Signal Balance as a Pluripotency Determinant

In vitro modeling of in vivo pluripotency states with WNT, FGF and BMP

Alexandru Valentin Neagu

ISBN: 978-94-6375-626-6
Layout: Alexandru Valentin Neagu
Cover design: Alexandru Valentin Neagu
Printing: Ridderprint, The Netherlands

The work described in this thesis was performed at the Department of Cell Biology at the Erasmus MC, Rotterdam, The Netherlands.

The research has been funded by NWO (NWO ECHO.10.B1.064).

Signal Balance as a Pluripotency Determinant

In vitro modeling of in vivo pluripotency states with WNT, FGF and BMP

Signaalbalans als een determinant van pluripotentie

In vitro modellering of in vivo pluripotentie met WNT, FGF en BMP

Proefschrift

ter verkrijging van de graad van doctor aan de
Erasmus Universiteit Rotterdam
op gezag van de rector magnificus
Prof. dr. R.C.M.E. Engels
en volgens het besluit van het College voor Promoties.
De openbare verdediging zal plaatsvinden op

dinsdag 14 januari 2020 om 13:30 uur

door

Alexandru Valentin Neagu

geboren in Constanta, Roemenië

Erasmus University Rotterdam

Promotiecommissie

Promotoren
Prof. dr. E.A. Dzierzak
Prof. dr. D.F.E. Huylebroeck

Overige leden
Prof. dr. J.H. Gribnau
Dr. R.A. Poot
Dr. B.A.J. Roelen

Copromotor
Dr. D. ten Berge

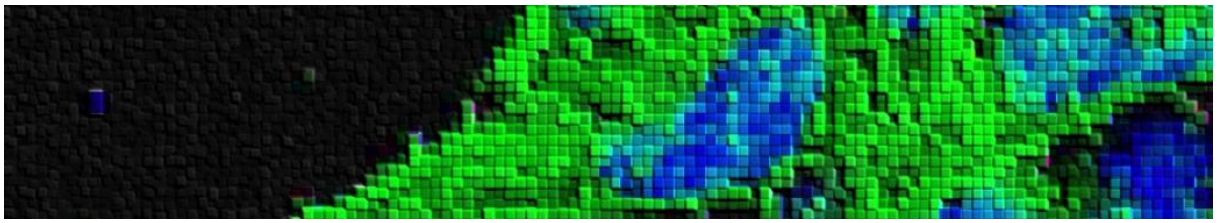

Contents

Chapter 1

Introduction

The first segregation of cells in the early mammalian embryo generates trophectoderm and inner mass cells. The latter will form the future epiblast cells and the primitive endoderm. The epiblast cells are a transient population of cells with a remarkable property: they can differentiate into all cell lineages of the embryo proper (giving rise to the entire adult organism) and a number of cell populations that will form extra-embryonal parts. This property of the inner cell mass cells is referred to as 'pluripotency'. Based mainly on experiments with inner cell mass like cells *in vitro*, i.e. embryonic stem cells, preserving it requires maintenance of self-renewal and inhibition of differentiation. Defining the molecular mechanisms and factors that control the initiation, maintenance and exit from pluripotency (which accompanies the onset of cell differentiation) is crucial in order to have a better understanding of early development. In addition to fundamental insights in development, pluripotent cells can be used to generate knockout or transgenic animals (through embryonic stem cells). In principle, these cells are also a cell source for cell therapy in regenerative medicine or personalized disease models (through induced pluripotent cells, which are obtained from somatic cells via reprogramming, and which are similar to pluripotent embryonic stem / epiblast cells). To fulfil the potential of induced pluripotent cells in personalized medicine, it is of fundamental importance to fully characterize pluripotency as it occurs in development. This introduction presents an overview of embryonic development, the events that generate pluripotency, the transition from one type of pluripotency to another, the signaling pathways involved in these processes and their molecular effects.

The core characteristics of pluripotent cells and their potential for developmental biology, regenerative medicine and establishment of tumor-initiating cells by cell de-differentiation in cancer have generated tremendous interest in understanding the molecular mechanisms controlling them. Although significant progress has been made in the past years in elucidating the cell extrinsic and intrinsic factors that regulate self-renewal and pluripotency, several major gaps still remain. In particular, this introduction provides an overview of the known mechanisms either triggered or inhibited by various signals which seemingly have opposing effects on the molecular machinery affecting pluripotency, depending on the particular developmental stage of the cells. This represents the crucial context in which the work presented in this thesis must be viewed from.

This thesis enriches the body of knowledge around pluripotency by describing a novel pluripotent state. It deepens our understanding of cell biology, the processes establishing pluripotency and provides new insights into improving the process of artificial generation of pluripotent cells.

1. The establishment and dismantling of pluripotency during embryogenesis

Vertebrate development starts after an egg is fertilized by a sperm cell. Although on a different time scale, the processes described in this section are similar between mice and humans. Both the egg cell and the sperm cell carry half of the genetic information of the parent they originate from. Upon fertilization, the nuclei of the two cells merge and thus lead to the formation of a single diploid cell: the zygote. The zygote can give rise to a whole embryo, as well as extra-embryonic tissues, like the placenta in mammals. Therefore, it is totipotent. At this stage, the proteins that wrap and condense the DNA still have modifications inherited from the parents (epigenetic marks, for example the methylation of histones that wrap the DNA). After four rounds of cell division with no significant growth, a process called cleavage, the embryo advances to a ball of 16 cells called a morula. During these stages, cells go through a process in which the epigenetic marks are removed. In mouse, 3 days after fertilization (embryonic day 3 or E3), the cells go through their first specification, answering to cues from

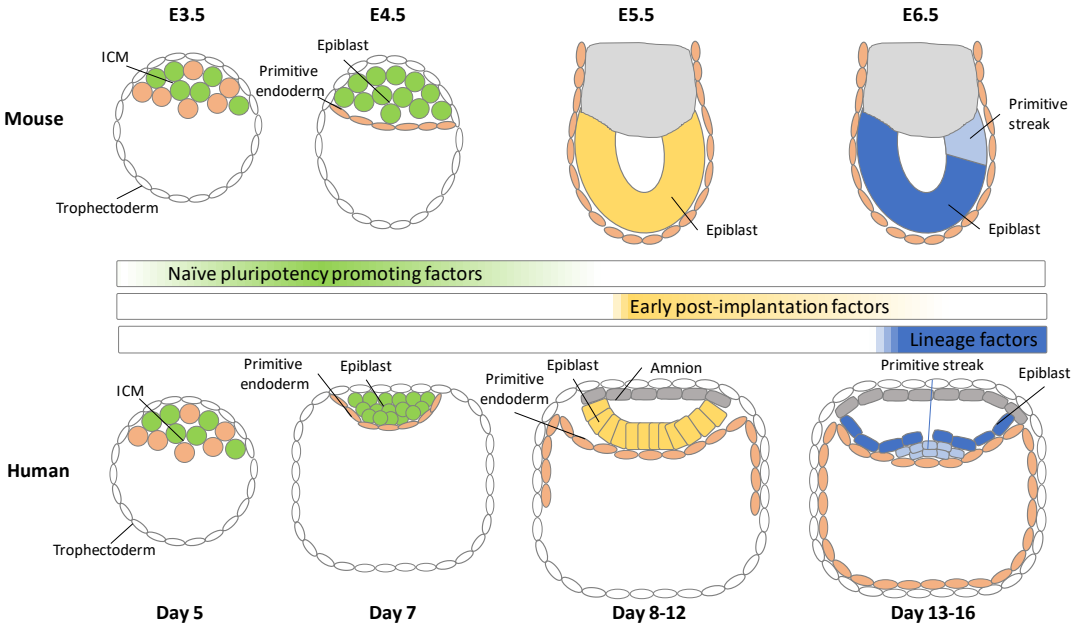

Figure 1. *Schematic representation of peri-implantation embryo development in mouse and human. Adapted from* (Smith A. , 2017).

neighboring cells that inform them, in part based on their relative position, on their position within the embryo (Krupa, et al., 2014). In the morula stage, a phenomenon unique to mammalian embryos occurs, compaction. This change in shape of the embryo leads to the formation of an outer layer of cells, called trophectoderm, from which extra-embryonic tissues will develop, and an inner clump of cells, the inner cell mass (ICM) (Morris, et al., 2010). Fluid collects between the trophoblast and the ICM, and following a cavitation process the morula transitions into a blastocyst (figure 1).

The cells in the ICM segregate into primitive endoderm and the pluripotent epiblast around E4 (in mouse) or day 7 of human embryonic development. The epiblast gives rise to all tissues of the embryo, a property called pluripotency. It is at this stage that methylation reaches an all-developmental low, meaning that the chromatin (DNA and proteins organized as chromosomes) is open and all marks inherited from parents have been removed (Smith Z. , et al., 2012). The cells are therefore said to be in a naïve pluripotency (Nichols & Smith , 2009). Shortly after reaching this step, information by way of cell-cell contacts leads to the gain of polarity in these cells and a re-arrangement of them in a rosette, with a basal membrane towards the outside and an apical side towards the middle, coinciding with implantation (Bedzhov & Zernicka-Goetz, 2014). Here, cells start secreting sialomucins that lead to the formation of another cavity, which expands until the epiblast cells form the egg cylinder (figure 2). The egg cylinder is a unique feature of mouse embryonic development.

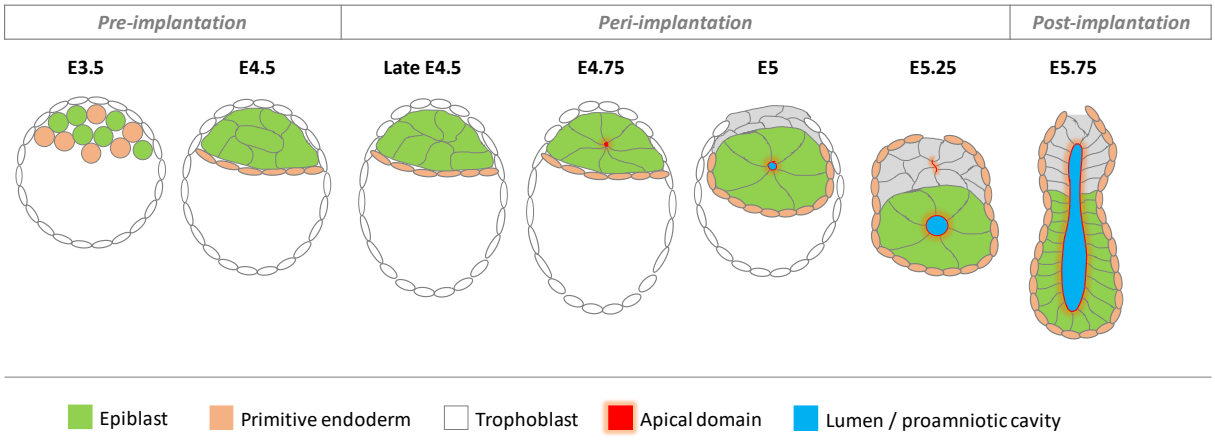

Figure 2. *Schematic representation of mouse peri-implantation development. Adapted from* (Bedzhov & Zernicka-Goetz, 2014)

After having went through 2 rounds of specification and in preparation to the next step, which is differentiation to one of the three germ layers, the cells that form the epiblast start undergoing epigenetic changes that enable the cells to undertake stable differentiation.

Because they still have the potential to differentiate into any cell type, depending on the signaling cues they receive, these cells are also pluripotent. As opposed to the cells in the ICM, due to their more advanced development, these cells are in a primed pluripotent state. The two types of pluripotency and their characteristics will be discussed in the following sections. The next developmental event after the formation of the egg cylinder is gastrulation. Gastrulation is a crucial stage in embryonic development, when pluripotent epiblast cells organize to generate the germ layers: mesendoderm (initially, later yielding mesoderm and definitive endoderm) and ectoderm. Gastrulation strongly rearranges these germ layers and lays down the basic, primitive body plan, which will further develop into the embryo. It starts approximately at E6.25 with (i) embryonic asymmetry (specification across the proximal-distal and anterior-posterior axes), (ii) the formation of the primitive streak, (iii) epithelial to mesenchymal transitions and (iv) an ingression at the primitive streak that will form the germ layers. Gastrulation is a process that continues for several days. The exit from pluripotency and early cell determination in the three germ layers of the embryo proper is guided by several signaling pathways, including additional interactions at the extra-embryonal and embryonal interface, at the future anterior (no primitive streak formation here) and posterior (gastrulation side, visible by primitive streak formation) side of the egg cylinder.

2. Naïve pluripotency - Embryonic stem cells

In 1981, Evans and Kaufman were the first ones to succeed in the *in vitro* derivation of mouse pluripotent stem cell lines, from the ICM of blastocysts (Evans & Kaufman, 1981). In the same year, Martin coined the term “embryonic stem cells” (Martin, 1981). It has been shown by clonal derived cell culture that the capacity of ICM cells to self-renew as embryonic stem cells is gained immediately following epiblast specification (Boroviak, Loos, Bertone, Smith, & Nichols, 2014). These first lines had a high degree of instability due to their culture conditions (i.e. readily differentiating), which were based on a feeder layer of mitotically inactivated fibroblasts together with fetal calf serum, with an unknown growth factor composition. A few years later, the first factor promoting ESC maintenance was identified by Austin Smith (Smith, et al., 1988), and Colin Stewart and collaborators (Williams, et al., 1988), as Leukemia Inhibitory Factor (LIF). LIF was demonstrated later as being one of the factors required for the maintenance of ESCs (Williams, et al., 1988). Serum, which has a variable and undefined composition, was still added to the culture. An important milestone in ESC maintenance was

the shift from a serum based medium to a defined, serum free culture. The derivation efficiency of ESCs and their stability in culture was shown to be increased by the addition of small-molecule inhibitors for MEK signaling (described below) (Burdon, Stracey, Chambers, Nichols, & Smith, 1999). This led to the development of several different defined conditions, most involving activators of the WNT pathway and MEK inhibitors (most notably three inhibitors – 3i, and two inhibitors – 2i) (Kielman, et al., 2002) (Ying, et al., 2008). Complete genetic ablation of *Erk1* and *Erk2* (MEK effectors), either individually or combined, does not lead to a maintenance of rodent ESC survival, nor does it yield an identical phenotype to that resulting from MEK inhibition, suggesting that MEK inhibition has additional, ERK-independent roles in the maintenance of ESCs (Chen, et al., 2015). In 2011, ten Berge et al. demonstrated that in addition to LIF, ESCs only require WNT signals for their homogenous maintenance and indefinite expansion (ten Berge, et al., 2011). Other studies contradict this and argue that ESCs can be maintained in the absence of WNT signals (Lyashenko, et al., 2011). These findings highlight the relevance of investigating ESCs in different combinations of factors or chemical inhibitors of their signaling that support the expansion of maintenance of the cells.

LIF and WNT signaling pathways act to retain the characteristics of ES cells. Morphologically, the cells are small and round, and form compact, dome-shaped colonies due to the strong adherence of the cells to each other. Upon breaking down a colony in a single cell suspension, each individual cell can give rise to a new colony. Their pluripotency can be tested in three ways: (i) by injecting the cells subcutaneously, which will lead to the formation of a teratoma that contains cell types of all the three germ layers, (ii) by injecting the cells in blastocysts, which will lead to the formation of a chimeric embryo, or (iii) by triggering *in vitro* differentiation through embryoid body formation. A fourth, more recent alternative, is to mix ESCs with TSCs, thereby generating 3D structures called ETS embryos (ESC- and TSC-derived embryos), to show morphogenesis similar to that of natural embryos (Ellys Harrison, Sozen, Christodoulou, Kyprianou, & Zernicka-Goetz, 2017).

Characteristic to these cells is the presence of several pluripotency regulators, which form a core pluripotency gene regulatory network. One of the core pluripotency factors is NANOG, first reported to be essential for sustaining pluripotency in ESCs (Mitsui, et al., 2003) (Chambers, et al., 2003). NANOG-null ESCs cannot be derived from mouse ICM, further indicating its indispensable role in establishing pluripotency *in vivo* (Festuccia, et al., 2012).

Another component of the pluripotency gene regulatory network is Octamer-binding transcription factor 4 (*Oct4*, also known as *Pou5f1*), which is expressed in ESCs and throughout the germ line, essential for both *in vivo* and *in vitro* pluripotency (Scholer, Hatzopoulos, Balling, Suzuku, & Gruss, 1989) (Nichols, et al., 1998) (Niwa, Miyazaki, & Smith, 2000). Upstream of OCT4 is SRY-box 2 (SOX2), a transcription factor required for the formation of the pluripotent epiblast (Avilion, et al., 2003) (Masui, et al., 2007). The loss of both OCT4 and SOX2 triggers differentiation of the cells into trophectoderm, whereas the overexpression of genes encoding both proteins leads to the differentiation of mesendoderm or neural ectoderm, respectively (Niwa, Miyazaki, & Smith, 2000) (Thomson, et al., 2011). SOX2, OCT4 and NANOG function together and co-occupy approximately 14,000 of potential regulatory elements in the genome, across approximately 3,200 genes, including their own promoters, forming densely interconnected feedback and feedforward regulatory loops (Marson, et al., 2008). Effectors of LIF, BMP4 and WNT pathways (STAT3, SMAD1 and β-catenin-TCF7L1, respectively) directly modulate the SOX2-OCT4-NANOG core circuit by co-occupying enhancers that are bound by these transcription factors (Young, 2011) (Hackett & Surani, 2014). In the absence of nuclear β-catenin, TCF7L1 (also known as TCF3) functions as a transcriptional repressor, and antagonizes the action of OCT4 and SOX2, which colocalize with TCF7L1 at pluripotency-associated genes (Cole, Johnstone, Newman, Kagey, & Young, 2008).

Other ESC-specific markers include alkaline phosphatase, *Stella*, *Klf4*, *Esrrb*, *Cd31* (Brons, et al., 2007) (Payer, et al., 2006) (Takahashi K. & Yamanaka S., 2006) (Festuccia, et al., 2012) (Li, et al., 2005). Their gene expression profile carries a unique signature dependent on the pluripotency transcription factors. Epigenetically, their genome can be described as “open”, as they have a reduced prevalence of repressive histone markers (H3K27me3) at promoters (Marks, et al., 2012). Most of the parental epigenetic marks have been erased and methylation reaches an all-developmental low in the ICM and ESCs respectively (Smith Z. , et al., 2012). In female cells both X chromosomes are active and repressive histone marks are limited, due to a continuous chromatin remodeling (Niwa H. , 2007) (Farthing, et al., 2008). Without inherited epigenetic modifications, or modifications that restrict the cells’ future development into one of the 3 germ layers, the cells are “naïve” (Ying, et al., 2008).

Several proteins produced in the ICM or by ESCs do not promote naïve pluripotency. Some of them actually promote the transition to primed pluripotency. Due to the highly optimized and

defined culture conditions, ESCs tolerate these factors *in vitro*. For instance, in a defined LIF/2i culture, TCF7L1 is neutralized by adding the inhibitor for GSK3, boosting naïve pluripotency (Wray, et al., 2011). In LIF/serum conditions, TCF7L1 is able to bind to its naïve pluripotency-promoting target genes, leading to their partial repression. Thus, the naïve pluripotent state is a "zero sum game" representing the outcome of stabilizing and destabilizing factors that act in concert (Loh & Lim, 2011).

3. Naïve to primed pluripotency transition: the formative state

The *in vitro* transition from naïve to primed pluripotency consists of a series of key events. *In vivo*, in mouse embryos, the transition from naïve (E3.75-4.75) to primed pluripotency (E6.0-6.5) covers a time span of approximately 2 days (Boroviak, Loos, Bertone, Smith, & Nichols, 2014). It was hypothesized that certain events occurring in this time window are essential for the transition, but until recently these events had not been described. For instance, cells that have lost ES cell identity do not immediately upregulate definitive lineage specification markers (Kalkan, et al., 2017). Accordingly, one author coined the term formative to describe the transient period between naïve and primed pluripotency (Kalkan & Smith, 2014) (Smith A. , 2017).

A discrete formative phase, intermediate between naïve and primed pluripotency is shown by tracking the ESCs' ability to revert to a naïve state in the absence of exogenous growth factors or serum components. Using a destabilized GFP knock-in to the *Rex1* locus enables tracking of the loss of naïve pluripotency by downregulation of the fluorescent reporter, and screens using the REX1-GFP as read-out (Kalkan, et al., 2017). Early after 2i withdrawal (16h), cells remain uniformly REX1::GFP-positive and can revert to self-renewal very efficiently. By 25h, the GFP expression profile becomes heterogenous: GFP-high cells are still able to self-renew if restored to LIF/2i, but this ability is effectively lost in GFP-low. Moreover, the GFP-low fraction readily responds to stimuli for the differentiation to the three embryonic germ layers (Mulas, Kalkan, & Smith, 2017). An *in vitro* intermediate state can be captured by culturing ESCs in a medium supplemented with FGF and Activin (two key pathways in epiblast stem cell maintenance). This leads to epiblast-like cells (EpiLCs), which have a transcriptional state similar to the E5.75 epiblast, which is just prior to the onset of gastrulation (Morgani, Nichols, & Hadjantonakis, 2017). EpiLCs obtained *in vitro* show markers of pluripotency that are intermediate between ESC and EpiSC: naïve gene markers (e.g. *Stella, Rex1* and *Klf4*) are

downregulated, while later markers, associated with differentiation (e.g. *T, FoxA2, Lefty, Sox1*) are not upregulated to the same extent as in EpiSCs, and early EpiSC markers such as *Fgf5* and *Oct6* are expressed at the same or higher levels than in EpiSCs (Morgani, Nichols, & Hadjantonakis, 2017). There are several significant differences between the formative phase and primed pluripotency, such as the formation of blastocyst chimaeras, germ cell competence, lower DNA methylation, expression of genes encoding early post-implantation transcription factors and no expression of genes encoding non-ectoderm lineage transcription factors (Smith A. , 2017).

The concept of formative pluripotency acts as a bridge between the two pluripotency states captured *in vitro,* but it is not limited to one cell type in particular. So far, formative pluripotency is not a self-renewing state and formative stem cell lines have not yet been established. EpiLCs, which may include formative cells, are currently considered as a transient type of cells (Hayashi, Ohta, Kurimoto, Aramaki, & Saitou, 2011). Deriving formative pluripotent stem cells is a significant challenge which has been suggested to rely on whether a stable balance of different signaling pathways exists and can be arrested *in vivo* (Enver, Pera, Peterson, & Andrews , 2009). These states all transiently and seamlessly occur within a sequence of developmental progression.

4. Primed pluripotency - Epiblast stem cells

In vitro, epiblast stem cell were initially derived from post-implantation epiblasts of rodents, in FGF2/Activin A supplemented medium. EpiSCs were shown to resemble more the pluripotent human ESCs (hESCs, see below) while showing patterns of gene expression and signaling responses that would normally function in the post-implantation epiblast (Tesar, et al., 2007). As opposed to ESCs, they are derived from the epiblast of the post-implantation embryo (E5.5-E7.5) (Joo, et al., 2014). *In vitro* they can be differentiated from ESCs by removing WNT and activating FGF and Activin signaling. If both WNT and FGF pathways are active, ESCs do not make the transition to EpiSCs, showing that WNT maintains naïve pluripotency regardless of FGF signaling. The two pluripotent stem cell types are easily distinguishable by their morphology, since EpiSCs form flat, irregular colonies and individual cells are easily identifiable. Furthermore, the maintenance and expansion of EpiSCs is done by breaking the colonies into clumps of cells and not a single cell suspension, from which they hardly recover because of interrupted cadherin signaling (Felicia Basilicata, Frank, Solter,

Brabletz, & Stemmler, 2016). Although pluripotent, as assessed by teratoma assays and to a lesser, much more inefficient way than ESCs, by chimera formation (Ohtsuka, Nishikawa-Torikai, & Niwa, 2012), there are striking differences between ESCs and EpiSCs in terms of the marker genes they express and their gene expression profiles. A lower but still detectable expression of the core pluripotency transcription factors (*Nanog*, *Oct4*, *Sox2*) is complemented by the upregulation of lineage commitment factors such as *Oct6* and *Otx2*, which also act as markers (Buecker, et al., 2014). In contrast to ESCs, this is the stage where *de novo* DNA methyltransferases (*Dnmt3* members) are expressed and epigenetic marks established, which will "prime" the cells in development by allowing lineage commitment and establishment of a somatic epigenome (Brons, et al., 2007). For example, naïve marker genes like *Stella* and *Rex1* are silenced by methylation upon the transition to EpiSCs (Bao, et al., 2009). One of the most important epigenetic events occurring at this stage is the random inactivation of one of the X chromosomes in female cells (Guo, et al., 2009). In terms of their culture requirements, EpiSCs thrive in defined, serum-free medium supplemented with FGF and Activin (Brons, et al., 2007) (ten Berge, et al., 2011).

The first hESCs derived from blastocysts showed significant differences with mouse ESCs in their characteristics and culture requirements (Thomson, et al., 1998). hESCs, either derived from blastocysts, or iPSCs obtained by direct *in vitro* reprogramming rely on FGF2 and Activin A, but not LIF signaling (Bertero, et al., 2015). Moreover, human ESCs do not upregulate the expression of *FGF5* or *N-CADHERIN* mRNAs, and they have high levels of several naïve pluripotency marker genes (*NANOG*, *PRDM14*) (Gafni, et al., 2013). Other naïve pluripotency marker genes (e.g. *REX1*, *KLF17*, *DPPA3*) show a low expression in hESCs, similar to mouse EpiSCs (Chia, et al., 2010). The active deposition of H3K27me3 over developmental genes, loss of pluripotency upon inhibition of MEK-ERK signaling, lack of global hypomethylation (as seen in the ICM), and lack of a pre-X inactivation state in most conventional female human pluripotent lines suggest that hESCs are developmentally closer to murine EpiSCs (Smith Z. , et al., 2014) (Mekhoubad, et al., 2012). A complete parallel between hESCs and murine epiblast stem cells (EpiSC) cannot be drawn. hESCs are functionally dependent on NANOG and PRDM14, as losing these factors induces differentiation (Chia, et al., 2010). Even the distribution of DNA methylation is similar to murine ESCs grown in serum-supplemented medium, rather than murine EpiSCs expanded in FGF2/Activin A (Hackett, et al., 2013)

(Shipony, et al., 2014). Lastly, the localization of TFE3, whose intracellular redistribution affects the exit from pluripotency (nuclear TFE3 – no differentiation; cytoplasmic TFE3 – exit from pluripotency), is different from both murine pluripotent states: whereas in murine ESCs, TFE3 is located exclusively in the nucleus and in EpiSCs exclusively in the cytoplasm (Betschinger, et al., 2013), hESCs show an intermediate configuration, in which TFE3 is present in both the cytoplasm and nucleus (Gafni, et al., 2013).

While we commonly tend to think of ESCs and EpiSCs as two completely separate cell types, the *in vitro* reality is that these two states are on opposite sides of a pluripotency spectrum. Each cell in culture has the ability to move closer or further away from naïve pluripotency, in the case of ESCs, or primed pluripotency, in the case of EpiSCs (Hayashi, Lopes, Tang, & Surani , 2008). This translates to some of the ESCs triggering differentiation to EpiSCs, as assayed for example by subtle changes in the expression of some genes. Depending on WNT activity, this transition can be completed or not. Vice-versa, EpiSCs do not normally revert to a "naïve" state, indicating a 'point of no return' in differentiation. The fully defined serum-free media supplemented with specific molecules helps keeping the naïve-primed differentiation/reversion processes in check and maintaining homogenous cultures. Whereas naïve pluripotency is maintained by LIF and WNT and primed pluripotency by FGF and Activin, exit from pluripotency is guided by an interplay between WNT, BMP and Nodal.

5. Signaling pathways affecting pluripotency

a. LIF signaling

The ability to maintain and propagate naïve pluripotency *in vitro* through ESCs relies on two essential signaling pathways. Chronologically, the first identified was the Leukemia inhibitory factor (LIF) (Smith, et al., 1988) (Williams, et al., 1988). LIF is a member of the family of interleukin (IL)-6-type cytokines, which signal through a heterodimer consisting of the receptor subunit gp130, in association with the low-affinity LIF receptor (LIFR), a ligand-specific receptor subunit (Graf, Casanova, & Cinelli, 2011). This complex leads to the activation of the receptor-associated Janus kinases (JAKs), which in turn phosphorylates receptor docking sites, and recruits the Src homology-2 (SH2) domain containing proteins such as STAT3 (signal transducer and activator of transcription 3). Upon binding to the receptor, STAT3

molecules dimerize. The dimers then translocate to the nucleus, where they bind to promoters and enhancer regions of their target genes (figure 3). In mouse ESCs, LIF does not only activate the STAT3-mediated cascade, but may also induce the ERK-pathway, through the mitogen-activated protein kinase (MAPK) (Shoni, et al., 2014).

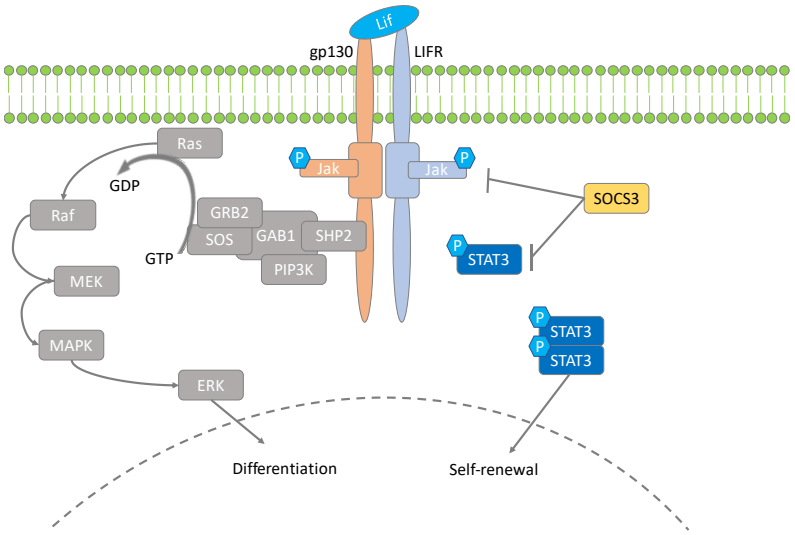

Figure 3. *Schematic representation of the LIF-pathway.*

LIF signaling was shown to be necessary to maintain self-renewal of mouse ESCs in the absence of feeders (Matsuda, et al., 1999) (Niwa, Burdon, Chambers, & Smith, 1998) (Cinelli, et al., 2008). Among its downstream targets, the transcription factor c-MYC was described to have a significant role in self-renewal by functioning as a key target of LIF/STAT3 signaling (Cartwright, et al., 2005). In support of this hypothesis, constitutive expression of *c-Myc* was shown to support self-renewal independent of LIF activity. This observation was made for other genes involved in the maintenance of pluripotency, such as *Nanog* (Chambers, et al., 2003) or *Klf2* (Hall, et al., 2009). Expression of a dominant negative form of c-MYC promotes differentiation (Cartwright, et al., 2005). 55% of the putative STAT3 target genes display binding sites for NANOG, and 41% of the putative NANOG target genes display binding sites for STAT3 (Chen, et al., 2008). LIF/STAT3 was also shown to target *Klf4* (Hall, et al., 2009) (Niwa, Ogawa, Shimosato, & Adachi, 2009). This emphasizes the co-regulation of the expression of a large set of target genes by these transcription factors, which are involved in the maintenance of naïve pluripotency.

b. WNT signaling

The WNT signaling pathways are a group of highly conserved signal transduction pathways formed by proteins that carry signals from outside of a cell through cell surface receptors to the inside of the cell. *In vivo*, WNT activity was detected in E3.5 and E4.5 mouse embryos, but

not in E5.5 implanted embryos (ten Berge, et al., 2011). WNT activity can once again be detected in the region of the primitive streak, starting from E6.5 (ten Berge, et al., 2008).

There are three pathways that have been described: (i) the canonical WNT pathway, which leads to the regulation of gene expression, (ii) the noncanonical planar cell polarity pathway, which is responsible for the shape of the cytoskeleton and (iii) the noncanonical WNT/calcium pathway, which regulates the intake of calcium (Komiya & Habas, 2008). First described in Drosophila as the *Wingless* gene (Wg), and in mouse as the *int1* (integration 1) oncogene, they were later discovered to be part of the same pathway which was renamed WNT (Wingless-related integration site) (Rijsewijk, et al., 1987) (Nusse, et al., 1991). Of relevance for pluripotency is the canonical WNT pathway (Wray, et al., 2011) (ten Berge, et al., 2011). The family is comprised of 19 WNT signaling proteins in human and mouse. Given the correct signals, a cell will start transcribing *Wnt* genes, which will be translated in the cytoplasm into 350-400 amino acid proteins. The proteins are post-translationally lipid-modified by palmitoylation, which is required for the initiation of the targeting of the WNT protein to the plasma membrane, followed by its secretion. The protein is also glycosylated to insure proper secretion (Kurayoshi, Yamamoto, Izumi, & Kikuchi, 2007). *In vitro*, WNT production can be blocked by using a synthetic molecule called Inhibitor of WNT Production 2 (IWP2) which inhibits the enzyme that palmytoylates WNT, porcupine (Chen, et al., 2009). After secretion, the WNT protein mostly acts in an autocrine or paracrine manner. In the canonical pathway, upon binding to its receptors, Frizzled and its co-receptor LRP5/6, the WNT signal reaches the phosphoprotein Dishevelled which in turn sequesters the "destruction complex" to the cell membrane (Rao & Kuhl, 2010) (Komiya & Habas, 2008) (figure 4). This complex is made of Axin, adenomatosis polyposis coli (APC), glycogen synthase kinase 3

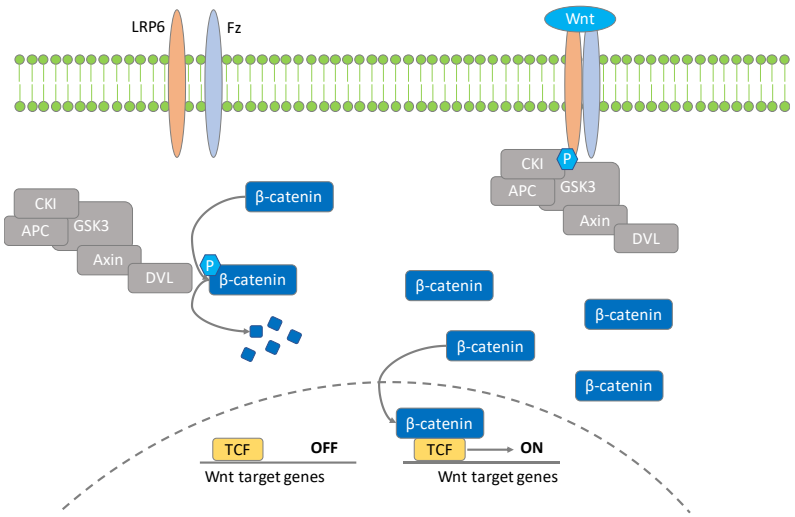

Figure 4. *Schematic representation of the WNT pathway.*

(GSK3) and casein kinase 1α (CK1α) (Minde, Anvarian, Rudiger, & Maurice, 2011). In the absence of WNT signaling, the "destruction complex" degrades β-catenin by targeting it for ubiquitination and proteasomal digestion (MacDonald, Tamai, & He, 2009). Immediately upon binding of a WNT protein to its receptors, the "destruction complex" is disturbed, which leads to an accumulation of β-catenin in the cytoplasm followed by its translocation to the nucleus. Here, it acts as a transcriptional coactivator of transcription factors belonging to the TCF/LEF family. *In vitro*, instead of soluble WNT proteins, the pathway can also be activated by the addition of a GSK3 inhibitor, as is the case in the 2i culture condition of ESCs. While TCF1, TCF4 and LEF1 are not bound to DNA when WNT is off and activate genes once beta-catenin translocates to the nucleus, TCF7L1 is bound to DNA even in the absence of WNT (without GSK3 inhibitor) and has a repressive role (Staal & Clevers, 2000) (Yi, et al., 2011). Upon WNT activation, this repression is relieved and active transcription begins (Wu, et al., 2012). Moreover, TCFf3 has been shown to act broadly, genome-wide, to reduce the levels of naïve genetic markers (*Nanog*, *Tbx3*, *Esrrb*) while not affecting genes that show a relatively similar expression in both ESCs and EpiSCs (*Oct4*, *Sox2*, *Fgf4*). This has led to the conclusion that TCF7L1 acts as an inhibitor of naïve pluripotency cell self-renewal (Yi, Pereira, & Merrill, 2008). Contradicting reports indicated that β-catenin may not be needed for transcription, but for cadherin-mediated cell adhesion (Lyashenko, et al., 2011). Other hypothesis implies that beta-catenin directly interacts with the pluripotency network by upregulating *Nanog* after physically associating with OCT4 (Takao, Yokota, & Koide, 2007) (Kelly, et al., 2011). In contrast, WNT signaling has a different function in primed pluripotency. Instead of stimulating self-renewal, WNT signaling effectively stimulated differentiation of EpiSCs.

Several earlier studies of the role WNT has in ES cells suggested that the signal triggers differentiation. Otero et al. observed neural differentiation in ESCs cultured with WNT3a conditioned medium (Otero, Fu, Kan, Cuadra, & Kessler, 2004). Overexpression of β-catenin yielded similar results. Not all reports, upon induction of WNT signaling, show differentiation or commitment towards the same lineage. Others reported that WNT signaling is required for mesoderm/endoderm specific differentiation in both human and mouse ES cells (Bakre, et al., 2007) (Lindsley, Gill, Kyba, Murphy, & Murphy , 2006). Activation of WNT signaling either by supplying cells with WNT3a or by inhibiting GSK3 resulted in the upregulation of certain mesoderm and endoderm specific markers in human and mouse ES cells. The progenitor cells

could still be maintained long term in culture despite the partial differentiation, suggesting that WNT signaling might be responsible for the self-renewal of these cells. Other studies showed that overexpression of stabilized β-catenin led to an increase in self-renewal and impaired neural differentiation in mouse cells after 14 days of embryonic body formation. Together, these studies suggest an important role for WNT signaling during early differentiation. All these results are in sharp contrast with other studies in which WNT3a (either purified protein or conditioned medium) did not induce differentiation but was instead reported to promote self-renewal of ESCs (ten Berge, et al., 2011) (Sato, Meijer, Skaltsounis, Greengard, & Brivanlou, 2004). In contrast, Davidson et al. found that activation of WNT signaling either by supplying hESCs with WNT3a or by inhibiting GSK3 reduced self-renewal, indicating a significantly different role for WNT in hESCs (Davidson, et al., 2012). The requirement of WNT signaling during differentiation does not exclude that WNT signaling is also paramount for ESC self-renewal.

c. FGF signaling

In 1974, a protein was identified that, upon tests in bioassays, was discovered to promote fibroblast proliferation (Gospodarowicz, 1974). It was later found that this protein belonged to a bigger family of proteins, fibroblast growth factors (FGF). FGFs are proteins that interact with membrane-associated heparan sulfate proteoglycans, in the form of four receptors (FGFR1, FGFR2, FGFR3 and FGFR4), driving FGF signal transduction and thus constituting the FGF signaling pathway. It is involved in several important processes, like angiogenesis, wound healing, proliferation, survival, migration and differentiation. Of relevance for this thesis is the role FGF signaling has in the early embryonic development *in vivo* and the loss of naïve pluripotency/gain of primed pluripotency.

After binding to its receptors, the FGF signal can be carried through four distinct pathways: the Janus kinase/signal transducer and activator of transcription (JAK/STAT), phosphoinositide phospholipase C (PLC), phosphatidylinositol 3-kinase (PI3K) and MAP kinase pathways (Dailey, Ambrosetti, Mansukhani, & Basilico, 2005). MAP kinases are a family of proteins that control the activity of downstream kinases and transcription factors. In pluripotent stem cells MAP kinase is active through MEK1 and MEK2, which in turn regulate the transcriptional activity of ERK1/2. Early in development (E3.0-E3.75) FGF regulates the formation of primitive endoderm from the ICM (no connection to the naïve-primed transition). Later in development (not clear

when this happens *in vivo* but peri-implantation), FGF is required for the transition to primed pluripotency. Upon activation of ERK1/2 by FGF stimulation, it was demonstrated that pluripotent ESCs lose the ability to self-renew and gain the capacity to undergo lineage commitment (Kunath, et al., 2007). While ESCs experience autocrine FGF4 signaling (Ma, et al., 1992), only after removal of WNT activity do the cells undergo the transition (ten Berge, et al., 2011). This indicates WNT and FGF have sequential roles in the naïve-primed transition. Since then, it was shown that ERK activation leads to the export of KLF4 from the nucleus of ESCs, which in turn leads to a rapid decline in *Nanog* and *Klf4* transcription. This disrupts the entire core pluripotency network, leading to differentiation (Dhaliwal, Miri, Davidson, Tamim El Jarkass, & Mitchell, 2018).

The report by ten Berge et al. in 2011 showed that using the same MEK inhibitor as in the 2i ESC culture condition, together with soluble WNT protein, lowers the level of WNT3a protein required for optimal self-renewal (ten Berge, et al., 2011). The existence of an interaction between the two pathways and at what level is still an open question in the field (Kurek & ten Berge, 2012). Consistent with the *in vitro* data, FGF4 was also detected in the inner cell mass of the blastocyst (Rappolee, Basilico, Patel, & Werb, 1994). WNT activity has been detected *in vivo* at E3.5 and E4.5, but not at E5.5, stages which developmentally correspond to naïve and primed pluripotent states, respectively (ten Berge, et al., 2011), suggesting that WNT activity must be inhibited for the transition from one state to another to occur. Additionally, suppression of ERK signaling stimulates the maintenance of naïve cells within the ICM in the mouse embryo by blocking specification of primitive endoderm (Nichols, Silva, Roode, & Smith, 2009).

d. Nodal/Activin signaling

The primitive streak formation is initiated by WNT and Nodal, on the posterior side of the embryo (Huelsken, et al., 2000) (Brennan, et al., 2001), while primitive streak formation is inhibited at the future anterior side of the embryo by growth factor antagonists and intracellular back-up mechanisms (Pereira, et al., 2012). A positive feedback loop is initiated where proNodal (Nodal precursor) induces the expression of *Bmp* in the extraembryonic ectoderm (Ben-Haim, et al., 2006). BMP then promotes the expression of *Wnt3* in the posterior epiblast, the site of the primitive streak. WNT signaling induces the T box transcription factor Brachyury, routinely used as a mesodermal marker, which has an

important role in the establishment of the anterior-posterior axis. WNT activity also positively regulates the levels of proNodal, which initiates the feedback loop.

Nodal belongs to the transformation growth factor beta (TGFβ) superfamily of secreted growth factors. Nodal (and Activin A, which mimics its effects) activates a complex of type I and type II cell surface serine threonine kinase receptors, that in turn phosphorylate the downstream cytoplasmic effector proteins SMAD2 and SMAD3. Phospho-SMAD complexes (usually 2/3), in association with the co-SMAD, SMAD4, translocate to the nucleus and, acting together with additional DNA-binding partners, selectively regulate target gene expression (figure 5) (Massague, Seoane, & Wotton, 2005). In the mouse embryo, Nodal activity peaks in the anterior primitive streak (Kaufman-Francis, et al., 2014). *In vitro*, mouse EpiSCs are maintained by culturing them in the presence of Activin A (another TGFβ-related factor) and FGF2, reminiscent of the provision of Nodal and FGF signals at the anterior primitive streak (Tam & Loebel, 2007). Similarly, TGFβ signaling through Activin/Nodal is necessary for the maintenance of pluripotency in human embryonic stem cells (James, Levine, Besser, & Hemmati-Brivanlou, 2005).

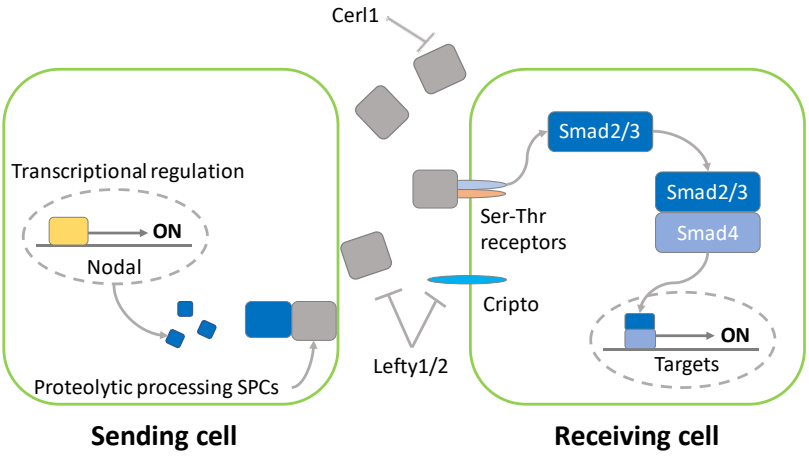

Figure 5. *Schematic representation of the Nodal pathway.*

e. BMP4 signaling

BMPs are also members of the TGFβ superfamily. They are involved in regulation of cell proliferation, differentiation, and apoptosis, and therefore play essential roles during embryonic development and pattern formation (Massague, TGF-beta signal transduction, 1998). BMP functions through receptor-mediated intracellular signaling and subsequently influences target gene transcription, similar to Nodal. Two types of receptors are required in this process, type I and type II. While there is only one type II BMP receptor (BMPRII), there

are three type I receptors: ALK2, ALK3 (BMPR1A) and ALK6 (BMPR1B). Different combinations of type II with any one of the type I receptors may determine the specificity and result in different consequences. There are two well-defined signaling pathways involved in BMP signal transduction (Derynck & Zhang, 2003). The canonical BMP pathway is through receptor I mediated phosphorylation of SMAD1, SMAD5 or SMAD9 (previously known as SMAD8) (figure 6). Two phosphorylated SMADs form a heterotrimeric complex with a common SMAD4. The SMAD heterotrimeric complex translocates into the nucleus and cooperates with other transcription factors to modulate target gene expression. A parallel pathway for the BMP signal is mediated by TGFβ1 activated tyrosine kinase 1 (TAK1, a MAPKKK) and through mitogen activated protein kinase (MAPK) (Derynck & Zhang, 2003) (Massague, 2000), which also involves cross-talk between the BMP and WNT pathways (Smit, et al., 2004) (Ishitani, et al., 2003). In Xenopus, dorsal-ventral polarity patterning was shown to be an effect of dorso-ventral BMP and antero-posterior WNT signaling, through inhibition of phospho-BMP-SMADs by concerted action of GSK3β and MAPK (Fuentealba, et al., 2007).

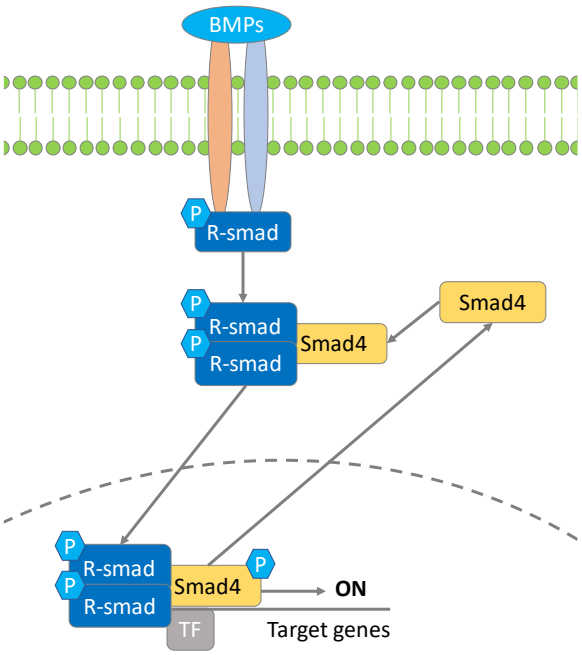

Figure 6. *Schematic representation of the BMP pathway.*

BMP4 was shown to induce the differentiation of primed pluripotent cells (Ying, Nichols, Chambers, & Smith, 2003). In contrast, LIF through STAT3 can block mesoderm and endoderm differentiation but favors neural differentiation (Ying, Nichols, Chambers, & Smith, 2003). BMP4 drives hESC differentiation into a mixture of mesoderm and trophoblast committed cells (Drukker, et al., 2012). In addition, supplementing the culture of hESCs with BMP4 induces a rapid decrease in the level of expression of *OCT4* and *SSEA3*, while increasing the expression of the differentiation gene marker *SSEA1* (Vallier, et al., 2009). This confirms that in contrast to mouse ESCs, hESCs are not maintained as pluripotent cells by BMP4 signaling.

6. Epigenetic seesaw

As important as signaling pathway effectors and transcription factors are, an additional layer of complexity is laid by the epigenetic machinery. Epigenetic modifications and cofactors play a significant role both in the maintenance of the two pluripotent states, but also in their transition. Transcriptional co-activators and co-repressors are protein complexes that do not bind DNA on their own, but regulate the action of sequence-specific transcription factors via chromatin-mediated mechanisms (Li & Belmonte, 2017).

Histone modifications have been extensively used to define and annotate distinct functional regions such as promoters and enhancers. The chromatin landscape of pluripotent cells was first described in murine ESCs. It showed that active and repressive chromatin marks colocalize genome-wide, for instance the trimethylation of lysine 4 on histone 3 (H3K4me3) and trimethylation of lysine 27 on histone 3 (H3K27me3) (Bernstein, et al., 2006) (Azuara, et al., 2006). This 'bivalent' chromatin signature is considered a key element that enables genes repressed in ESCs to follow alternative fates. In hESCs, a significant set of genes shows the same bivalent H3K4me3 and H3K27me3 marking, but few genes exhibit H3K27me3 alone (Pan, et al., 2007) (Zhao, et al., 2007). This indicates that, at least in hESCs, bivalency is the default chromatin state at genes essential for proper developmental control. A particular feature associated with the naïve phase of pluripotency is the presence of two active X chromosomes in female cells. In XX embryos the paternal X is initially inactive (Takagi & Sasaki, 1975) and is reactivated in the naïve epiblast (Mak, et al., 2004). Subsequently, one of the X chromosomes is randomly inactivated in each cell. In common with the naïve epiblast, female ESCs exhibit two active X chromosomes that undergo random inactivation during differentiation (Rastan & Robertson, 1985).

ESCs are extremely sensitive to oscillations in several cofactors, such as Mediator and cohesin (Kagey, et al., 2010), the Tat-interactive protein – p400 chromatin remodelling complex (Fazzio, Huff, & Panning, 2008), the RNA polymerase-associated factor 1 (PAF1) complex (Ding, et al., 2015), and the co-repressors CCR4-NOT transcription complex subunit 3 (CNOT3) and tripartite motif-containing protein 28 (TRIM28) (Hu, et al., 2009). Mediator and cohesin are especially relevant for the maintenance of naïve pluripotency, due to their role in the 3D genome organization of the core pluripotency transcription machinery. Mediator and cohesin are relatively large protein complexes that enable physical interaction between transcription

factor-bound enhancers and promoters (Li, Liu, & Izpisua Belmonte, 2012) (Gorkin, Leung, & Ren, 2014). The transcription of pluripotency-associated genes depends on interactions between distant regulatory elements. For instance, the expression of *Oct4* requires its upstream enhancer, bound by OCT4, SOX2, KLF4, Mediator and cohesin, to come into contact with its promoter (Wei, et al., 2013) (Zhang, et al., 2013).

EpiSCs show several differences, when compared to ESCs, in enhancer histone modifications. For example, *Oct4* enhancer usage switches from a distal enhancer (DE, preferentially used in the naïve state) to a proximal enhancer (PE, primarily used in the primed state) (Tesar, et al., 2007) (Yeom, et al., 1996). DNA methylation also varies: whereas ESCs have hypomethylated genomic DNA, EpiSCs are hypermethylated (Weinberger, Ayyash, Novershtern, & Hanna, 2016) (Hackett, et al., 2013) (Hayashi, Lopes, Tang, & Surani , 2008). Perhaps the difference easiest to observe in the status of the X-chromosome inactivation in female cells. Whereas female ESCs have both X chromosomes active, in EpiSCs the random inactivation of one of them is already completed (Guo, et al., 2009) (Bao, et al., 2009).

Thus, the transition from naïve (ESCs) to primed (EpiSCs) pluripotency is induces significant changes in the chromatin landscape. It then becomes essential for naïve cells to undergo an intermediary state, where they remove naïve marks and lay primed ones, as it allows proper remodeling in order to prepare for the correct segregation of all definitive embryonic lineages. The exact steps and sequence of events in the naïve-to-primed remodeling, as well as their function, are currently poorly understood. Learning more about this process could provide insight into how to direct it in the reverse way (i.e. reprogramming), to increase its efficiency.

7. Reprogramming somatic cells to pluripotent stem cells

In 2006, the direct *in vitro* reprogramming of somatic cells to pluripotency by ectopic expression of defined factors was achieved in groundbreaking research by Yamanaka, with the final aim of using these "induced pluripotent stem cells" for gene therapy (Takahashi K. & Yamanaka S., 2006). In theory, one could harvest cells (e.g., fibroblasts) from a diseased patient, reprogram them to a pluripotent stem cell state which can expand indefinitely, use gene editing technologies to fix the underlying defect (with, for example, CRISPR/Cas9), differentiate the stem cells back to cell types of interest and perform an autologous transplant back into the patient, thus curing the disease. Viewed as a "Holy Grail" in modern medicine,

this approach to personalized medicine is sidestepping the ethical issues of working with human embryonic stem cells but it is still hindered by a number of factors, mainly inefficient reprogramming/differentiating, especially in the human cells, of most clinical importance. That is due to a failure to erase their epigenetic memory; instead they acquire a state that resembles developmentally-primed cells, with a differentiation potential biased towards their lineage of origin (Kim, et al., 2010). In contrast, mouse iPSCs acquire a state of naïve pluripotency that supports complete reprogramming. Ultimately, it is the growth conditions that are used to expand such cells *in vitro* that determine the pluripotent state they attain (i.e. complete erasure of developmental history or developmentally-primed) (Hanna, et al., 2009). The key to unlock the full potential of human iPSCs rests therefore in understanding the essential differences between the different types of pluripotency.

8. Scope of the thesis

The focus of this thesis is on extending our knowledge on stem cell biology by investigating different aspects of pluripotency in mouse and human pluripotent stem cells. Specifically, we aimed to thoroughly describe the effect key signaling pathways have on pluripotency, with a particular view towards providing a more complete view of the controversy of the role of WNT signaling in pluripotency. This thesis aimed to investigate the major differences between naïve and primed pluripotent cells derived from both mouse and human, the balance between various signaling pathways that lead to pluripotency maintenance or exit, and how their downstream effectors lead to different pluripotency states.

Chapter 2 investigates EpiSCs and the cues these cells respond to. Specifically, we aimed to describe the effect of WNT signaling on primed pluripotency. *In vivo*, the corresponding cells see a pulse of BMP and WNT during gastrulation. We proceeded with describing this process *in vitro*. We found that BMP induces *Wnt*. Consequently, the activation of WNT pathway leads to loss of pluripotency in EpiSCs and hESCs. Moreover, in EpiSCs, WNT inhibition confines the cells to a pregastrula epiblast state which is able to contribute to blastocyst chimeras. Our findings led to a clear model of how WNT affects exit from pluripotency, ending the controversy around the contradicting findings previously published which indicated that WNT can both maintain naïve pluripotency but also trigger differentiation. This chapter also describes new culture conditions that maintain homogenous cultures of mouse EpiSCs and human ESCs.

Chapter 3 addresses the question of identifying the specific roles WNT and MEK inhibition have in naïve pluripotency, in the mouse early embryo, as they are not needed simultaneously for a homogenous culture. In doing so, we identified a novel pluripotent stem cell type, which shares characteristics with both ESCs and EpiSCs, while also having unique features. Interestingly, cells with similar properties are found in the peri-implantation embryo, shortly after the cells gain polarity and form the embryonic rosette, indicating that they occupy an intermediate pluripotent state. This chapter focuses on the characterization of this newly identified stem cell type, which we named Rosette-like stem cells. The identification and in vitro capture of rosette-stage pluripotency allows new insights into the processes that install functional pluripotency.

Chapter 4 is based on the findings from Chapter 2, that WNT signals regulate the transition from naïve pluripotency to rosette-stage pluripotency. Our focus in this chapter was to obtain mechanistic insight into the regulation of this pluripotent state transition by WNT signals. Therefore, we set out to identify and characterize the transcription factor complexes that mediate the effects of WNT signals in these states.

Chapter 5 presents an exploratory study that identifies downstream targets of the pluripotency signaling pathways regulating the naïve-rosette transition. We identify possible synergies in targets between signaling pathways which may highlight key players in the transition. Moreover, we found a specific link between the MEK signaling pathway and the DNA hypomethylation observed in naïve pluripotency *in vitro.*

References

Avilion, A., Nicolis, S., Pevny, L., Perez, L., Vivian, N., & Lovell-Badge, R. (2003). Multipotent cell lineages in early mouse development depend on SOX2 function. *Genes Dev*, 17(1): 126-40.

Azuara, V., Perry, P., Sauer, S., Spivakov, M., Jorgensen, H., John, R., . . . Fisher, A. (2006). Chromatin signatures of pluripotent cell lines. *Nat Cell Biol*, 8(5): 532-8.

Bakre, M., Hoi, A., Mong, J., Koh, Y., Wong, K., & Stanton, L. (2007). Generation of multipotential mesendodermal progenitors from mouse embryonic stem cells via sustained Wnt pathway activation. *J. Biol. Chem.*, 282: 31703-31712.

Bao, S., Tang, F., Li, X., Hayashi, K., Gillich, A., Lao, K., & Surani, M. (2009). Epigenetic reversion of post-implantation epiblast to pluripotent embryonic stem cells. *Nature*, 1292-1295.

Bedzhov, I., & Zernicka-Goetz, M. (2014). Self-Organizing Properties of Mouse Pluripotent Cells Initiate Morphogenesis upon Implantation. *Cell*, 1032-1044.

Ben-Haim, N., Lu, C., Guzman-Ayala, M., Pescatore, L., Mesnard, D., Bischofberger, M., . . . Constam, D. (2006). The nodal precursor acting via activin receptors induces mesoderm by maintaining a source of its convertases and BMP4. *Dev Cell*, 11(3): 313-23.

Bernstein, B., Mikkelsen, T., Xie, X., Kamal, M., Huebert, D., Cuff, J., . . . Lander , E. (2006). A bivalent chromatin structure marks key developmental genes in embryonic stem cells. *Cell*, 125(2): 315-26.

Bertero, A., Madrigal, P., Galli, A., Hubner, N., Moreno, I., Burks, D., . . . Vallier, L. (2015). Activin/nodal signaling and NANOG orchestrate human embryonic stem cell fate decisions by controlling the H3K4me3 chromatin mark. *Genes Dev*, 29(7): 702-17.

Betschinger, J., Nichols, J., Dietmann, S., Corrin, P., Paddison, P., & Smith, A. (2013). Exit from pluripotency is gated by intracellular redistribution of the bHLH transcription factor Tfe3. *Cell*, 153(2): 335-47.

Biechele, S., Cockburn, K., Lanner, F., Cox, B., & Rossant, J. (2013). Porcn-dependent Wnt signaling is not required prior to mouse gastrulation. *Development*, 2961-71.

Bonnet, D., & Dick, JE. (1997). Human acute myeloid leukemia is organized as a hierarchy that originates from a primitive hematopoietic cell. *Nature Medicine*, 730-737.

Boroviak, T., Loos, R., Bertone, P., Smith, A., & Nichols, J. (2014). The ability of inner-cell-mass cells to self-renew as embryonic stem cells is acquired following epiblast specification. *Nat Cell Biol*, 516-528.

Brennan, J., Lu, C., Norris, D., Rodriguez, T., Beddington, R., & Robertson, E. (2001). Nodal signalling in the epiblast patterns the early mouse embryo. *Nature*, 411(6840): 965-9.

Brons, I., Smithers, L., Trotter, M., Rugg-Gunn, P., Sun, B., Chuva de Sousa Lopes, S., . . . Vallier, L. (2007). Derivation of pluripotent epiblast stem cells from mammalian embryos. *Nature*, 191-195.

Buecker, C., Srinivasan, R., Wu, Z., Calo, E., Acampora, D., Faial, T., . . . Wysocka, J. (2014). Reorganization of enhancer patterns in transition from naive to primed pluripotency. *Cell Stem Cell*, 14(6): 838-53.

Burdon, T., Stracey, C., Chambers, I., Nichols, J., & Smith, A. (1999). Suppression of SHP-2 and ERK signaling promotes self-renewal of mouse embryonic stem cells. *Dev. Biol*, 210: 30-43.

Cartwright, P., McLean, C., Sheppard, A., Rivett, D., Jones, K., & Dalton, S. (2005). LIF/STAT3 controls ES cell self-renewal and pluripotency by a Myc-dependent mechanism. *Development*, (132) 885-896.

Chambers, I., Colby, D., Robertson, M., Nichols, J., Lee, S., Tweedie, S., & Smith, A. (2003). Functional expression of cloning of Nanog, a pluripotency sustaining factor in embryonic stem cells. *Cell*, (113) 643-655.

Chen, B., Dodge, M., Tang, W., Lu, J., Ma, Z., Fan, C., . . . Lum, L. (2009). Small molecule-mediated disruption of Wnt-dependent signaling in tissue regeneration and cancer. *Nat Chem Biol*, 100-107.

Chen, H., Guo, R., Zhang, Q., Guo, H., Yang, M., Wu, Z., . . . Chen, L. (2015). Erk signaling is indispensable for genomic stability and self-renewal of mouse embryonic stem cells. *Proc. Natl. Acad. Sci. USA*, 112(44):E5936-43.

Chen, X., Xu, H., Yuan, P., Fang, F., Huss, M., Vega, V., . . . Ng, H. (2008). Integration of external signaling pathways with the core transcriptional network in embryonic stem cells. *Cell*, (133): 1106-1117.

Cheng, N., Chytil, A., Shyr, Y., Joly, A., & Moses, H. (2008). Transforming growth factor-beta signaling-deficient fibroblasts enhance hepatocyte growth factor signaling in mammary carcinoma cells to promote scattering and invasion. *Mol. Cancer Res.*, 6, 1521-1533.

Chia, N., Chan, Y., Feng, B., Lu, X., Orlov, Y., Moreau, D., . . . Ng, H. (2010). A genome-wide RNAi screen reveals determinants of human embryonic stem cell identity. *Nature*, 468(7321): 316-20.

Cinelli, P., Casanova, E., Uhlig, S., Lochmatter, P., Matsuda, T., Yokota, T., . . . Burki, K. (2008). Expression profiling in transgenic FVB/N embryonic stem cells overexpressing STAT3. *BMC Dev Biol*, 57.

Cole, M., Johnstone, S., Newman, J., Kagey, M., & Young, R. (2008). Tcf3 is an integral component of the core regulatory circuitry of embryonic stem cells. *Genes Dev*, 22: 746-55.

Dailey, L., Ambrosetti, D., Mansukhani, A., & Basilico, C. (2005). Mechanisms underlying differential responses to FGF signaling. *Cytokine & Growth Factor Reviews*, 233-247.

Davidson, K., Adams, A., Goodson, J., McDonald, C., Potter, J., Berndt, J., . . . Moon, R. (2012). Wnt/beta-catenin signaling promotes differentiation, not self-renewal, of human embryonic stem cells and is repressed by Oct4. *Proc. Natl. Acad. Sci. U.S.A.*, 109: 4485-4490.

Derynck, R., & Zhang, Y. (2003). Smad-dependent and Smad-independent pathways in TGF-beta family signalling. *Nature*, 425: 577-584.

Dhaliwal, N., Miri, K., Davidson, S., Tamim El Jarkass, H., & Mitchell, J. (2018). KLF4 Nuclear Export Requires ERK Activation and Initiates Exit from Naive Pluripotency. *Stem Cell Reports* , 10(4): 1308-1323.

Ding, L., Paszkowski-Rogacz, M., Winzi, M., Chakraborty, D., Theis, M., Singh, S., . . . Buchholz, F. (2015). Systems Analyses Reveal Shared and Diverse Attributes of Oct4 Regulation in Pluripotent Cells. *Cell Syst*, 1(2): 141-51.

Drukker, M., Tang, C., Ardehali, R., Rinkevich, Y., Seita, J., Lee, A., . . . Soen, Y. (2012). Isolation of primitive endoderm, mesoderm, vascular endothelial and trophoblast progenitors from human pluripotent stem cells. *Nat Biotechnol*, 30(6): 531-42.

Ellys Harrison, S., Sozen, B., Christodoulou, N., Kyprianou, C., & Zernicka-Goetz, M. (2017). Assembly of embryonic and extraembryonic stem cells to mimic embryogenesis in vitro. *Science*, 356: eaal1810.

Enver, T., Pera, M., Peterson, C., & Andrews , P. (2009). Stem cell states, fates, and the rules of attraction. *Cell Stem Cell*, 4(5): 387-97.

Evans, M., & Kaufman, M. (1981). Establishment in culture of pluripotential cells from mouse embryos. *Nature*, 154-156.

Farthing, C., Ficz, G., Ng, R., Chan, C., Andrews, S., Dean , W., . . . Reik, W. (2008). Global mapping of DNA methylation in mouse promoters reveals epigenetic reprogramming of pluripotency genes. *PLoS Genetics*.

Fazzio, T., Huff, J., & Panning, B. (2008). An RNAi screen of chromatin proteins identifies Tip60-p400 as a regulator of embryonic stem cell identity. *Cell*, 134: 162-74.

Felicia Basilicata, M., Frank, M., Solter, D., Brabletz, T., & Stemmler, M. (2016). Inappropriate cadherin switching in the mouse epiblast compromises proper signaling between the epiblast and the extraembryonic ectoderm during gastrulation. *Scientific Reports*, 6, article number 26562.

Festuccia, N., Osorno, R., Halbritter, F., Karwacki-Neisius, V., Navarro, P., Colby, D., . . . Chambers , I. (2012). Esrrb is a direct Nanog target gene that can substitute for Nanog function in pluripotent cells. *Cell Stem Cell*, 11(4): 477-90.

Fuentealba, L., Eivers, E., Ikeda, A., Hurtado, C., Kuroda, H., Pera, E., & De Robertis, E. (2007). Integrating Patterning Signals: Wnt/GSK3 Regulates the Duration of the BMP/Smad1 Signal. *Cell*, 131(5): 980-993.

Gafni, O., Weinberger, L., Mansour , A., Manor, Y., Chomsky, E., Ben-Yosef, D., . . . Hanna, J. (2013). Derivation of novel human ground state naive pluripotent stem cells. *Nature*, 504(7479): 282-6.

Gorkin, D., Leung, D., & Ren, B. (2014). The 3D genome in transcriptional regulation and pluripotency. *Cell Stem Cell*, 14: 762-75.

Gospodarowicz, D. (1974). Localization of a fibroblast growth factor and its effect alone and with hydrocortisone on 3T3 cell growth. *Nature* , 123-127.

Graf, U., Casanova, E., & Cinelli, P. (2011). The role of the Leukemia Inhibitory Factor (LIF) - Pathway in derivation and maintenance of murine pluripotent stem cells. *Genes*, 2(1): 280-297.

Guo, G., Yang, J., Nichols , J., Hall, J., Eyres, I., Mansfield, W., & Smith , A. (2009). Klf4 reverts developmentally programmed restriction of ground state pluripotency. *Development*, 1063-1069.

Hackett, J., & Surani, M. (2014). Regulatory principles of pluripotency: from the ground state up. *Cell Stem Cell*, 15: 416-30.

Hackett, J., Dietmann, S., Murakami, K., Down, T., Leitch, H., & Surani, M. (2013). Synergistic mechanisms of DNA demethylation during transition to ground-state pluripotency. *Stem Cell Reports*, 1(6): 518-31.

Hall, J., Guo, G., Wray, J., Eyres, I., Nichols, J., Grotewold, L., . . . Smith, A. (2009). Oct4 and LIF/Stat3 additively induce Kruppel Factors to sustain embryonic stem cell self-renewal. *Cell Stem Cell*, (5): 597-609.

Hanahan, D., & Weinberg, R. (2011). Hallmarks of cancer: the next generation. *Cell*, 144(5), pp. 646-74.

Hanna, J., Markoulaki, S., Mitalipova, M., Cheng, A., Cassady , J., Staerk, J., . . . Jaenisch, R. (2009). Metastable pluripotent states in NOD-mouse-derived ESCs. *Cell Stem Cell*, 4(6): 513-24.

Hayashi, K., Lopes, S., Tang, F., & Surani , M. (2008). Dynamic equilibrium and heterogeneity of mouse pluripotent stem cells with distinct functional and epigenetic states. *Cell Stem Cell*, 391-401.

Hayashi, K., Ohta, H., Kurimoto, K., Aramaki, S., & Saitou, M. (2011). Reconstitution of the mouse germ cell specification pathway in culture by pluripotent stem cells. *Cell*, 146(4): 519-32.

Hayflick L., & Moorhead PS. (1961). The serial cultivation of human diploid cell strains. *Exp Cell Res*, 585-621.

Hu, G., Kim, J., Xu, Q., Leng, Y., Orkin, S., & Elledge, S. (2009). A genome-wide RNAi screen identifies a new transcriptional module required for self-renewal. *Genes Dev*, 23(7): 837-48.

Huelsken, J., Vogel, R., Brinkmann, V., Erdmann, B., Birchmeier, C., & Birchmeier, W. (2000). Requirement for beta-catenin in anterior-posterior axis formation in mice. *J Cell Biol*, 148(3): 567-78.

Ishitani, T., Kishida, S., Hyodo-Miura, J., Ueno, N., Yasuda, J., Waterman , M., . . . Matsumoto, K. (2003). The TAK1-NLK mitogen-activated protein kinase cascade functions in the Wnt-5a/Ca(2+) pathway to antagonize Wnt/beta-catenin signaling. *Mol. Cell Biol.*, 23: 131-139.

James, D., Levine, A., Besser, D., & Hemmati-Brivanlou, A. (2005). TGF-beta/activin/nodal signaling is necessary for the maintenance of pluripotency in human embryonic stem cells. *Development*, 132: 1273-1282.

Joo, J., Choi, H., Kim, M., Zaehres, H., Tapia, N., Stehling, M., . . . Scholer, H. (2014). Establishment of a primed pluripotent epiblast stem cell in FGF4-based conditions. *Scientific Reports*.

Kagey, M., Newman, J., Bilodeau, S., Zhan, Y., Orlando, D., van Berkum, N., . . . Young, R. (2010). Mediator and cohesin connect gene expression and chromatin architecture. *Nature*, 467(7314): 430-5.

Kalkan, T., & Smith, A. (2014). Mapping the route from naive pluripotency to lineage specification. *Philos Trans R Soc Lond B Biol Sci*, 369: 20130540.

Kalkan, T., Olova, N., Roode, M., Mulas, C., Lee, H., Nett, I., . . . Smith, A. (2017). Tracking the embryonic stem cell transition from ground state pluripotency. *Development*, 144: 1221-34.

Kaufman-Francis, K., Ngee Goh, H., Kojima, Y., Studdert, J., Jones, V., Power, M., . . . Tam, P. (2014). Differential response of epiblast stem cells to Nodal and Activin signalling: a paradigm of early endoderm development in the embryo. *Phil. Trans. R. Soc. B.*, 369: 20130550.

Kelly, K., Ng, D., Jayakumaran, G., Wood, G., Koide, H., & Doble, B. (2011). Beta-catenin enhances Oct-4 activity and reinforces pluripotency through a TCF-independent mechanism. *Cell Stem Cell*, 214-227.

Kielman, M., Rindapaa, M., Gaspar, C., van Poppel, N., Breukel, C., van Leeuwen, S., . . . Fodde, R. (2002). Apc modulates embryonic stem-cell differentiation by controlling the dosage of beta-catenin signaling. *Nature Genetics*, 32: 594-605.

Kim, J., Woo, A., Chu, J., Snow, J., Fujiwara, Y., Kim, C., . . . Orkin, S. (2010). A Myc network accounts for similarities between embryonic stem and cancer cell transcription programs. *Cell*, 313-324.

Kim, K., Doi, A., Wen , B., Ng, K., Zhao, R., Cahan , P., . . . Daley, G. (2010). Epigenetic memory in induced pluripotent stem cells. *Nature*, 285-290.

Komiya, Y., & Habas, R. (2008). Wnt signal transduction pathways. *Organogenesis*, 68-75.

Krupa, M., Mazur, E., Szczepanska, K., Filimonow, K., Maleszewski, M., & Suwinska, A. (2014). Allocation of inner cells to epiblast vs primitive endoderm in the mouse embryo is biased but not determined by the round of asymmetric divisions (8->16- and 16->32-cells). *Dev Biol*, 136-148.

Kunath, T., Saba-El-Leil, M., Almousailleakh, M., Wray, J., Meloche, S., & Smith, A. (2007). FGF stimulation of the Erk1/2 signalling cascade triggers transition of pluripotent embryonic stem cells from self-renewal to lineage commitment. *Development*, 2895-2902.

Kurayoshi, M., Yamamoto, H., Izumi, S., & Kikuchi, A. (2007). Post-translational palmitoylation and glycosylation of Wnt-5a are necessary for its signalling. *Biochemical Journal*, 515-523.

Kurek, D., & ten Berge, D. (2012). The signaling requirements for mouse embryonic stem cells. *Cell Cycle*, 207-208.

Lanner, F., & Rossant, J. (2010). The role of FGF/Erk signaling in pluripotent cells. *Development*, 3351-3360.

Li, M., & Belmonte, J. (2017). Ground rules of the pluripotency gene regulatory network. *Nature Reviews Genetics*, 18: 180-91.

Li, M., Liu, G., & Izpisua Belmonte, J. (2012). Navigating the epigenetic landscape of pluripotent stem cells. *Nat Rev Mol Cell Biol*, 13: 524-35.

Li, Z., Wang, Z., Zheng, Y., Xu, B., Scadden, D., & Han, Z. (2005). Kinetic expression of platelet endothelial cell adhesion molecule-1 (PECAM-1/CD31) during embryonic stem cell differentiation. *J Cell Biochem*, 95(3): 559-70.

Lindsley, R., Gill, J., Kyba, M., Murphy, T., & Murphy , K. (2006). Canonical Wnt signaling is required for development of embryonic stem cell-derived mesoderm. *Development*, 133: 3787-3796.

Loh, K., & Lim, B. (2011). A precarious balance: pluripotency factors as lineage specifiers. *Cell Stem Cell*, 8: 363-369.

Lyashenko, N., Winter, M., Migliorini, D., Biechele, T., Moon, R., & Hartmann, C. (2011). Differential requirement for the dual functions of beta-catenin in embryonic stem cell self-renewal and germ layer formation. *Nat Cell Biol*, 753-761.

Ma, Y., Rosfjord, E., Huebert, C., Wilder, P., Tiesman, J., Kelly, D., & Rizzino, A. (1992). Transcriptional regulation of the murine k-FGF gene in embryonic cell lines. *Developmental Biology*, 45-54.

MacDonald, B., Tamai, K., & He, X. (2009). Wnt/beta-catenin signaling: components, mechanisms and diseases. *Developmental Cell*, 9-26.

Mak, W., Nesterova, T., de Napoles, M., Appanah, R., Yamanaka, S., Otte, A., & Brockdorff, N. (2004). Reactivation of the paternal X chromosome in early mouse embryos. *Science*, 303: 666-9.

Marks, H., Kalkan, T., Menafra , R., Denissov, S., Jones, K., Hofemeister, H., . . . Stunnenberg, H. (2012). The transcriptional and epigenomic foundations of ground state pluripotency. *Cell*, 590-604.

Marson, A., Levine, S., Cole, M., Frampton, G., Brambrink, T., Johnstone, S., . . . Young, R. (2008). Connecting microRNA genes to the core transcriptional regulatory circuitry of embryonic stem cells. *Cell*, 134(3): 521-533.

Martello, G., Sugimoto, T., Diamanti, E., Joshi, A., Hannah, R., Ohtsuka, S., . . . Smith, A. (2012). Esrrb is a pivotal target of the Gsk3/Tcf3 axis regulating embryonic stem cell self-renewal. *Cell Stem Cell*, 491-504.

Martin, G. (1981). Isolation of a pluripotent cell line from early mouse embryos cultured in medium conditioned by teratocarcinoma stem cells. *PNAS*, 7634-7638.

Massague, J. (1998). TGF-beta signal transduction. *Annu. Rev. Biochem.*, 67: 753-791.

Massague, J. (2000). How cells read TGF-beta signals. *Nat. Rev., Mol. Cell. Biol.*, 1: 169-178.

Massague, J., Seoane, J., & Wotton, D. (2005). Smad transcription factors. *Genes Dev.*, 134: 1023-34.

Masui, S., Nakatake, Y., Toyooka, Y., Shimosato, D., Yagi, R., Takahashi, K., . . . Niwa, H. (2007). Pluripotency governed by Sox2 via regulation of Oct3/4 expression in mouse embryonic stem cells. *Nat Cell Biol*, 9(6): 625-35.

Matsuda, T., Nakamura, T., Nakao, K., Arai, T., Katsuki, M., Heike, T., & Yokota, T. (1999). STAT3 activation is sufficient to maintain an undifferentiated state of mouse embryonic stem cells. *EMBO Journal*, 4261-4269.

Mekhoubad, S., Bock, C., de Boer, A., Kiskinis, E., Meissner, A., & Eggan, K. (2012). Erosion of dosage compensation impacts human iPSC disease modeling. *Cell Stem Cell*, 10(5): 595-609.

Minde, D., Anvarian, Z., Rudiger, S., & Maurice, M. (2011). Messing up disorder: how do missense mutations in the tumor suppressor protein APC lead to cancer? *Molecular Cancer*, 10-19.

Mitsui, K., Tokuzawa, Y., Itoh, H., Segawa, K., Murakami, M., Takahashi, K., . . . Yamanaka, S. (2003). The Homeoprotein Nanog Is Required for Maintenance of Pluripotency in Mouse Epiblast and ES Cells. *Cell*, 113: 631-642.

Morgani, S., Nichols, J., & Hadjantonakis, A. (2017). The many faces of Pluripotency: in vitro adaptations of a continuum of in vivo states. *BMC Developmental Biology*, 17:7.

Morris, S., Graham, S., Jedrusik, A., & Zernicka-Goetz, M. (2013). The differential response to Fgf signaling in cells internalized at different times influences lineage segregation in preimplantation mouse embryos. *Open Biol*.

Morris, S., Guo, Y., & Zernicka-Goetz, M. (2012). Developmental plasticity is bound by pluripotency and the Fgf and Wnt signaling pathways. *Cell Rep*, 756-765.

Morris, S., Guo, Y., & Zernicka-Goetz, M. (2012). Developmental plasticity is bound by pluripotency and the Fgf and Wnt signaling pathways. *Cell Rep*, 756-765.

Morris, S., Teo, R., Li, H., Robson , P., Glover , D., & Zernicka-Goetz, M. (2010). Origin and formation of the first two distinct cell types of the inner cell mass in the mouse embryo. *PNAS*, 6364-6369.

Mulas, C., Kalkan, T., & Smith, A. (2017). NODAL secures pluripotency upon embryonic stem cell progression from the ground state. *Stem Cell Reports*, 20: 1215-28.

Nichols, J., & Smith , A. (2009). Naive and primed pluripotent states. *Cell Stem Cell*, 487-492.

Nichols, J., Silva, J., Roode, M., & Smith, A. (2009). Suppression of Erk signallig promotes ground state pluripotency in the mouse embryo. *Development*, 3215-3222.

Nichols, J., Zevnik, B., Anastassiadis, K., Niwa, H., Klewe-Nebenius, D., Chambers, I., . . . Smith, A. (1998). Formation of pluripotent stem cells in the mammalian embryo depends on the POU transcription factor Oct4. *Cell*, 95(3): 379-91.

Niwa, H. (2007). Open conformation chromatin and pluripotency. *Genes Dev*, 2671-2676.

Niwa, H., Burdon, T., Chambers, I., & Smith, A. (1998). Self-renewal of pluripotent embryonic stem cells is mediated via activation of STAT3. *Genes Dev*, 2048-2060.

Niwa, H., Miyazaki, J., & Smith, A. (2000). Quantitative expression of Oct-3/4 defines differentiation, dedifferentiation or self-renewal of ES cells. *Nat. Genet.*, 24: 372-6.

Niwa, H., Ogawa, K., Shimosato, D., & Adachi, K. (2009). A parallel circuit of LIF signalling pathways maintains pluripotency of mouse ES cells. *Nature*, (460): 118-122.

Nusse, R., Brown, A., Papkoff, J., Scambler, P., Shackleford, G., McMahon, A., . . . Varmus, H. (1991). A new nomenclature for int-1 and related genes: the Wnt gene family. *Cell*, 231.

Ohtsuka, S., Nishikawa-Torikai, S., & Niwa, H. (2012). E-Cadherin Promotes Incorporation of Mouse Epiblast Stem Cells into Normal Development. *PLOS One*, 7(9): e45220.

Otero, J., Fu, W., Kan, L., Cuadra, A., & Kessler, J. (2004). Beta-catenin signaling is required for neural differentiation of embryonic stem cells. *Development*, 131: 3545-3557.

Pan, G., Tian, S., Nie, J., Yang, C., Ruotti, V., Wei, H., . . . Thomson, J. (2007). Whole-genome analysis of histone H3 lysine 4 and lysine 27 methylation in human embryonic stem cells. *Cell Stem Cell*, 1: 299-312.

Payer, B., de Sousa Lopes, C., Barton, S., Lee, C., Saitou, M., & Surani, M. (2006). Generation of stella-GFP transgenic mice: a novel tool to study germ cell development. *Genesis*, 44(2): 75-83.

Pereira, P., Dobreva, M., Maas, E., Cornelis, F., Moya, I., Umans, L., . . . Zwijsen, A. (2012). Antagonism of Nodal signaling by BMP/Smad5 prevents ectopic primitive streak formation in the mouse amnion. *Development*, 139: 3343-3354.

Rao, T., & Kuhl, M. (2010). An updated overview on Wnt signaling pathways. *Circulation Research*, 1798-1806.

Rappolee, D., Basilico, C., Patel, Y., & Werb, Z. (1994). Expression and function of FGF-4 in peri-implantation development in mouse embryos. *Development*, 2259-2269.

Rastan, S., & Robertson, E. (1985). X-chromosome deletions in embryo-derived (EK) cell lines associated with lack of X-chromosome inactivation. *J Embryol Exp Morphol*, 90: 379-88.

Rijsewijk, F., Schuermann, M., Wagenaar, E., Parren, P., Weigel, D., & Nusse, R. (1987). The Drosophila homolog of the mouse mammary oncogene int-1 is identical to the segment polarity gene wingless. *Cell*, 649-657.

Sato, N., Meijer, L., Skaltsounis, L., Greengard, P., & Brivanlou, A. (2004). Maintenance of pluripotency in human and mouse embryonic stem cells through activation of Wnt signaling by a pharmacological GSK-3-specific inhibitor. *Nat. Met.*, 10: 55-63.

Scholer, H., Hatzopoulos, A., Balling, R., Suzuku, N., & Gruss, P. (1989). A family of octamer-specific proteins present during mouse embryogenesis: evidence for germline-specific expression of an Oct factor. *EMBO J.*, 8: 2543-2550.

Shipony, Z., Mukamel, Z., Cohen, N., Landan, G., Chomsky, E., Zeliger, S., . . . Tanay, A. (2014). Dynamic and static maintenance of epigenetic memory in pluripotent and somatic cells. *Nature*, 513(7516): 115-9.

Shoni, M., Lui, K., Vavvas, D., Muto, M., Berkowitz, R., Vlahos, N., & Ng, S. (2014). Protein kinases and associated pathways in pluripotent states and lineage differentiation. *Curr Stem Cell Res Ther*, 9(5): 366-387.

Silva, J., Nichols, J., Theunissen , T., Guo, G., van Oosten, A., Barrandon, O., . . . Smith, A. (2009). Nanog is the gateway to the pluripotent ground state. *Cell*, 138(4): 722-37.

Smit, L., Baas, A., Kuipers, J., Korswagen, H., van de Wetering, M., & Clevers, H. (2004). Wnt activates the Tak1/Nemo-like kinase pathway. *J. Biol. Chem.*, 279: 17232-17240.

Smith, A. (2017). Formative pluripotency: the executive phase in a developmental continuum. *Development*, 144: 365-73.

Smith, A., Heath, J., Donaldson, D., Wong, G., Moreau, J., Stahl, M., & Rogers , D. (1988). Inhibition of pluripotential embryonic stem cell differentiation by purified polypeptides. *Nature*, 688-690.

Smith, Z., Chan , M., Mikkelsen, T., Gu, H., Gnirke, A., Regev , A., & Meissner , A. (2012). A unique regulatory phase of DNA methylation in the early mammalian embryo. *Nature*, 339-344.

Smith, Z., Chan, M., Humm, K., Karnik, R., Mekhoubad, S., Regev, A., . . . Meissner, A. (2014). DNA methylation dynamics of the human preimplantation embryo. *Nature*, 511(7511): 611-5.

Staal, F., & Clevers, H. (2000). Tcf/Lef transcription factors during T-cell development: unique and overlapping functions. *Hematol J*, 3-6.

Takagi, N., & Sasaki, M. (1975). Preferential inactivation of the paternally derived X chromosome in the extraembryonic membranes of the mouse. *Nature*, 256: 640-2.

Takahashi K., & Yamanaka S. (2006). Induction of pluripotent stem cells from mouse embryonic and adult fibroblast cultures by defined factors. *Cell*, 663-676.

Takao, Y., Yokota, T., & Koide, H. (2007). Beta-catenin up-regulates Nanog expression through interactions with Oct-3/4 in embryonic stem cells. *Biochem Biophys Res Commun*, 699-705.

Tam, P., & Loebel, D. (2007). Gene function in mouse embryogenesis: get set for gastrulation. *Nat. Rev. Genet.*, 8: 368-381.

ten Berge, D., Koole, W., Fuerer, C., Fish, M., Eroglu, E., & Nusse, R. (2008). Wnt signaling mediates self-organisation and axis formation in embryoid bodies. *Cell Stem Cell*, 3: 508-518.

ten Berge, D., Kurek, D., Blauwkamp, T., Koole, W., Maas, A., Eroglu, E., . . . Nusse, R. (2011). Embryonic stem cells require Wnt proteins to prevent differentiation to epiblast stem cells. *Nature Cell Biology*, 1070-1075.

Tesar, P., Chenoweth, J., Brook, F., Davies, T., Evans, E., Mack, D., . . . McKay, R. (2007). New cell lines from mouse epiblast share defining features with human embryonic stem cells. *Nature*, 196-199.

Thomson, J., Itskovitz-Eldor, J., Shapiro, S., Waknitz, M., Swiergiel, J., Marshall, V., & Jones, J. (1998). Embryonic stem cell lines derived from human blastocysts. *Science*, 282(5391): 1145-7.

Thomson, M., Liu, S., Zou, L., Smith, Z., Meissner, A., & Ramanathan, S. (2011). Pluripotency factors in embryonic stem cells regulate differentiation into germ layers. *Cell*, 145(6): 875-89.

Tropepe, V., Hitoshi, S., Sirard, C., Mak, T., Rossant, J., & van der Kooy, D. (2001). Direct neural fate specification from embryonic stem cells: a primitive mammalian neural stem cell stage acquired through a default mechanism. *Neuron*, 30: 65-78.

Vallier, L., Touboul, T., Chng, Z., Brimpari , M., Hannan, N., Millan, E., . . . Pedersen, R. (2009). Early cell fate decisions of human embryonic stem cells and mouse epiblast stem cells are controlled by the same signaling pathways. *PLoS One*, 4(6): e6082.

Wei, Z., Gao, F., Kim, S., Yang, H., Lyu, J., An, W., . . . Lu, W. (2013). Klf4 organizes long-range chromosomal interactions with the oct4 locus in reprogramming and pluripotency. *Cell Stem Cell*, 13(1): 36-47.

Weinberger, L., Ayyash, M., Novershtern, N., & Hanna, J. (2016). Dynamic stem cell states: naive to primed pluripotency in rodents and humans. *Nat Rev Mol Cell Biol*, 17: 155-69.

Williams, R., Hilton, D., Pease, S., Willson, T., Stewart, C., Gearing , D., . . . Gough, N. (1988). Myeloid leukemia inhibitory factor maintains the developmental potential of embryonic stem cells. *Nature*, 336(6200): 684-7.

Wilson, S., & Edlund, T. (2001). Neural induction: toward a unifying mechanism. *Nat. Neuroscience*, 4(4): 1161-1168.

Wray, J., Kalkan, T., Gomez-Lopez, S., Eckardt, D., Cook, A., Kemler, R., & Smith, A. (2011). Inhibition of glycogen synthase kinase-3 alleviates Tcf3 repression of the pluripotency network and increases embryonic stem cell resistance to differentiation. *Nat Cell Biol*, 13(7): 838-45.

Wu, C., Hoffman, J., Shy, B., Ford, E., Fuchs, E., Nguyen, H., & Merrill , B. (2012). Function of Wnt/beta-catenin in counteracting Tcf3 repression through the Tcf3-beta-catenin interaction. *Development*, 2118-2129.

Yeom, Y., Fuhrmann, G., Ovitt, C., Brehm, A., Ohbo, K., Gross, M., . . . Scholer, H. (1996). Germline regulatory element of Oct-4 specific for the totipotent cycle of embryonal cells. *Development*, 122: 881-94.

Yi, F., Pereira , L., Hoffman, J., Shy, B., Yuen, C., Liu, D., & Merrill, B. (2011). Opposing effects of Tcf3 and Tcf1 control Wnt stimulation of embryonic stem cell self-renewal. *Nat Cell Biol*, 762-770.

Yi, F., Pereira, L., & Merrill, B. (2008). Tcf3 functions as a steady-state limiter of transcriptional programs of mouse embryonic stem cell self-renewal. *Stem Cells*, 1951-1960.

Ying, Q., Nichols, J., Chambers, I., & Smith, A. (2003). BMP induction of Id proteins suppresses differentiation and sustains embryonic stem cell self renewal in collaboration with STAT3. *Cell*, 115: 281-292.

Ying, Q., Wray, J., Nichols, J., Batlle-Morera, L., Doble , B., Woodgett, J., . . . Smith, A. (2008). The ground state of embryonic stem cell self-renewal. *Nature*, 519-523.

Young, R. (2011). Control of the embryonic stem cell state. *Cell* , 144: 940-54.

Zhang, H., Jiao, W., Sun, L., Fan, J., Chen, M., Wang, H., . . . Hu, J. (2013). Intrachromosomal looping is required for activation of endogenous pluripotency genes during reprogramming. *Cell Stem Cell*, 13(1): 30-5.

Zhao, X., Han, X., Chew, J., Liu, J., Chiu, K., Choo, A., . . . Wei, C. (2007). Whole-genome mapping of histone H3 Lys4 and 27 trimethylations reveals distinct genomic compartments in human embryonic stem cells. *Cell Stem Cell*, 1(3): 286-98.

Chapter 2

Endogenous WNT Signals Mediate BMP-Induced and Spontaneous Differentiation of Epiblast Stem cells and Human Embryonic Stem Cells

Stem Cell Reports
Article
ISSCR
OPEN ACCESS

Endogenous WNT Signals Mediate BMP-Induced and Spontaneous Differentiation of Epiblast Stem Cells and Human Embryonic Stem Cells

Dorota Kurek,[1,2] Alex Neagu,[1,2] Melodi Tastemel,[1,2] Nesrin Tüysüz,[1,2] Johannes Lehmann,[1,2] Harmen J.G. van de Werken,[2] Sjaak Philipsen,[2] Reinier van der Linden,[1,2] Alex Maas,[2] Wilfred F.J. van IJcken,[3] Micha Drukker,[4] and Derk ten Berge[1,2,*]
[1]Erasmus MC Stem Cell Institute, Erasmus MC, Wytemaweg 80, 3015 CN Rotterdam, the Netherlands
[2]Department of Cell Biology, Erasmus MC, Wytemaweg 80, 3015 CN Rotterdam, the Netherlands
[3]Erasmus MC Center for Biomics, Erasmus MC, Wytemaweg 80, 3015 CN Rotterdam, the Netherlands
[4]Institute of Stem Cell Research, German Research Center for Environmental Health, Helmholtz Center Munich, Ingolstädter Landstraße 1, 85764 Neuherberg, Germany
*Correspondence: d.tenberge@erasmusmc.nl
http://dx.doi.org/10.1016/j.stemcr.2014.11.007

SUMMARY

Therapeutic application of human embryonic stem cells (hESCs) requires precise control over their differentiation. However, spontaneous differentiation is prevalent, and growth factors induce multiple cell types; e.g., the mesoderm inducer BMP4 generates both mesoderm and trophoblast. Here we identify endogenous WNT signals as BMP targets that are required and sufficient for mesoderm induction, while trophoblast induction is WNT independent, enabling the exclusive differentiation toward either lineage. Furthermore, endogenous WNT signals induce loss of pluripotency in hESCs and their murine counterparts, epiblast stem cells (EpiSCs). WNT inhibition obviates the need to manually remove differentiated cells to maintain cultures and improves the efficiency of directed differentiation. In EpiSCs, WNT inhibition stabilizes a pregastrula epiblast state with novel characteristics, including the ability to contribute to blastocyst chimeras. Our findings show that endogenous WNT signals function as hidden mediators of growth factor-induced differentiation and play critical roles in the self-renewal of hESCs and EpiSCs.

INTRODUCTION

Pluripotent stem cells can generate all cell types of the body and hold great potential for transplantation medicine and the study of early development. Pluripotency arises in the inner cell mass of blastocyst-stage embryos during formation of the epiblast, and both human and mouse blastocysts can give rise to pluripotent embryonic stem cells (ESCs). Differentiation of the pluripotent epiblast toward the primary germ layers occurs after implantation of the embryo during the process of gastrulation. Signaling proteins belonging to the BMP and WNT families are key gastrulation factors that mediate induction of the primitive streak in the embryo and can induce primitive streak derivatives in human ESCs (hESCs) and mouse ESCs (mESCs) (Bakre et al., 2007; Blauwkamp et al., 2012; Davidson et al., 2012; Drukker et al., 2012; Gadue et al., 2006; Lako et al., 2001; Lindsley et al., 2006; Nostro et al., 2008; Sumi et al., 2008; ten Berge et al., 2008). However, BMP4 additionally induces trophoblast (Drukker et al., 2012; Xu et al., 2002), complicating efforts to obtain single lineages. Furthermore, other reports show that both BMP and WNT signals support the self-renewal of mESCs instead (Hao et al., 2006; Ogawa et al., 2006; Singla et al., 2006; ten Berge et al., 2011; Ying et al., 2003). These conflicting reports may reflect the action of BMP and WNT signals on different pluripotent states, as the epiblast of post implantation mouse embryos can also give rise to a pluripotent cell type, the epiblast stem cell (EpiSC) (Brons et al., 2007; Tesar et al., 2007). EpiSCs are developmentally more advanced than mESCs and possess different morphology, growth factor requirements, gene expression profile, and epigenetic state (Brons et al., 2007; Tesar et al., 2007). They can generate teratomas, a measure of pluripotency, but unlike mESCs are not competent to contribute to blastocyst chimeras.

EpiSCs express many differentiation factors present in the primitive streak (Brons et al., 2007; Tesar et al., 2007) and were found to comprise heterogeneous populations of cells with distinct potency (Bernemann et al., 2011; Tsakiridis et al., 2014). This suggests that EpiSCs are to some extent prespecified, and their pluripotent state has therefore been designated "primed," as opposed to the unspecified "naïve" pluripotent state of mESCs (Nichols and Smith, 2009). Similar observations were made for hESCs, consistent with them occupying a primed pluripotent state (Blauwkamp et al., 2012; Davidson et al., 2012; Drukker et al., 2012; Stewart et al., 2006). Interestingly, for both EpiSCs and hESCs, it has been shown that endogenous WNT proteins, produced by the cells themselves, drive prespecification of the cells (Blauwkamp et al., 2012; Frank et al., 2012; Sumi et al., 2013; Tsakiridis et al., 2014).

Here we address the consequences of endogenous WNT signals for directed differentiation and self-renewal of human and mouse pluripotent cells. We show that

endogenous WNT signals mediate differentiation decisions in response to BMP signals and furthermore that they are the main cause of spontaneous differentiation in both hESCs and EpiSCs.

RESULTS

BMP4-Induced Differentiation of EpiSCs Is Mediated by WNT Signals

Both WNT and BMP signals are implicated in the initiation of gastrulation and induction of the primitive streak. To monitor these processes in vitro, we established EpiSCs carrying the T-GFP reporter for the primitive streak marker *Brachyury* by differentiating T-GFP ESCs (Fehling et al., 2003) into EpiSCs by culture in FGF2 and ACTIVIN. We included IWP2, a small molecule inhibitor that blocks the biosynthesis of mature WNT proteins (Chen et al., 2009), to increase the efficiency of differentiation (ten Berge et al., 2011). Phenotypic and functional assays verified the complete differentiation (Figures S1A–S1D available online).

Treatment of the T-GFP EpiSCs with either WNT3A or BMP4, in the presence of ACTIVIN and FGF2, strongly induced reporter expression, followed by loss of the pluripotency marker SSEA1 (Figure 1A). However, in the BMP4-treated cells, these events were delayed, possibly because BMP4 may act indirectly, by inducing WNT signals in EpiSCs (Figure 1A). Indeed, BMP4 protein strongly induced a reporter for WNT signaling in Axin2-LacZ EpiSCs (ten Berge et al., 2011) (Figure 1B). This was due to the induction of endogenous WNT proteins as reporter expression was inhibited by IWP2 (Figure 1B). Importantly, IWP2 prevented not only the induction of T-GFP but also the loss of SSEA1 in response to BMP4 (Figure 1A), suggesting that BMP4-mediated exit from pluripotency requires the activation of WNT. Indeed, while both WNT3A and BMP4 induced expression of differentiation markers and loss of EpiSC markers, IWP2 prevented the gain or loss of these markers in response to BMP4, demonstrating that it relied on the induction of WNT signals (Figures 1C and S1E). IWP2 did not interfere with WNT signal transduction or differentiation per se since it did not block the effects of WNT3A (Figure S1F).

We used RNA-Seq to analyze the interactions between BMP4 and WNT in EpiSCs treated for 48 hr in the presence of ACTIVIN and FGF2. Principal component analysis showed that the BMP4- and/or WNT3A-treated samples separated from all other samples along the first component, whereas the IWP2-treated samples clustered together, regardless of the presence of BMP4 (Figure 1D). Interestingly, the WNT3A-treated samples clustered together with the BMP4-treated sample and induced the same mesodermal markers, such as *Kdr*, *Mesp1*, and *Tbx6* (Figures 1D and 1E). BMP4 was unable to induce these markers in the presence of IWP2 despite inducing the canonical BMP target *Id1*, showing that IWP2 did not interfere with BMP signal transduction (Figure 1E). These data show that the gene-expression changes induced by BMP4 in EpiSCs are to a large extent secondary to activation of WNT proteins.

Feedback loops between signaling factors are an important element of gastrulation (Ben-Haim et al., 2006; Tortelote et al., 2013). We therefore analyzed the short-term (2–6 hr) induction of the gastrulation factors *Nodal*, *Wnt3*, and *Fgf8* by BMP4 and/or WNT3A. While BMP4 induced *Wnt3*, WNT3A induced all three factors, and the highest induction of *Wnt3* was obtained using both signals (Figure 1F). These observations explain why BMP signals are not required for primitive streak induction once WNT signals have been activated. No induction of the WNT target *Axin2* by BMP4 or the BMP-target *Id1* by WNT3A was observed within the 6 hr timeframe (Figure 1F). However, *Id1* is somewhat induced in the 48 hr WNT3A-only condition, suggesting that the differentiating cells activate endogenous BMP signals (Figure 1E). Nonetheless, T-GFP induction was not suppressed by the BMP inhibitor LDN193189, indicating that it did not require BMP signals (Figure 1A). Finally, IWP2 prevented the loss of both OCT4- and SOX2-positive as well as SSEA1-positive EpiSCs in response to BMP4 (Figures 1G and S1G). Combined, these data indicate that induction of EpiSC differentiation by BMP4 is mediated by the induction of WNT signals.

Endogenous WNT Proteins Induce Differentiation and Loss of Pluripotency in EpiSCs

In the course of our studies, we found that T-GFP EpiSCs spontaneously induced a significant GFP-positive population (Figure 1A, +vehicle). This induction was suppressed either by IWP2 or by the WNT antagonist FZ8CRD, a soluble domain of the WNT receptor that binds and sequesters WNT proteins, indicating that it was due to endogenous WNT proteins (Figure 1A). The presence of endogenous WNT activity was further confirmed by the spontaneous LACZ activity evident in Axin2-LacZ EpiSCs, which was also suppressed by IWP2 (Figure 1B). Moreover, multiple *Wnt* genes were expressed in EpiSCs, in particular *Wnt3* (Figure S2A). These observations are in line with a recent report showing that endogenous WNT signals specify a fraction of EpiSCs toward primitive-streak lineages (Tsakiridis et al., 2014). Clonal assays showed that these specified cells were not committed to differentiation and maintained a pluripotent phenotype (Tsakiridis et al., 2014).

However, we noticed that the GFP-positive cells showed a shift to lower SSEA1 expression, suggesting that some of them lost pluripotency (Figure 1A). We therefore sorted the cells based on T-GFP intensity and assessed their potential to establish colonies or to form embryoid bodies (EBs), both measures of pluripotency. A clear negative correlation

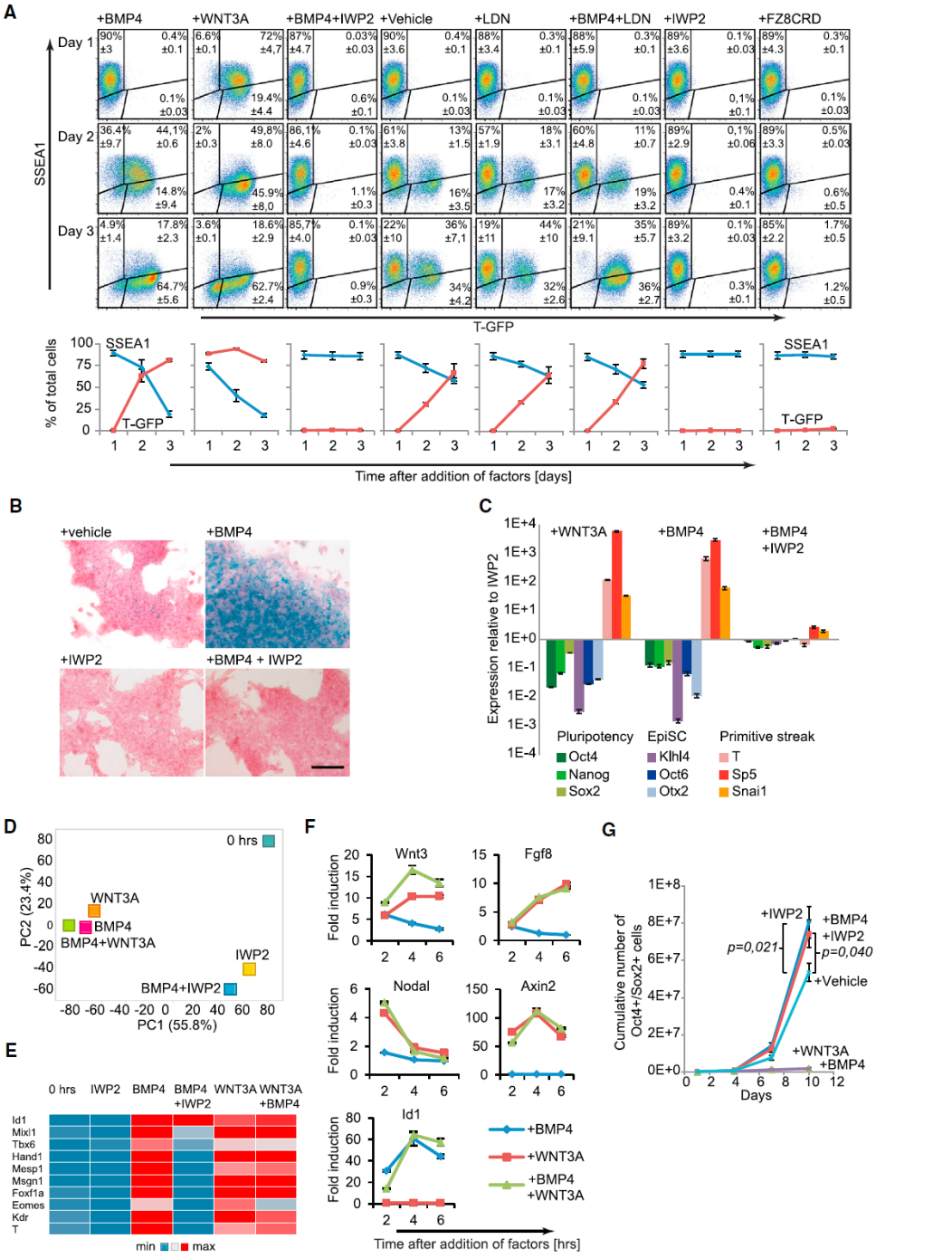

(legend on next page)

was visible between the level of GFP and potential to establish NANOG-positive colonies (Figures 2A, S2B, and S2C). Likewise, cells with higher levels of GFP produced smaller EBs, while the cells with the highest level failed to form EBs at all (Figures 2B and S2D). Moreover, these cells downregulated SOX2 and OCT4 (Figure 2B). These data show that the T-GFP-positive population is enriched for cells that have lost pluripotency.

We next tested whether WNT inhibition would prevent this loss of pluripotency. When analyzed for SSEA1, multiple EpiSC lines all displayed substantial levels of SSEA1-negative cells, indicating significant differentiation (Figures 2C and S2E, vehicle). However, in the presence of IWP2, more than 90% of the cells expressed SSEA1 (Figures 2C and S2E). In addition, RT-PCR and immunostaining showed that IWP2 not only repressed primitive streak markers but also raised the level of the pluripotency markers *Oct4*, *Nanog*, and *Sox2* (Figures 2D and S1E). Moreover, IWP2 substantially enhanced the expansion of OCT4- and SOX2-positive or SSEA1-positive cells (Figures 1G and S1G). In line with a recent report (Sumi et al., 2013), suppression of endogenous WNT signals also greatly enhanced the derivation of novel EpiSC lines from 25% (four lines from 16 E5.5 embryos) to 79% (15 of 19). These data show that endogenous WNT signals induce loss of pluripotency in a subset of EpiSCs, and WNT inhibition suppresses this spontaneous differentiation, greatly enhancing their self-renewal and derivation efficiency. In fact, certain cell lines, e.g., the T-GFP EpiSCs, could essentially not be maintained in the absence of IWP2 as they progressively accumulated differentiated cells (Figure 1A, +vehicle).

To identify the differentiation pathways induced by endogenous WNT signals we compared the transcriptomes of EpiSCs maintained in the presence or absence of IWP2. Most differences were due to a set of genes that was repressed by IWP2 (Figure 2E), with 321 genes downregulated and 87 genes upregulated in response to IWP2 (Table S1). Using gene set enrichment analysis (Subramanian et al., 2005), we found that a set of 29 genes first expressed around the start of gastrulation (Pfister et al., 2007) was strongly enriched in conventional EpiSCs when compared with EpiSCs treated with IWP2 (Figure 2F; Table S2). We next looked for signatures of more committed cell types that derive from the primitive streak. A set of 98 genes expressed in committed human- and mouse-definitive endoderm and endoderm precursors (Hou et al., 2007; McLean et al., 2007; Ogaki et al., 2011; Tada et al., 2005) was highly enriched in conventional EpiSCs (Figure 2F; Table S3). Since some of these genes are also expressed in mesoderm progenitors, we created a gene set consisting of 154 genes specifically expressed in E7.5 endoderm versus mesoderm and ectoderm (Gu et al., 2004) and found strong enrichment of this set in conventional EpiSCs (Figure 2F; Table S4). Furthermore, a panel of genes associated with the committed endoderm state showed consistent repression in response to IWP2 (Figure 2G). In contrast, a set of 155 genes expressed in E7.5 mesoderm and ectoderm versus endoderm (Gu et al., 2004) showed no enrichment (Figure 2F; Table S5) and committed mesoderm markers such as *Mesp1*, *Meox1*, *Kdr*, *Hand1*, *Msgn1*, *Foxf1a*, *Tlx2*, or *Tbx6* ranked low in the comparison (Table S5). Anterior neurectoderm genes did not increase in response to IWP2 (Figure S2F), indicating that endogenous WNT signals were not required to inhibit neural differentiation. These findings show that endogenous WNT signals induce a committed definitive endoderm state in a subset of EpiSCs, explaining the loss of pluripotency in response to endogenous WNT signals.

WNT Inhibition Maintains EpiSCs in a Pregastrula Epiblast Stage

Despite their origin from the pregastrula epiblast, transcriptome comparisons indicate that EpiSCs are more similar to the late-gastrula-stage epiblast (Kojima et al., 2014). To test whether WNT inhibition maintains EpiSCs in a state closer to that of the pregastrula epiblast, we compared their transcriptomes with those of epiblasts derived from embryos ranging from the cavity (Cav) stage to the prestreak (PS),

Figure 1. BMP4-Induced Differentiation of EpiSCs Depends on WNT Signals

(A) Flow cytometry plots of T-GFP EpiSCs treated with the indicated factors and analyzed for T-GFP and SSEA1. The cells were maintained in the presence of IWP2 prior to the experiment. Line plots indicate the mean of three independent experiments ± SEM.

(B) Axin2-LacZ EpiSCs treated for 3 days with the indicated factors and stained for LACZ (blue).

(C) RT-PCR gene expression profiles of GFP9 EpiSCs treated for 2 days with the indicated factors, plotted relative to EpiSCs maintained in the presence of IWP2 (n = 3, mean ± SEM).

(D) Principal component analysis of transcriptomes of GFP9 EpiSCs treated for 48 hr with the indicated factors or untreated (0 hr). The percentage of variance explained by the principal components is indicated between parentheses.

(E) Heat map of selected gene expression levels in GFP9 EpiSCs treated for 48 hr with the indicated factors, determined by RNA-Seq.

(F) Time course RT-PCR analysis of indicated genes in GFP9 EpiSCs following treatment with the indicated factors (n = 3, mean ± SEM).

(G) Plot showing the expansion of OCT4- and SOX2-positive 129S2C1a EpiSCs in the indicated conditions (three independent experiments, mean ± SEM).

The scale bar represents 200 μm. See also Figure S1.

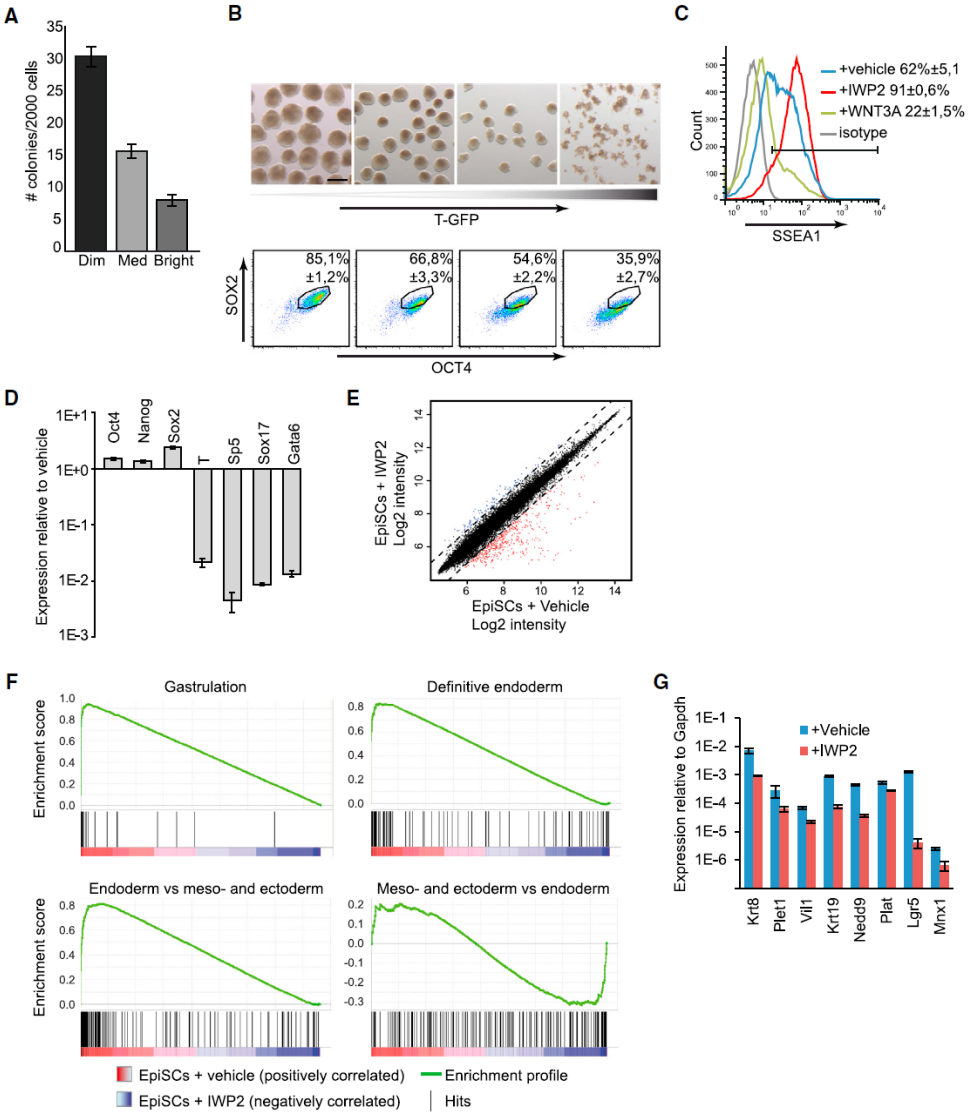

Figure 2. Endogenous WNT Proteins Induce Loss of Pluripotency in EpiSCs

(A) T-GFP EpiSCs were sorted into three categories based on GFP and assayed for their ability to establish NANOG-positive colonies (three independent experiments, mean ± SEM).

(B) T-GFP EpiSCs were sorted into four categories based on GFP and assayed for their ability to establish EBs (top) or analyzed by flow cytometry for SOX2 and OCT4 (bottom, three independent experiments, mean ± SEM).

(C) Flow cytometry histogram showing T-GFP EpiSCs treated for 3 days with the indicated factors and analyzed for SSEA1 (three independent experiments, mean ± SEM).

(D) Real-time RT-PCR gene expression profiles of 129S2C1a EpiSCs cells treated for 3 days with IWP2, plotted relative to untreated EpiSCs (three independent experiments, mean ± SEM).

(E) Scatter plot comparing the global gene expression levels of GFP9 EpiSCs cultured in the presence or absence of IWP2. The dotted lines delineate the boundaries of 2-fold difference in gene expression levels. Genes expressed more than 2-fold higher or lower in the presence of IWP2 are plotted in blue or red, respectively.

(legend continued on next page)

late mid streak (LMS), late streak (LS), no bud (OB), early bud (EAB), and late bud (LB) stage, obtained using Illumina bead-chip arrays (Kojima et al., 2014). A normalization procedure matched the distribution of the expression values from our Affymetrix to the Illumina platform, and the genes that were at least 1.5-fold differentially expressed in response to IWP2 (1,066 gene identifications shared between both platforms) were analyzed using principal component analysis. As observed before (Kojima et al., 2014), the first component separated the embryo-derived samples from the EpiSCs, whereas the second component separated the embryo-derived samples according to their developmental stage (Figure 3A). Importantly, while the regular EpiSCs aligned at the early bud stage, EpiSCs maintained in the presence of IWP2 aligned between the prestreak and early-streak stages, showing that their transcriptome is indeed more similar to that of the pregastrula epiblast (Figure 3A).

We tested the pregastrula state of EpiSCs maintained with IWP2 using two functional assays. First, a small percentage of EpiSCs can revert to the ESC state when transferred to ESC conditions (Greber et al., 2010), and we found that IWP2 treatment strongly raised this reversal efficiency (Figure 3B). This indicates that IWP2 caused many more cells to occupy a state of pluripotency sufficiently close to that of ESCs to make the transition. Second, in contrast to epiblast from the gastrula, the pregastrula epiblast can contribute to chimeras upon blastocyst injection (Gardner et al., 1985). However, EpiSCs rarely contribute to blastocyst chimeras but rather, corresponding to their late-gastrula stage character, can integrate when introduced into the primitive streak (Huang et al., 2012; Kojima et al., 2014). We derived EpiSCs from E6.5 transgenic embryos carrying either a Rosa26-LacZ or Actin-GFP reporter in the presence of IWP2, cultured the cells for five passages, and performed blastocyst injections. We obtained 3 chimeras out of 14 E10.5 embryos from the Rosa26-LacZ EpiSCs, and 1 chimera out of 14 embryos from the Actin-GFP-derived EpiSC line GFP9 (Figure 3C). X-gal and immunostainings demonstrated integration into multiple tissues, including the neural tube, somite, nephrogenic cord, body wall, splanchnopleure, and parts of the gut tube (Figure S3A). Together, these tests strongly support the pregastrula character of EpiSCs shielded from WNT signals. Moreover, they indicate that the ability to contribute to blastocyst chimeras does not distinguish naive from primed pluripotent cells.

We considered several explanations for the blastocyst compatibility of IWP2-treated EpiSCs. First, some cells may be reprogrammed to the naive state. However, IWP2 induced no increase in *Tbx3*, *Dppa3*, *Zfp42*, *Klf4*, *Dppa5*, or other naive markers (Figure 3D; Table S1). Second, IWP2 may stabilize a minor fraction of EpiSCs that contributes to blastocyst chimeras, marked by the Oct4-GFP reporter GOF18 (Han et al., 2010). IWP2 did however not enhance the GFP-positive fraction and sorted GFP-positive cells lost GFP expression regardless of the presence of IWP2 (Figures S3B and S3C). Third, E-CADHERIN overexpression allows EpiSCs to participate in blastocyst chimeras (Ohtsuka et al., 2012). We observed higher *E-cadherin* expression and strong E-CADHERIN staining throughout the cultures in the presence of IWP2, similar in strength as in ESCs, whereas staining was faint and patchy in regular EpiSCs (Figures 3E and 3F). Furthermore, WNT3A induced the *E-cadherin* repressor *Snai1* and *N-cadherin* and downregulated *E-cadherin* in EpiSCs (Figure 3G). These observations indicate that endogenous WNT proteins repress *E-cadherin* in EpiSCs, thereby reducing their ability to integrate in the pregastrulation epiblast.

WNT inhibition repressed multiple differentiation genes, including *Eomes*, *Foxa2*, *Gata6*, *Lefty2*, and *Sox17*, to the same level as in ESCs, indicating that they are not EpiSC markers (Figure 3D). We screened our gene expression data for potential markers for genuine EpiSCs, maintained in the presence of WNT inhibition (Figure 3H), and identified CD38, CD107/KIT, CD105/ENDOGLIN, and CD44 as cell surface markers suitable to separate ESCs and EpiSCs by flow cytometry (Figure 3I) and OCT6 as a nuclear marker for genuine EpiSCs (Figure 3J).

Next, we addressed whether the differentiation-inducing effect of WNT on EpiSCs explains the conflicting reports on the role of WNT in ESCs. While we previously demonstrated that endogenous WNT signals support ESC self-renewal by inhibiting their differentiation into EpiSCs (ten Berge et al., 2011), we and others also demonstrated that WNT signals induce differentiation of ESCs in EBs (Nostro et al., 2008; ten Berge et al., 2008). However, a transient EpiSC signature has been detected in differentiating EBs (Zhang et al., 2010). This could be the result of a shutdown of the WNT pathway in EBs, which would induce differentiation of ESCs into EpiSCs. When we generated EBs from ESCs carrying the 7xTcf-GFP reporter for WNT signaling (ten Berge et al., 2008), we observed rapid downregulation of the WNT reporter, followed by loss of the ESC

(F) Gene set enrichment analysis plots demonstrating the enrichment of the indicated gene sets in EpiSCs cultured in the absence versus the presence of IWP2.
(G) RT-PCR analysis for definitive endoderm genes in EpiSCs, in response to IWP2 (three biological replicates using 129S2C1a, Axin2LacZ, and GFP9 EpiSCs, mean ± SEM).
Scale bar represents 200 μm. See also Figure S2.

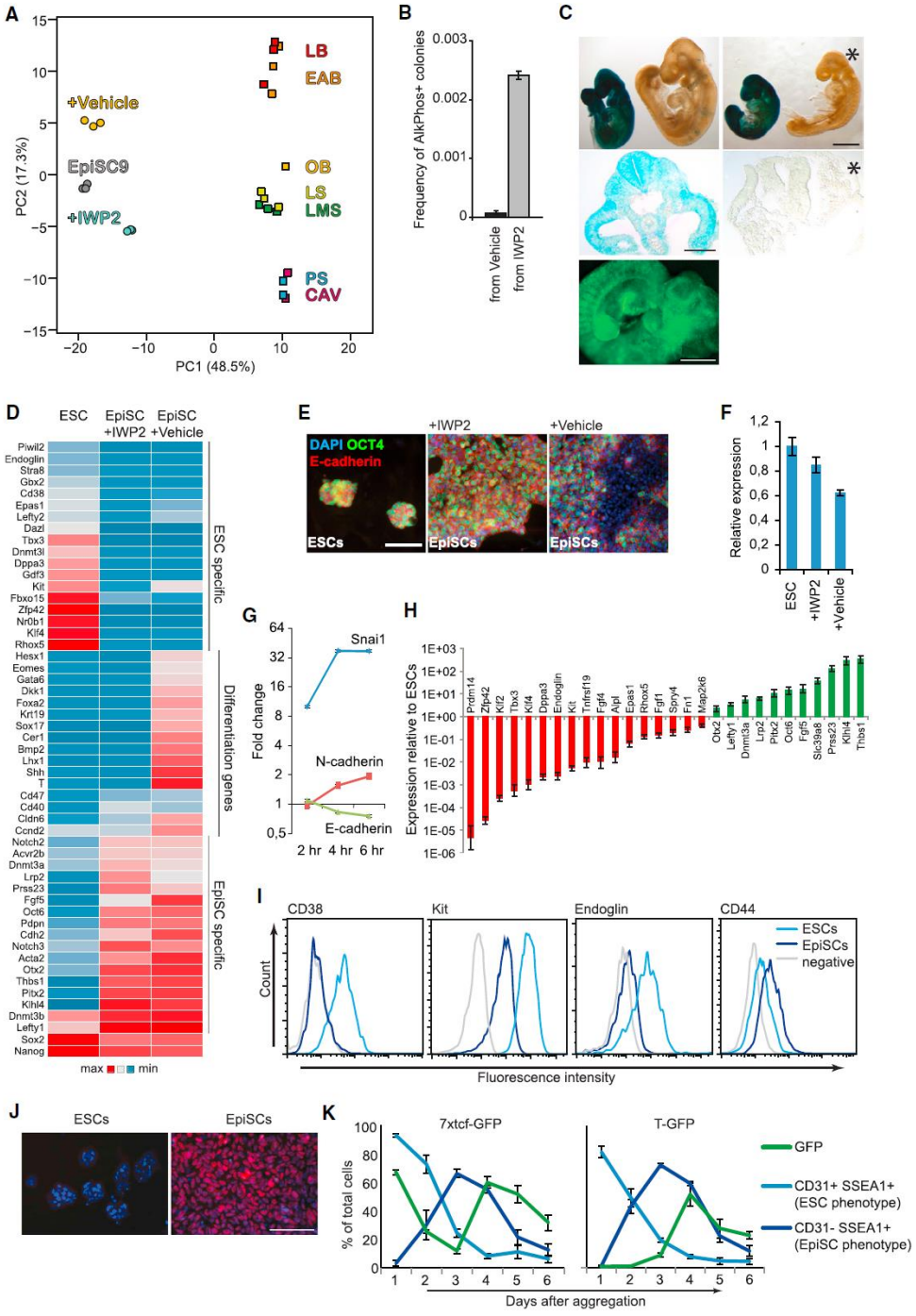

(legend on next page)

marker CD31 (Figure 3K). However, the cells maintained expression of the pluripotency marker SSEA1, suggesting they converted into EpiSCs. Following this transition, the WNT reporter was induced while SSEA1 was lost (Figure 3K), suggesting that endogenous WNTs now acted as differentiation signals. Indeed, using T-GFP ESCs, we observed induction of the differentiation reporter following the transition of the ESCs into EpiSCs (Figure 3K). Thus, EBs first mediate the conversion of ESCs into EpiSCs; only then are endogenous WNT signals activated that induce their differentiation.

Inhibition of Endogenous WNT Signals Prevents the Accumulation of Differentiated Cells in hESC Cultures

It is thought that hESCs occupy a state of primed pluripotency like that of mouse EpiSCs, rather than the naive pluripotency of mESCs (Nichols and Smith, 2009). hESC cultures experience substantial spontaneous differentiation and require frequent manual removal of accumulations of differentiated cells. We investigated whether commitment to differentiation could be prevented by inhibition of endogenous WNT signals, similar to what we showed for EpiSCs.

In the presence of IWP2 or FZ8CRD, both H1 and H9 hESCs established flatter, sharper edged colonies with very little evidence of differentiated cells, whether cultured on mouse embryo fibroblasts (MEFs) or in mTESR1, a serum- and feeder-free medium (Figures 4A and S4A). When cultured in standard conditions, both H1 and H9 hESCs formed patches of BRACHYURY- and GATA4-positive cells (Figures S4B and S4C), and significant proportions of the cells lacked NANOG, OCT4, or SOX2 (Figures 4B and S4D). In contrast, no BRACHYURY or GATA4 was visible when the cells were cultured in the presence of IWP2 (Figures S4B and S4C), and the proportion of cells lacking the pluripotency factors was strongly reduced (Figures 4B and S4D). A recently introduced defined medium, E8, performed better yet IWP2 significantly improved the proportion of cells expressing the pluripotency factors (Figure 4B). RT-PCR analysis confirmed that IWP2 repressed multiple markers of mesendodermal differentiation and enhanced expression of pluripotency markers, while neurectodermal markers either showed minor changes or were downregulated (Figures 4C and S4E). These data suggest that WNT inhibition prevents the spontaneous mesendodermal differentiation of hESCs, while not increasing neurectodermal differentiation.

We next tested whether WNT inhibition obviated the need for manual removal of differentiated cells during routine culture of hESCs. With manual cleaning, both H1 and H9 hESCs maintained persistent populations of cells lacking one or more of the pluripotency factors, while in the absence of cleaning this population progressively increased (Figures 4D, S4F, and S4H). Strikingly, IWP2 maintained pluripotency factor expression in most cells in the absence of cleaning (Figures 4D, S4F, and S4H). Furthermore, IWP2 prevented the accumulation of cells expressing the hESC differentiation marker SSEA1, which otherwise rapidly accumulated (Figures 4E, S4G, and S4H). Finally, both H1 and H9 cells cultured for 10 passages in IWP2 efficiently formed teratomas, indicating that they retained their pluripotency (Figure S4I). Combined, these

Figure 3. WNT Inhibition Maintains EpiSCs in a Pregastrula Epiblast Stage

(A) Transcriptomes from primary epiblasts dissected from embryos ranging from cavity to late bud stages and from the EpiSC line EpiSC9 were obtained from GEO (GSE46227) and combined with six microarray gene expression data sets from GFP9 EpiSCs cultured with and without IWP2 and analyzed by principal component analysis. The percentage of variance explained by the principal components is indicated between parentheses.

(B) Reversal efficiency of T-GFP EpiSCs. Prior to start of the reversal experiment, the cells were maintained in the presence or absence of IWP2 as indicated (n = 3, mean ± SEM).

(C) (Upper) X-gal stained chimeras derived from blastocyst injections of passage 5 Rosa26-LacZ EpiSCs. (Middle) Sections to indicate EpiSC contribution (blue). Asterisk indicates a nonchimeric littermate. (Lower) Chimera derived from blastocyst injections of passage 5 GFP9 EpiSCs. Green fluorescence indicates EpiSC contribution.

(D) Heat map of selected gene expression levels of ESCs and GFP9 EpiSCs cultured in the presence or absence of IWP2 and analyzed by microarray.

(E) E-CADHERIN and OCT4 immunofluorescence images of EpiSCs and ESCs.

(F) RT-PCR for *E-cadherin* in EpiSCs and ESCs (three biological replicates using 129S2C1a, Axin2LacZ, and GFP9 EpiSCs, mean ± SEM).

(G) Time course RT-PCR analysis of indicated genes in GFP9 EpiSCs following treatment with WNT3A (n = 3, mean ± SEM).

(H) Real-time RT-PCR gene expression analysis of FVB EpiSCs relative to ESCs for a range of genes found by microarray to be differentially expressed between EpiSCs and ESCs (n = 3, mean ± SEM).

(I) Flow cytometry histograms showing surface markers distinguishing ESCs (CD38, KIT, and ENDOGLIN) and EpiSCs (CD44).

(J) OCT6 immunostaining (red) of 129S2C1a EpiSCs and ESCs (blue, DAPI).

(K) The indicated ESC lines were aggregated into EBs and analyzed daily by flow cytometry for expression of reporter and the indicated cell surface markers (three independent experiments, mean ± SEM).

Scale bar represents 1 mm (C, embryos), 200 μm (C, section), 100 μm (E and J). See also Figure S3.

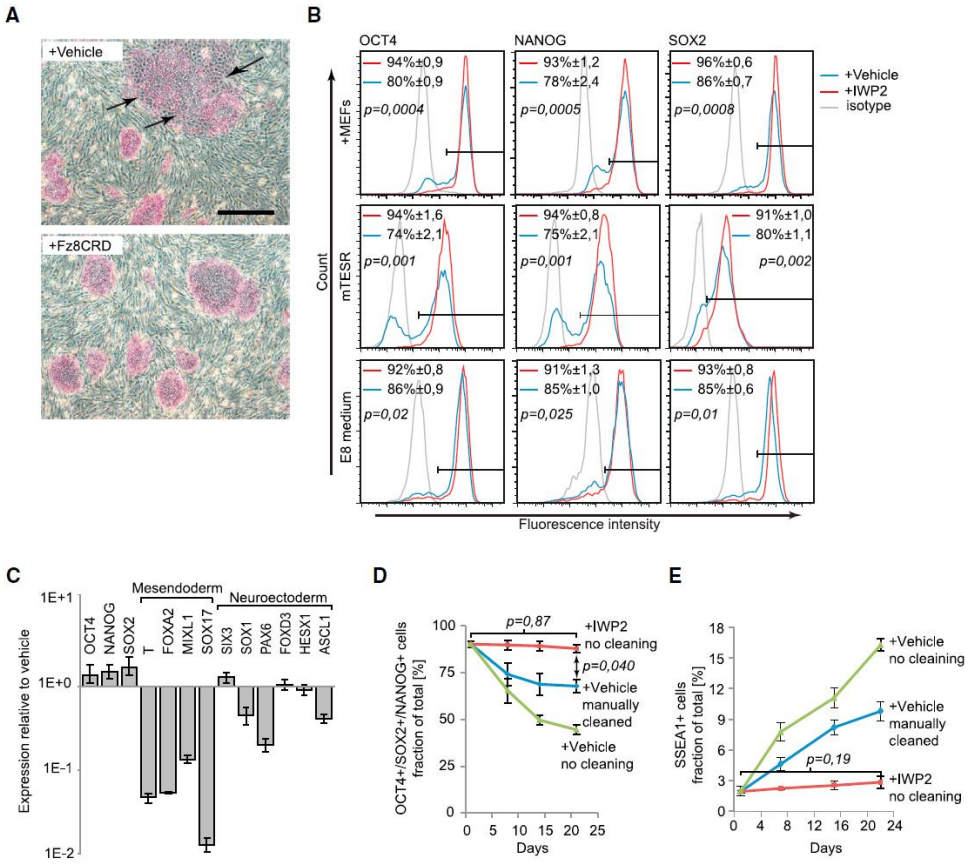

Figure 4. Inhibition of Endogenous WNT Signals Prevents Accumulation of Differentiated Cells in hESC Cultures

(A) H1 hESCs cultured for 5 days at the indicated conditions and stained for alkaline phosphatase (red). Arrows indicate differentiating areas of the colonies.

(B) Flow cytometry histograms showing H1 hESCs cultured for 7 days in the presence or absence of IWP2 and analyzed for NANOG, OCT4, and SOX2 (three independent experiments, mean ± SEM).

(C) Real-time RT-PCR gene expression profiles of H1 hESCs cultured for 6 days in the presence of IWP2, plotted relative to untreated cells (n = 3, mean ± SEM).

(D) Percentage of H1 hESCs triple positive for NANOG, OCT4, and SOX2 in the indicated conditions and procedures (three independent experiments, mean ± SEM).

(E) Percentage of H1 hESCs expressing SSEA1 in the indicated conditions and procedures (three independent experiments, mean ± SEM). Scale bar represents 500 μm. See also Figure S4.

data show that inhibition of endogenous WNT signals prevents the accumulation of differentiated cells in hESC cultures and obviates the need for their manual removal.

BMP4 Induces Both WNT-Dependent and WNT-Independent Differentiation Pathways in hESCs

We next investigated whether WNT signals mediate BMP-induced differentiation in hESCs. Similar to the observations with mouse EpiSCs, both WNT3A and BMP4 protein induced BRACHYURY and GATA4 in H1 hESCs, with concomitant loss of OCT4 (Figure S5A). Flow cytometry indicated a strong induction of the mesoderm marker ROR2 (Drukker et al., 2012), together with suppression of pluripotency factors (Figures 5A, S5B, and S5C). RT-PCR analysis showed induction of additional primitive streak and mesoderm markers (Figure 5B). Furthermore, induction of *WNT3* in response to BMP4 suggested that in hESCs too mesodermal induction was mediated by

Stem Cell Reports
Endogenous WNT in Pluripotent Cell Differentiation

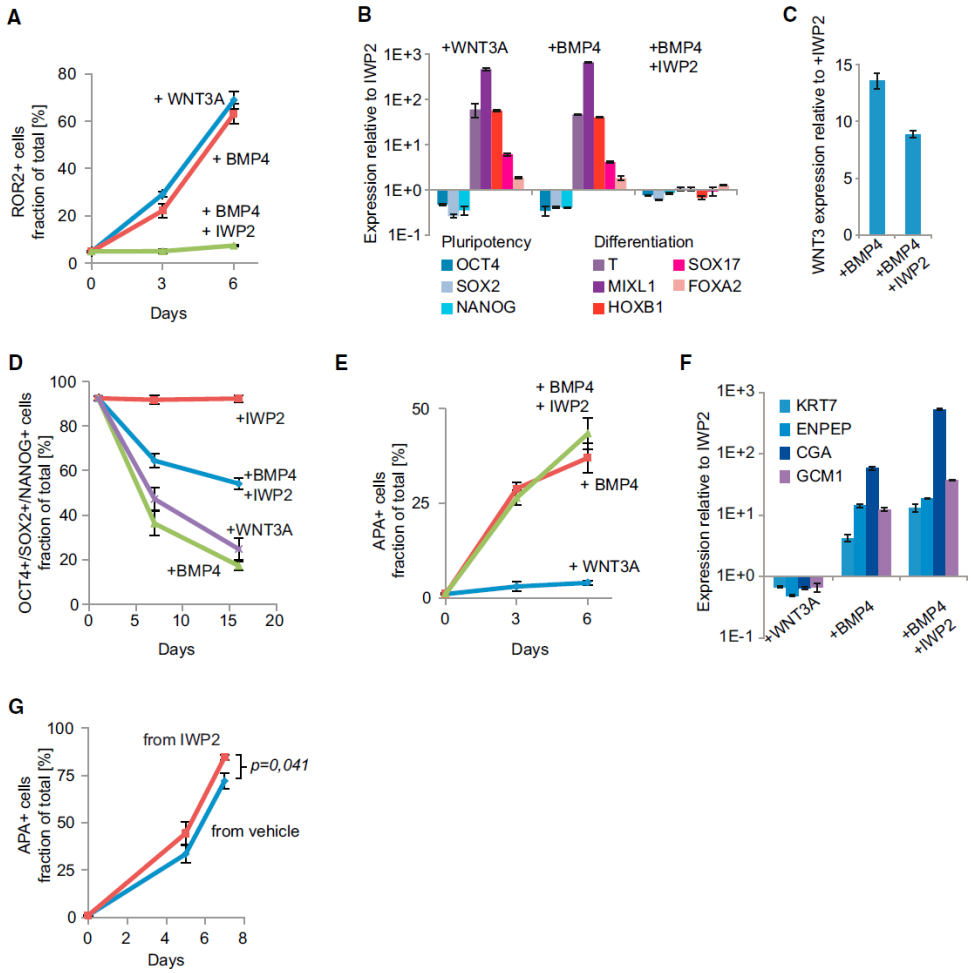

Figure 5. BMP4 Induces Both WNT-Dependent and WNT-Independent Differentiation Pathways in hESCs

(A) H1 hESCs were cultured with the indicated factors for 3 or 6 days and analyzed by flow cytometry for the mesodermal marker ROR2 (three independent experiments, mean ± SEM).

(B) Real-time RT-PCR gene expression profiles of H1 hESCs cultured for 3 days in the indicated factors, plotted relative to cells maintained in the presence of IWP2 (n = 3, mean ± SEM).

(C) *WNT3* expression level 6 hr after induction of H1 hESCs with the indicated factors, plotted relative to cells maintained in IWP2 (n = 3, mean ± SEM).

(D) H1 hESCs cultured in the presence of the indicated factors and analyzed at several time points by flow cytometry for NANOG, OCT4, and SOX2. Plotted is the percentage of cells positive for all three markers (three independent experiments, mean ± SEM).

(E) H1 hESCs cultured with the indicated factors for 3 or 6 days and analyzed by flow cytometry for the trophoblast marker APA (three independent experiments, mean ± SEM).

(F) Real-time RT-PCR gene expression profiles of H1 hESCs cultured for 4 days in the indicated factors, plotted relative to cells maintained in the presence of IWP2 (n = 3, mean ± SEM).

(G) H1 hESCs maintained in the presence or absence of IWP2 prior to the experiment were differentiated with BMP4 in the presence of IWP2 and analyzed by flow cytometry for the trophoblast marker APA (three independent experiments, mean ± SEM).

See also Figure S5.

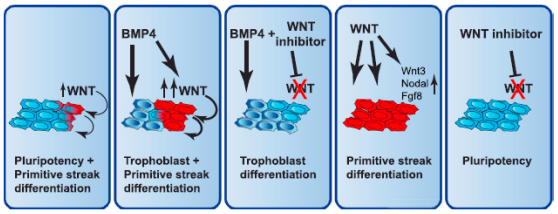

Figure 6. BMP and Endogenous WNT Signals Act Sequentially to Induce Shared and Distinct Differentiation Pathways in hESCs

(Left to right) Endogenous WNT proteins induce differentiation toward primitive streak lineages (red), reducing self-renewal. BMP4 induces both trophoblast (dark blue) and, mediated by endogenous WNTs, primitive streak lineages. In the presence of WNT inhibitors, BMP4 induces only trophoblast and no primitive streak lineages. WNT signals upregulate gastrulation factors and induce primitive streak lineages. WNT inhibitors block spontaneous differentiation, obviating the need to remove differentiated cells during culture.

endogenous WNT (Figure 5C). Indeed, IWP2 prevented mesodermal induction in response to BMP4 (Figures 5A, 5B, and S5A). IWP2 did not abolish the induction of *WNT3*, indicating that it did not directly interfere with BMP4 signaling (Figure 5C). Importantly, IWP2 reduced but did not prevent the loss of the pluripotency markers in response to BMP4 (Figures 5D and S5C). These data show that BMP4 induces mesodermal lineages in hESCs indirectly, via induction of WNT proteins, but also suggest that it induces an alternative differentiation pathway that is WNT independent.

In addition to mesodermal lineages, hESCs have the ability to differentiate into trophoblast (Pera et al., 2004; Xu et al., 2002), and it has recently been shown that a mixture of mesoderm- and trophoblast-committed cells emerge in response to BMP4 (Drukker et al., 2012). In agreement with this study, both flow cytometry for the trophoblast surface marker APA (Drukker et al., 2012), and RT-PCR for the trophoblast markers *KRT7*, *ENPEP*, *CGA*, and *GCM1* show that BMP4 induces the emergence of trophoblast progenitors (Figures 5E, 5F, and S5D). Importantly, WNT3A did not induce trophoblast differentiation, nor was the induction of the trophoblast markers by BMP4 inhibited by IWP2 (Figures 5E and 5F). Combined, these data show that BMP4 can induce the emergence of trophoblast-committed cells from hESCs in a WNT-independent manner, whereas the induction of mesoderm-committed cells requires the action of WNT proteins, either induced endogenously by BMP4 or added directly to the cells.

Finally, a reasonable assumption would be that hESCs maintained in the presence of IWP2 are better substrates for differentiation as they contribute fewer undesired lineages to the population. Indeed, when differentiated toward trophoblast by BMP4+IWP2, H1 hESCs that were maintained in the presence of IWP2 produced more APA+ cells than regular H1 cells (Figures 5G and S5E).

DISCUSSION

This work shows that endogenous WNT signals are major hidden factors in the differentiation of hESCs and EpiSCs and affect the outcome of directed differentiation protocols in hitherto unappreciated ways. We show that WNT signals induce the main gastrulation factors *Nodal*, *Wnt3*, and *Fgf8* and are required and sufficient for the induction of mesoderm by the commonly used mesoderm inducer BMP4. A surprising finding is that BMP4 induces both mesoderm as well as trophoblast-committed cells from hESCs, but only mesoderm induction requires the activation of *WNT* genes by BMP4.

We further show that endogenous WNT signals interfere with self-renewal of hESCs and mEpiSCs. Endogenous WNTs push the aggregate developmental phenotype of EpiSCs to that reminiscent of late-gastrula stage epiblast, consisting of a mixture of genuine EpiSCs with cells in various stages of differentiation, including cells committed to the definitive endoderm lineage. WNT inhibition prevents the induction of differentiation genes and commitment to endoderm, thereby maintaining a high percentage of genuine EpiSCs displaying their pregastrula phenotype, as evidenced by their contribution to blastocyst chimeras. A similar process takes place in hESCs, where we show that WNT inhibition is so effective in suppressing differentiation that it obviates the need for manual removal of differentiated cells during routine culture.

These findings are summarized in Figure 6, and they have obvious ramifications for the guided differentiation of hESCs. For instance, to induce trophoblast one should stimulate with BMP4 in the presence of a WNT inhibitor to avoid induction of mesoderm. Conversely, mesoderm is best obtained using WNT3A in lieu of BMP4 to avoid trophoblast induction. Furthermore, WNT-inhibited hESCs differentiate more efficiently to the trophoblast lineage, suggesting that genuine EpiSCs and hESCs, maintained as homogeneous undifferentiated populations by WNT inhibition, are superior substrates for differentiation as they contribute fewer undesired lineages to the population. We also find that different cell lines and culture media display various tendencies for endogenous WNT-induced differentiation, affecting their suitability for specific purposes such as mesoderm or neural differentiation. This may also influence to what extent WNT inhibition supports their self-renewal or improves their subsequent differentiation. Another interesting observation is that spontaneous endogenous WNT signals induce endoderm

in EpiSCs, consistent with the finding that low levels of WNT3A (25 ng/ml) induce definitive endoderm (D'Amour et al., 2006), whereas high levels of WNT3A (250 ng/ml) induce mesoderm. This may reflect a later function for WNT in redirecting primitive streak-specified cells from endoderm to mesoderm (Loh et al., 2014). Finally, ESCs are commonly aggregated into EBs for the derivation of mesendodermal lineages. We now show that EBs mediate the transition of mESCs into EpiSCs, which is followed by activation of an endogenous WNT gradient and primitive streak induction (ten Berge et al., 2008). A more controlled way of inducing mesendodermal lineages would be by directly inducing genuine EpiSCs with defined levels of WNT signals.

The sequential action of BMP and WNT signals that we uncover here is consistent with embryological findings: *Bmp4* is expressed prior to gastrulation in the extraembryonic ectoderm (Waldrip et al., 1998), both *Wnt3* and active beta-catenin have been detected in the prestreak epiblast bordering this *Bmp4*-expressing region (Mohamed et al., 2004; Rivera-Pérez and Magnuson, 2005), and WNT pathway activation in the epiblast is required for primitive streak induction (Haegel et al., 1995; Huelsken et al., 2000; Liu et al., 1999). The spatiotemporal expression patterns of *Bmp4* and *Wnt3* are therefore consistent with a role for BMP4 in inducing *Wnt3* in the primitive streak-forming region. This is supported by the observations that BMP4 induces *Wnt3* expression in epiblast explants (Ben-Haim et al., 2006), and *Bmp4* loss of function mutants fail to initiate gastrulation (Winnier et al., 1995). Since we find that WNT signals induce the essential gastrulation factors *Wnt3*, *Nodal*, and *Fgf8* in the epiblast, this suggests that, upon WNT3 induction, the primitive streak can continue to expand distally because of continuous induction of the gastrulation factors, including WNT3 itself, by WNT3.

A recent study shows that a subpopulation of EpiSCs expressing a transgenic *Brachyury* reporter displays reversible primitive streak characteristics, i.e., while biased toward mesoderm and endoderm fates, these cells retain their pluripotency (Tsakiridis et al., 2014). In contrast, we find that a significant fraction of the cells labeled by our *Brachyury* reporter has lost pluripotency, as indicated by the inability to establish EpiSC colonies or to contribute to EBs. In support of this, our gene expression data indicate the presence of cells committed to a definitive endoderm fate in EpiSC cultures. The differences in our results may be explained by the *Brachyury* reporters used; the T-GFP reporter is targeted into the endogenous *Brachyury* locus and faithfully replicates its expression (Fehling et al., 2003). In contrast, the Tps/tb-RED reporter used by Tsakiridis et al. (2014) fails to recapitulate *Brachyury* expression in the anterior streak region which, importantly, is the source of definitive endoderm precursors (Clements et al., 1996). Therefore, while the T-GFP-labeled population would include the cells that have lost pluripotency because they committed to a definitive endoderm state, the Tps/tb-RED reporter would not identify this population.

Recently, there has been debate about the nature of the trophoblast-committed cells induced by BMP4 in hESCs, with one study reporting that these cells represent a subpopulation of mesodermal cells that go through a BRACHYURY-positive state (Bernardo et al., 2011). However, the absence of BRACHYURY and other mesendodermal and mesodermal markers in our BMP4+IWP2-differentiated trophoblast cells argues against a mesodermal character.

EXPERIMENTAL PROCEDURES

Statistics

All data are presented as mean ± SEM. Technical replicates are meant unless further specified; p values < 0.05 determined using Student's t test were considered significant.

Cell Culture

EpiSCs were cultured on gelatin and fetal calf serum-coated plates in N2B27 supplemented with 20 ng/ml ACTIVIN A and 12 ng/ml FGF2 (Peprotech). H1 and H9 hESCs were cultured on MEFs in Dulbecco's modified Eagle's medium/F12 supplemented with 20% knockout serum replacement and 10 ng/ml human FGF2 (Millipore). Feeder free culture was done on Matrigel (BD) in mTeSR1 medium (StemCell Technologies). Media, recombinant proteins, and small molecules were changed daily.

Animal Experiments

All animal experiments were conducted after approval by the Erasmus MC animal ethical committee.

Transcriptome Analysis

Total RNA from GFP9 EpiSCs was prepared using TriPure (Roche), converted to biotin-labeled cRNA, hybridized to Affymetrix Mouse Genome 430 2.0 Arrays, and analyzed with the Affymetrix GeneChip Scanner 3000. RNA-Seq was performed at the Erasmus MC Center for Biomics using the Illumina HiSeq platform. We combined Illumina BeadArray gene expression data (Kojima et al., 2014) with our microarray data using a similar approach as described (Heider and Alt, 2013). Microarray (GSE62155) and RNA-Seq (GSE62205) data are available in Gene Expression Omnibus (GEO). Further details are provided in the Supplemental Experimental Procedures.

SUPPLEMENTAL INFORMATION

Supplemental Information includes Supplemental Experimental Procedures, five figures, and five tables and can be found with this article online at http://dx.doi.org/10.1016/j.stemcr.2014.11.007.

ACKNOWLEDGMENTS

129S2C1a EpiSCs were donated by L. Vallier, GOF18 EpiSCs by H.R. Schöler, and T-GFP ESCs by G. Keller. DtB was supported by NWO ECHO.10.B1.064, TI Pharma D5-402, Marie Curie FP7-PEOPLE-2009-RG-256560, ZonMW 911-09-036 and FES NIRM (Dutch Innovation Award), HvdW by NGI Zenith 93511036, and SP by LSBR 1040, ZonMW TOP 40-00812-98-12128, and EU fp7 THALAMOSS 306201.

Received: May 29, 2014
Revised: November 26, 2014
Accepted: November 26, 2014
Published: December 24, 2014

REFERENCES

Bakre, M.M., Hoi, A., Mong, J.C., Koh, Y.Y., Wong, K.Y., and Stanton, L.W. (2007). Generation of multipotential mesendodermal progenitors from mouse embryonic stem cells via sustained Wnt pathway activation. J. Biol. Chem. *282*, 31703–31712.

Ben-Haim, N., Lu, C., Guzman-Ayala, M., Pescatore, L., Mesnard, D., Bischofberger, M., Naef, F., Robertson, E.J., and Constam, D.B. (2006). The nodal precursor acting via activin receptors induces mesoderm by maintaining a source of its convertases and BMP4. Dev. Cell *11*, 313–323.

Bernardo, A.S., Faial, T., Gardner, L., Niakan, K.K., Ortmann, D., Senner, C.E., Callery, E.M., Trotter, M.W., Hemberger, M., Smith, J.C., et al. (2011). BRACHYURY and CDX2 mediate BMP-induced differentiation of human and mouse pluripotent stem cells into embryonic and extraembryonic lineages. Cell Stem Cell *9*, 144–155.

Bernemann, C., Greber, B., Ko, K., Sterneckert, J., Han, D.W., Araúzo-Bravo, M.J., and Schöler, H.R. (2011). Distinct developmental ground states of epiblast stem cell lines determine different pluripotency features. Stem Cells *29*, 1496–1503.

Blauwkamp, T.A., Nigam, S., Ardehali, R., Weissman, I.L., and Nusse, R. (2012). Endogenous Wnt signalling in human embryonic stem cells generates an equilibrium of distinct lineage-specified progenitors. Nat Commun *3*, 1070.

Brons, I.G., Smithers, L.E., Trotter, M.W., Rugg-Gunn, P., Sun, B., Chuva de Sousa Lopes, S.M., Howlett, S.K., Clarkson, A., Ahrlund-Richter, L., Pedersen, R.A., and Vallier, L. (2007). Derivation of pluripotent epiblast stem cells from mammalian embryos. Nature *448*, 191–195.

Chen, B., Dodge, M.E., Tang, W., Lu, J., Ma, Z., Fan, C.W., Wei, S., Hao, W., Kilgore, J., Williams, N.S., et al. (2009). Small molecule-mediated disruption of Wnt-dependent signaling in tissue regeneration and cancer. Nat. Chem. Biol. *5*, 100–107.

Clements, D., Taylor, H.C., Herrmann, B.G., and Stott, D. (1996). Distinct regulatory control of the Brachyury gene in axial and non-axial mesoderm suggests separation of mesoderm lineages early in mouse gastrulation. Mech. Dev. *56*, 139–149.

D'Amour, K.A., Bang, A.G., Eliazer, S., Kelly, O.G., Agulnick, A.D., Smart, N.G., Moorman, M.A., Kroon, E., Carpenter, M.K., and Baetge, E.E. (2006). Production of pancreatic hormone-expressing endocrine cells from human embryonic stem cells. Nat. Biotechnol. *24*, 1392–1401.

Davidson, K.C., Adams, A.M., Goodson, J.M., McDonald, C.E., Potter, J.C., Berndt, J.D., Biechele, T.L., Taylor, R.J., and Moon, R.T. (2012). Wnt/β-catenin signaling promotes differentiation, not self-renewal, of human embryonic stem cells and is repressed by Oct4. Proc. Natl. Acad. Sci. USA *109*, 4485–4490.

Drukker, M., Tang, C., Ardehali, R., Rinkevich, Y., Seita, J., Lee, A.S., Mosley, A.R., Weissman, I.L., and Soen, Y. (2012). Isolation of primitive endoderm, mesoderm, vascular endothelial and trophoblast progenitors from human pluripotent stem cells. Nat. Biotechnol. *30*, 531–542.

Fehling, H.J., Lacaud, G., Kubo, A., Kennedy, M., Robertson, S., Keller, G., and Kouskoff, V. (2003). Tracking mesoderm induction and its specification to the hemangioblast during embryonic stem cell differentiation. Development *130*, 4217–4227.

Frank, S., Zhang, M., Schöler, H.R., and Greber, B. (2012). Small molecule-assisted, line-independent maintenance of human pluripotent stem cells in defined conditions. PLoS ONE *7*, e41958.

Gadue, P., Huber, T.L., Paddison, P.J., and Keller, G.M. (2006). Wnt and TGF-beta signaling are required for the induction of an in vitro model of primitive streak formation using embryonic stem cells. Proc. Natl. Acad. Sci. USA *103*, 16806–16811.

Gardner, R.L., Lyon, M.F., Evans, E.P., and Burtenshaw, M.D. (1985). Clonal analysis of X-chromosome inactivation and the origin of the germ line in the mouse embryo. J. Embryol. Exp. Morphol. *88*, 349–363.

Greber, B., Wu, G., Bernemann, C., Joo, J.Y., Han, D.W., Ko, K., Tapia, N., Sabour, D., Sterneckert, J., Tesar, P., and Schöler, H.R. (2010). Conserved and divergent roles of FGF signaling in mouse epiblast stem cells and human embryonic stem cells. Cell Stem Cell *6*, 215–226.

Gu, G., Wells, J.M., Dombkowski, D., Preffer, F., Aronow, B., and Melton, D.A. (2004). Global expression analysis of gene regulatory pathways during endocrine pancreatic development. Development *131*, 165–179.

Haegel, H., Larue, L., Ohsugi, M., Fedorov, L., Herrenknecht, K., and Kemler, R. (1995). Lack of beta-catenin affects mouse development at gastrulation. Development *121*, 3529–3537.

Han, D.W., Tapia, N., Joo, J.Y., Greber, B., Araúzo-Bravo, M.J., Bernemann, C., Ko, K., Wu, G., Stehling, M., Do, J.T., and Schöler, H.R. (2010). Epiblast stem cell subpopulations represent mouse embryos of distinct pregastrulation stages. Cell *143*, 617–627.

Hao, J., Li, T.G., Qi, X., Zhao, D.F., and Zhao, G.Q. (2006). WNT/beta-catenin pathway up-regulates Stat3 and converges on LIF to prevent differentiation of mouse embryonic stem cells. Dev. Biol. *290*, 81–91.

Heider, A., and Alt, R. (2013). virtualArray: a R/bioconductor package to merge raw data from different microarray platforms. BMC Bioinformatics *14*, 75.

Hou, J., Charters, A.M., Lee, S.C., Zhao, Y., Wu, M.K., Jones, S.J., Marra, M.A., and Hoodless, P.A. (2007). A systematic screen for genes expressed in definitive endoderm by Serial Analysis of Gene Expression (SAGE). BMC Dev. Biol. *7*, 92.

Huang, Y., Osorno, R., Tsakiridis, A., and Wilson, V. (2012). In Vivo differentiation potential of epiblast stem cells revealed by chimeric embryo formation. Cell Rep *2*, 1571–1578.

Huelsken, J., Vogel, R., Brinkmann, V., Erdmann, B., Birchmeier, C., and Birchmeier, W. (2000). Requirement for beta-catenin in anterior-posterior axis formation in mice. J. Cell Biol. *148*, 567–578.

Kojima, Y., Kaufman-Francis, K., Studdert, J.B., Steiner, K.A., Power, M.D., Loebel, D.A., Jones, V., Hor, A., de Alencastro, G., Logan, G.J., et al. (2014). The transcriptional and functional properties of mouse epiblast stem cells resemble the anterior primitive streak. Cell Stem Cell *14*, 107–120.

Lako, M., Lindsay, S., Lincoln, J., Cairns, P.M., Armstrong, L., and Hole, N. (2001). Characterisation of Wnt gene expression during the differentiation of murine embryonic stem cells in vitro: role of Wnt3 in enhancing haematopoietic differentiation. Mech. Dev. *103*, 49–59.

Lindsley, R.C., Gill, J.G., Kyba, M., Murphy, T.L., and Murphy, K.M. (2006). Canonical Wnt signaling is required for development of embryonic stem cell-derived mesoderm. Development *133*, 3787–3796.

Liu, P., Wakamiya, M., Shea, M.J., Albrecht, U., Behringer, R.R., and Bradley, A. (1999). Requirement for Wnt3 in vertebrate axis formation. Nat. Genet. *22*, 361–365.

Loh, K.M., Ang, L.T., Zhang, J., Kumar, V., Ang, J., Auyeong, J.Q., Lee, K.L., Choo, S.H., Lim, C.Y., Nichane, M., et al. (2014). Efficient endoderm induction from human pluripotent stem cells by logically directing signals controlling lineage bifurcations. Cell Stem Cell *14*, 237–252.

McLean, A.B., D'Amour, K.A., Jones, K.L., Krishnamoorthy, M., Kulik, M.J., Reynolds, D.M., Sheppard, A.M., Liu, H., Xu, Y., Baetge, E.E., and Dalton, S. (2007). Activin a efficiently specifies definitive endoderm from human embryonic stem cells only when phosphatidylinositol 3-kinase signaling is suppressed. Stem Cells *25*, 29–38.

Mohamed, O.A., Clarke, H.J., and Dufort, D. (2004). Beta-catenin signaling marks the prospective site of primitive streak formation in the mouse embryo. Dev. Dyn. *231*, 416–424.

Nichols, J., and Smith, A. (2009). Naive and primed pluripotent states. Cell Stem Cell *4*, 487–492.

Nostro, M.C., Cheng, X., Keller, G.M., and Gadue, P. (2008). Wnt, activin, and BMP signaling regulate distinct stages in the developmental pathway from embryonic stem cells to blood. Cell Stem Cell *2*, 60–71.

Ogaki, S., Harada, S., Shiraki, N., Kume, K., and Kume, S. (2011). An expression profile analysis of ES cell-derived definitive endodermal cells and Pdx1-expressing cells. BMC Dev. Biol. *11*, 13.

Ogawa, K., Nishinakamura, R., Iwamatsu, Y., Shimosato, D., and Niwa, H. (2006). Synergistic action of Wnt and LIF in maintaining pluripotency of mouse ES cells. Biochem. Biophys. Res. Commun. *343*, 159–166.

Ohtsuka, S., Nishikawa-Torikai, S., and Niwa, H. (2012). E-cadherin promotes incorporation of mouse epiblast stem cells into normal development. PLoS ONE *7*, e45220.

Pera, M.F., Andrade, J., Houssami, S., Reubinoff, B., Trounson, A., Stanley, E.G., Ward-van Oostwaard, D., and Mummery, C. (2004). Regulation of human embryonic stem cell differentiation by BMP-2 and its antagonist noggin. J. Cell Sci. *117*, 1269–1280.

Pfister, S., Steiner, K.A., and Tam, P.P. (2007). Gene expression pattern and progression of embryogenesis in the immediate post-implantation period of mouse development. Gene Expr. Patterns *7*, 558–573.

Rivera-Pérez, J.A., and Magnuson, T. (2005). Primitive streak formation in mice is preceded by localized activation of Brachyury and Wnt3. Dev. Biol. *288*, 363–371.

Singla, D.K., Schneider, D.J., LeWinter, M.M., and Sobel, B.E. (2006). wnt3a but not wnt11 supports self-renewal of embryonic stem cells. Biochem. Biophys. Res. Commun. *345*, 789–795.

Stewart, M.H., Bossé, M., Chadwick, K., Menendez, P., Bendall, S.C., and Bhatia, M. (2006). Clonal isolation of hESCs reveals heterogeneity within the pluripotent stem cell compartment. Nat. Methods *3*, 807–815.

Subramanian, A., Tamayo, P., Mootha, V.K., Mukherjee, S., Ebert, B.L., Gillette, M.A., Paulovich, A., Pomeroy, S.L., Golub, T.R., Lander, E.S., and Mesirov, J.P. (2005). Gene set enrichment analysis: a knowledge-based approach for interpreting genome-wide expression profiles. Proc. Natl. Acad. Sci. USA *102*, 15545–15550.

Sumi, T., Tsuneyoshi, N., Nakatsuji, N., and Suemori, H. (2008). Defining early lineage specification of human embryonic stem cells by the orchestrated balance of canonical Wnt/beta-catenin, Activin/Nodal and BMP signaling. Development *135*, 2969–2979.

Sumi, T., Oki, S., Kitajima, K., and Meno, C. (2013). Epiblast ground state is controlled by canonical Wnt/β-catenin signaling in the postimplantation mouse embryo and epiblast stem cells. PLoS ONE *8*, e63378.

Tada, S., Era, T., Furusawa, C., Sakurai, H., Nishikawa, S., Kinoshita, M., Nakao, K., Chiba, T., and Nishikawa, S. (2005). Characterization of mesendoderm: a diverging point of the definitive endoderm and mesoderm in embryonic stem cell differentiation culture. Development *132*, 4363–4374.

ten Berge, D., Koole, W., Fuerer, C., Fish, M., Eroglu, E., and Nusse, R. (2008). Wnt signaling mediates self-organization and axis formation in embryoid bodies. Cell Stem Cell *3*, 508–518.

ten Berge, D., Kurek, D., Blauwkamp, T., Koole, W., Maas, A., Eroglu, E., Siu, R.K., and Nusse, R. (2011). Embryonic stem cells require Wnt proteins to prevent differentiation to epiblast stem cells. Nat. Cell Biol. *13*, 1070–1075.

Tesar, P.J., Chenoweth, J.G., Brook, F.A., Davies, T.J., Evans, E.P., Mack, D.L., Gardner, R.L., and McKay, R.D. (2007). New cell lines from mouse epiblast share defining features with human embryonic stem cells. Nature *448*, 196–199.

Tortelote, G.G., Hernández-Hernández, J.M., Quaresma, A.J., Nickerson, J.A., Imbalzano, A.N., and Rivera-Pérez, J.A. (2013). Wnt3 function in the epiblast is required for the maintenance but not the initiation of gastrulation in mice. Dev. Biol. *374*, 164–173.

Tsakiridis, A., Huang, Y., Blin, G., Skylaki, S., Wymeersch, F., Osorno, R., Economou, C., Karagianni, E., Zhao, S., Lowell, S., and Wilson, V. (2014). Distinct Wnt-driven primitive streak-like populations reflect in vivo lineage precursors. Development *141*, 1209–1221.

Waldrip, W.R., Bikoff, E.K., Hoodless, P.A., Wrana, J.L., and Robertson, E.J. (1998). Smad2 signaling in extraembryonic tissues determines anterior-posterior polarity of the early mouse embryo. Cell *92*, 797–808.

Winnier, G., Blessing, M., Labosky, P.A., and Hogan, B.L. (1995). Bone morphogenetic protein-4 is required for mesoderm formation and patterning in the mouse. Genes Dev. *9*, 2105–2116.

Xu, R.H., Chen, X., Li, D.S., Li, R., Addicks, G.C., Glennon, C., Zwaka, T.P., and Thomson, J.A. (2002). BMP4 initiates human embryonic stem cell differentiation to trophoblast. Nat. Biotechnol. *20*, 1261–1264.

Ying, Q.L., Nichols, J., Chambers, I., and Smith, A. (2003). BMP induction of Id proteins suppresses differentiation and sustains embryonic stem cell self-renewal in collaboration with STAT3. Cell *115*, 281–292.

Zhang, K., Li, L., Huang, C., Shen, C., Tan, F., Xia, C., Liu, P., Rossant, J., and Jing, N. (2010). Distinct functions of BMP4 during different stages of mouse ES cell neural commitment. Development *137*, 2095–2105.

Stem Cell Reports, Volume *4*
Supplemental Information

Endogenous WNT Signals Mediate BMP-Induced and Spontaneous Differentiation of Epiblast Stem Cells and Human Embryonic Stem Cells

Dorota Kurek, Alex Neagu, Melodi Tastemel, Nesrin Tüysüz, Johannes Lehmann, Harmen J.G. van de Werken, Sjaak Philipsen, Reinier van der Linden, Alex Maas, Wilfred F.J. van IJcken, Micha Drukker, and Derk ten Berge

Supplemental Figure Legends

Figure S1, related to Figure 1. (A-D) T-GFP ESCs were differentiated into EpiSCs by culture in FGF2 and ACTIVIN for 4 passages. The cells acquired the characteristic flattened EpiSC morphology (A), lost expression of the ESC markers *Stella* and *Rex1*, and gained expression of the EpiSC markers *Fgf5* and *Dnmt3b* (B). To verify that the cells had truly differentiated, we transferred them back into ESC conditions as a single cell suspension. On average 8 per 100,000 cells regenerated an ESC colony (n=3) (C), in line with the reversal efficiency of epiblast-derived EpiSCs (Bernemann et al., 2011; Greber et al., 2010), indicating complete differentiation. Teratoma assays demonstrated that the cells retained their pluripotency as they produced teratomas containing derivatives of all 3 germ layers (D). E) Immunofluorescence images of 129S2C1a EpiSCs cultured for 3 days with the indicated factors and immunostained as indicated (blue: DAPI). F) Flow cytometry plots of T-GFP EpiSCs treated with WNT3A and IWP2 and analyzed for T-GFP and SSEA1. G) Plot showing the expansion of SSEA1-positive 129S2C1a EpiSCs in the indicated conditions (mean +/- s.e.m.; n=3 independent experiments). Scale bar: 200 µm (A), 100 µm (D,E).

Figure S1

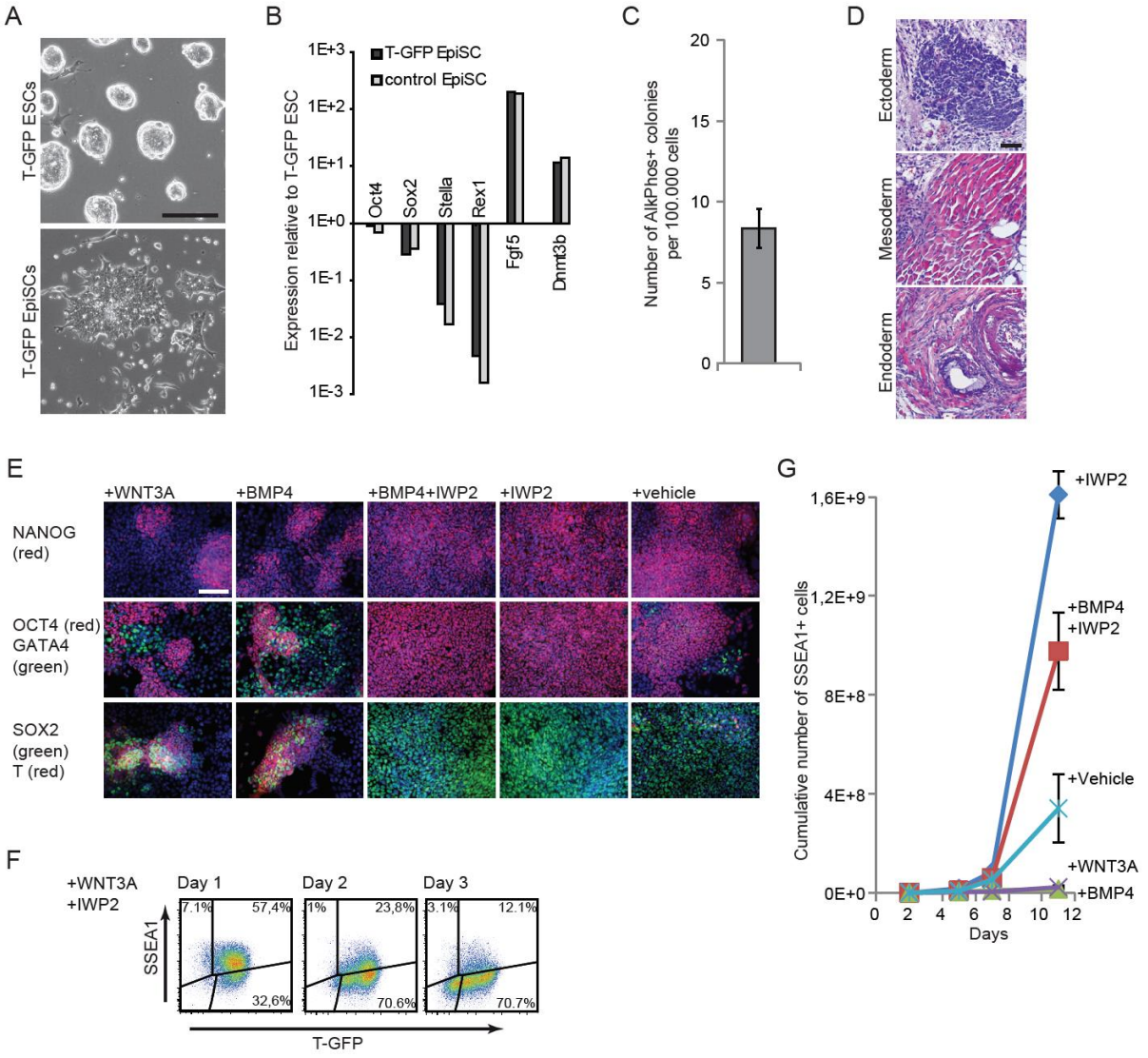

Figure S2, related to Figure 2. A) Expression level of *Wnt* genes in 129S2C1a EpiSCs relative to *Gapdh* (mean +/- s.e.m., n=3; ND, not detected). B) Representative examples of EpiSC colonies obtained from sorted T-GFP EpiSCs, stained for NANOG (red), and quantified in Figure 2A. All colonies stained positive for NANOG, while NANOG-negative cells only formed dispersed clusters. C) Gating strategy relating to Figure 2A.D) Gating strategy relating to Figure 2B. E) Flow cytometry histograms showing several EpiSC lines treated for 3 days with the indicated factors and analyzed for SSEA1. F) Heat map of selected gene expression levels of GFP9 EpiSCs cultured in the presence or absence of IWP2 and analyzed by microarray. Scale bar: 100 µm.

Figure S2

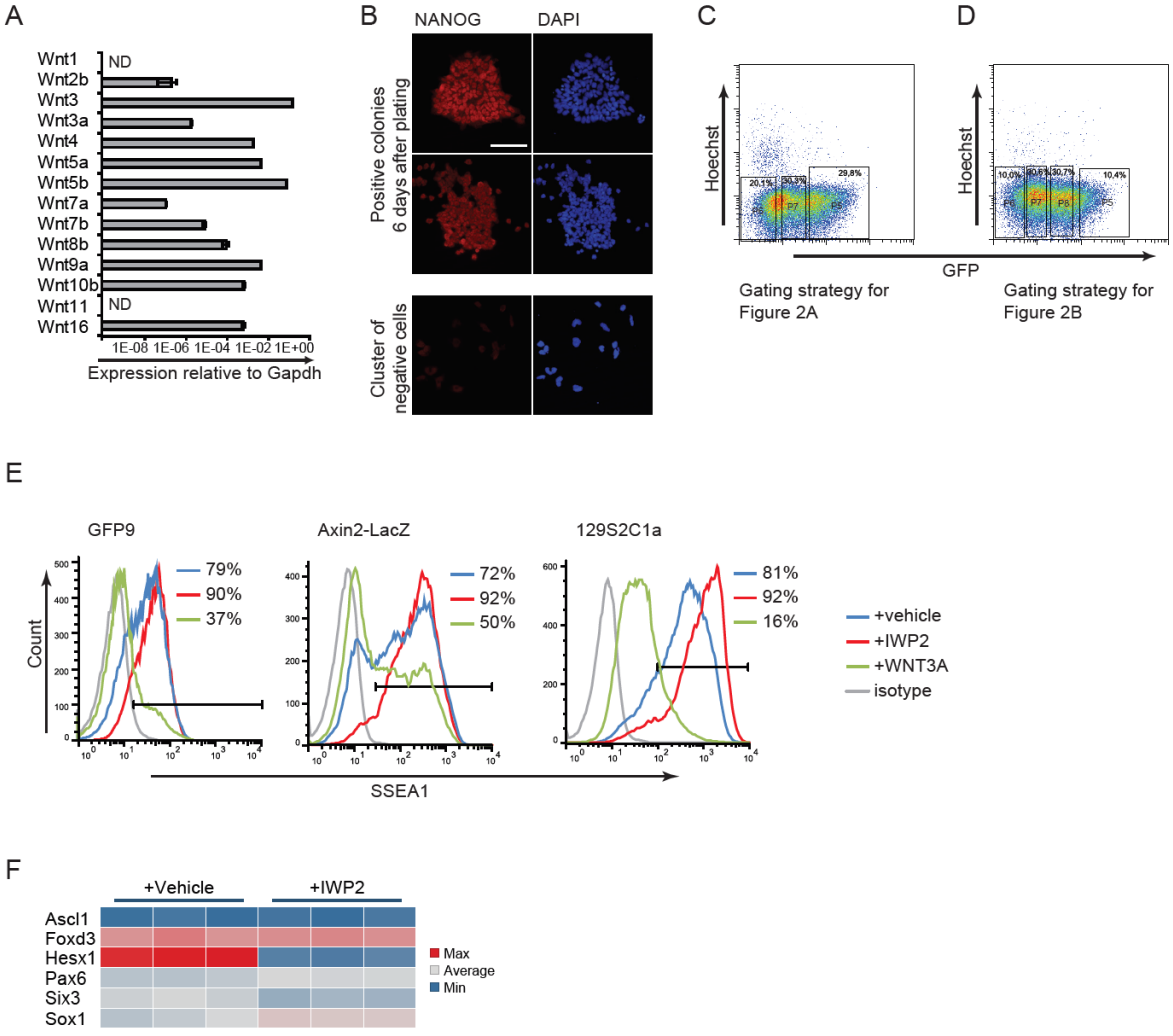

Figure S3, related to Figure 3. A) Immunofluorescence images of sections of X-gal stained chimeras immunostained as indicated. B) Flow cytometry plots of GOF18 EpiSCs cultured at indicated conditions for 4 passages and analyzed for SSEA1 and GFP (mean +/- s.e.m.; n=3 independent experiments). C) Flow cytometry histograms showing percentage of GFP positive cells from GFP-positive and GFP-negative GOF18 EpiSCs analyzed 4 and 18 days after sorting. Scale bar: 50 µm.

Figure S3

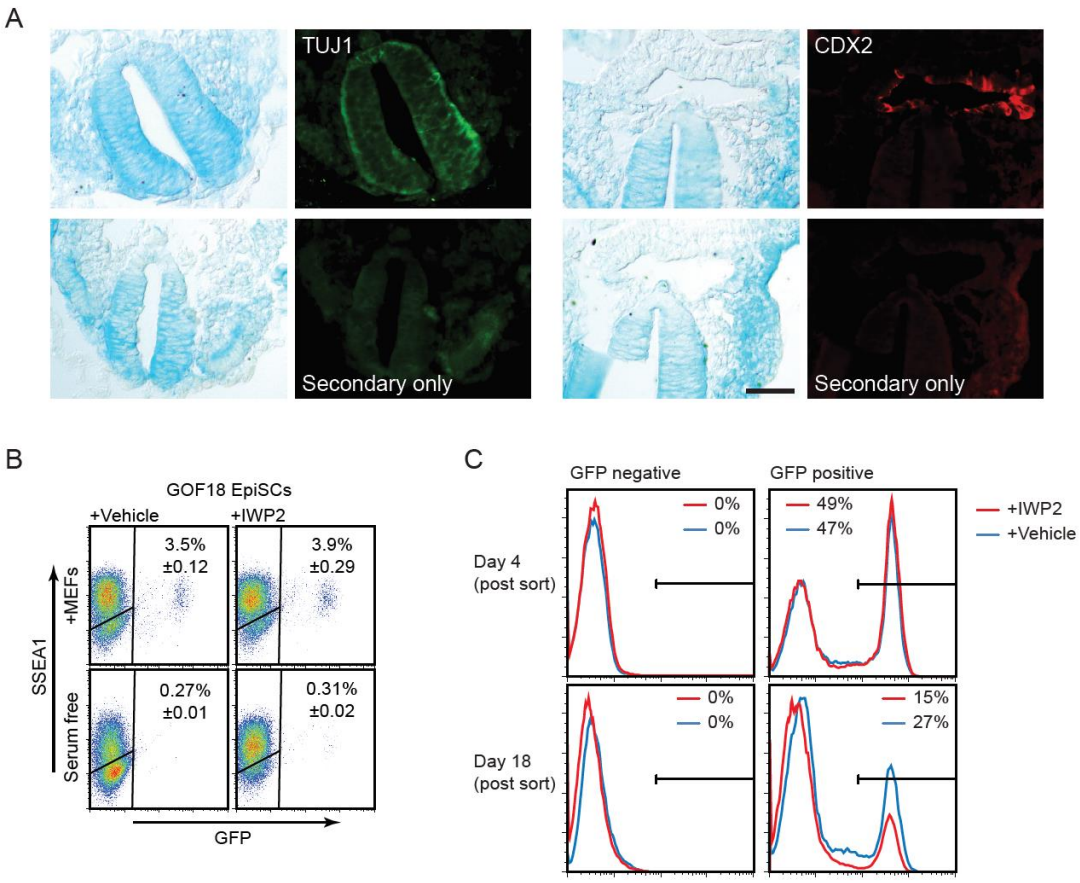

Figure S4, related to Figure 4. A) Representative phase contrast images of H9 (on MEFs) or H1 (mTESR1) hESCs cultured for 6 days at the indicated conditions. Arrows indicate differentiating areas of the colonies. B,C) Immunofluorescence images of H1 (B) or H9 (C) hESCs cultured for 6 days with the indicated factors and immunostained as indicated (blue: DAPI). D) Flow cytometry histograms showing H9 hESCs cultured in the indicated conditions for 7 days and analyzed for NANOG, OCT4 and SOX2. E) Real-time RT-PCR gene expression profile of H9 hESCs cultured for 6 days in the presence of IWP2, plotted relative to cells maintained in the absence of IWP2 (+/- s.e.m.; n=3). F) Percentage of H9 hESCs triple positive for NANOG, OCT4 and SOX2, cultured using the indicated conditions and procedures (mean +/- s.e.m.; n=3 independent experiments). G) Percentage of H9 hESCs expressing SSEA1 cultured using the indicated conditions and procedures (mean +/- s.e.m.; n=3 independent experiments). H) Flow cytometry histograms for SSEA1 and pluripotency transcription factors in H9 and H1 hESCs cultured using the indicated conditions and procedures. Pluripotency factor expression was determined either at day 19 (H9) or day 21 (H1). I) H9 or H1 hESCs were cultured in the presence of IWP2 for 10 passages and then used to establish teratomas. Hematoxylin and eosin staining shows the presence of all 3 germ layers in the teratomas. Scale bar: 200 µm (A,C and I), 100 µm (B).

Figure S4

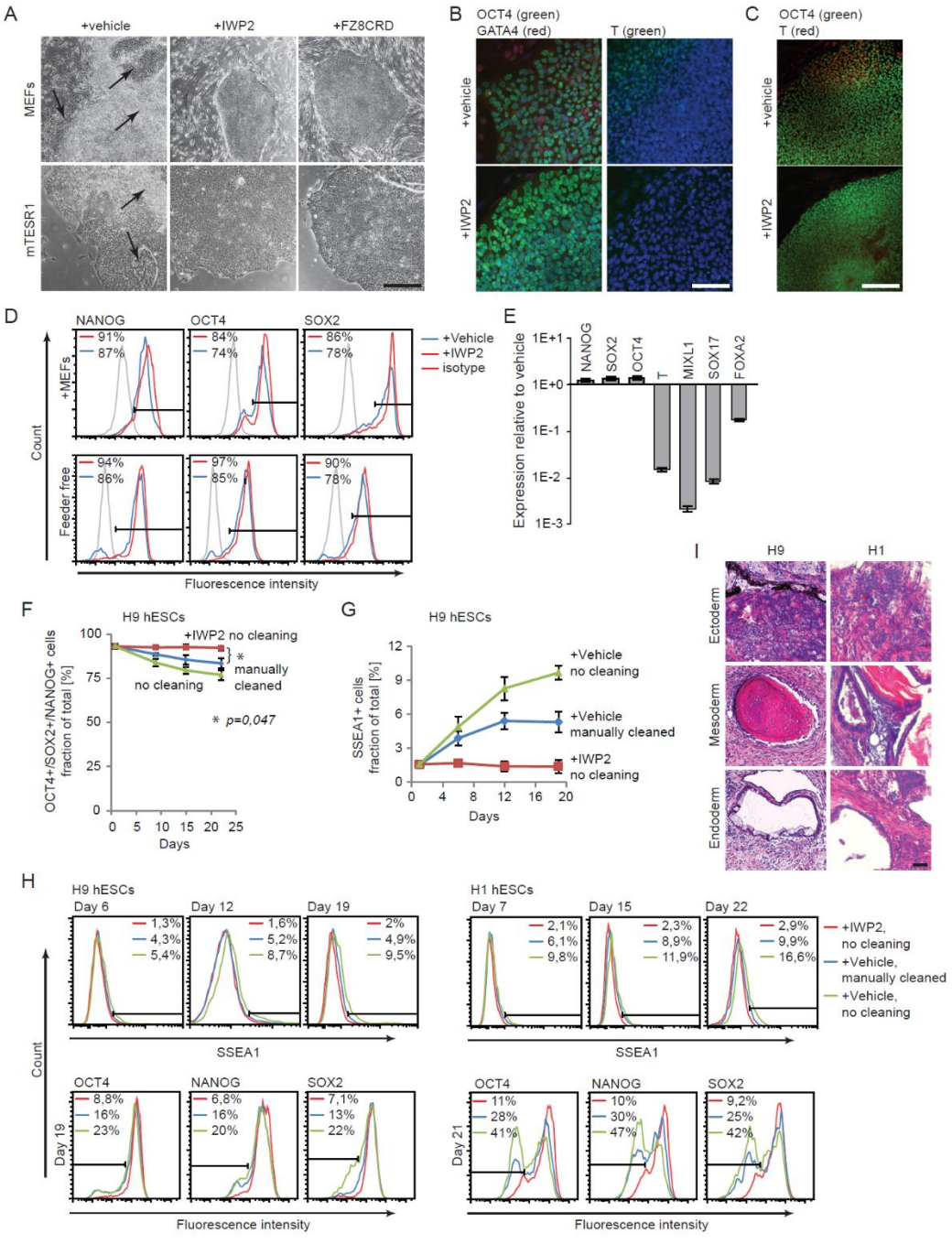

Figure S5, related to Figure 5. A) Immunofluorescence images of H1 hESCs cultured with the indicated factors for 7 days and immunostained as indicated (blue: DAPI). B) Flow cytometry plots from the experiment shown in Figure 5A, showing H1 hESCs cultured with the indicated factors for 3 or 6 days and analyzed for ROR2. C) Flow cytometry histograms showing H1 hESCs cultured with the indicated factors for 4 and 12 days and analyzed for NANOG, OCT4 and SOX2. D) Flow cytometry plots from the experiment shown in Figure 5E, showing H1 hESCs cultured with the indicated factors for 3 or 6 days and analyzed for APA. E) Flow cytometry histograms showing H1 hESCs differentiated with BMP4 in the presence of IWP2 for 5 and 7 days and analyzed for APA (mean +/- s.e.m.; n=3 independent experiments). Scale bar: 100 µm.

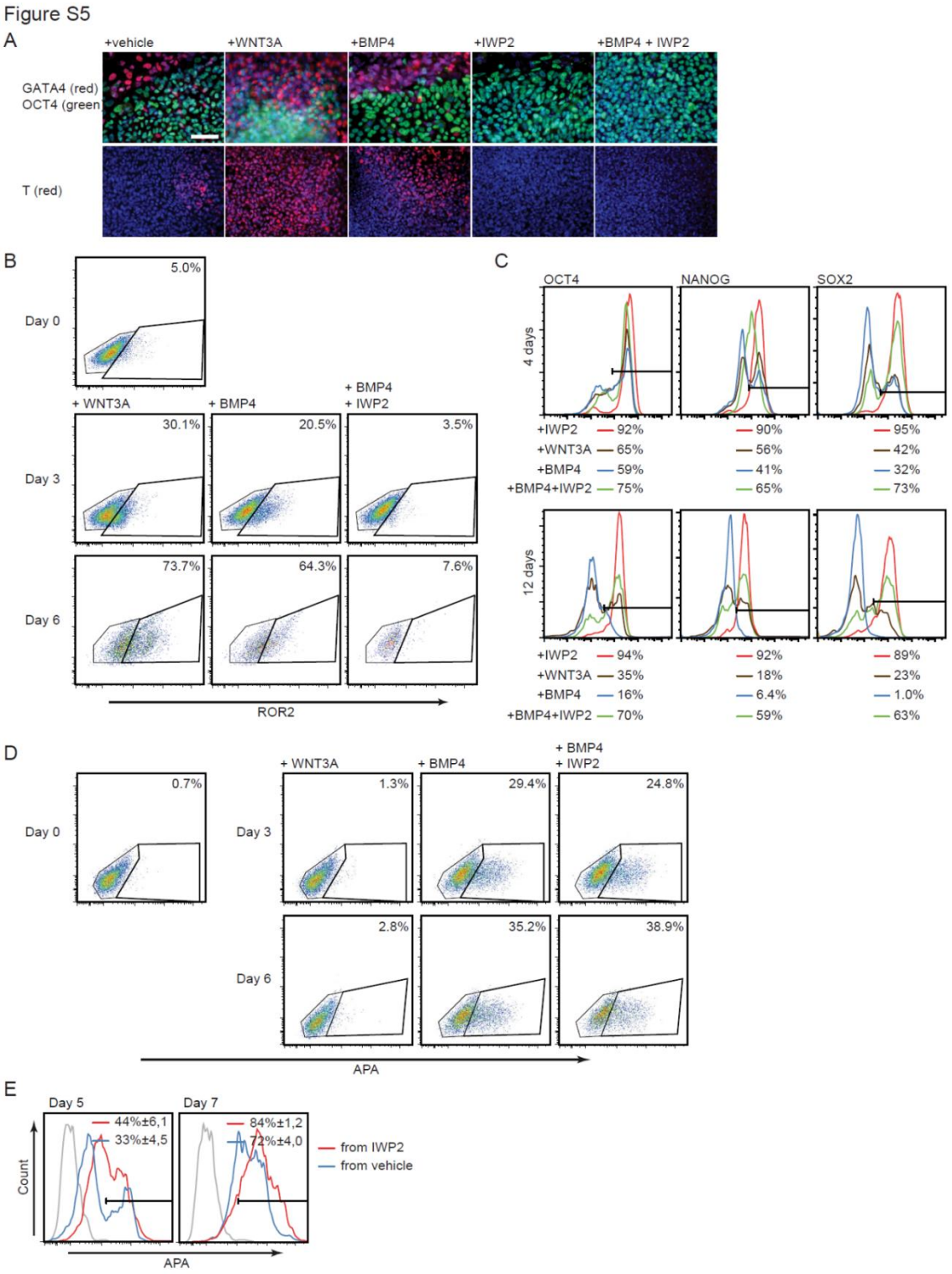

Supplemental Experimental Procedures

Cell culture. Epiblast stem cells (EpiSCs) were cultured on gelatin and fetal calf serum coated plates in EpiSC medium: N2B27 medium supplemented with 20 ng/ml ActivinA and 12 ng/ml bFGF (both Peprotech). N2B27 medium consisted of one volume DMEM/F12 combined with one volume Neurobasal medium, supplemented with 0.5% N2 Supplement, 1% B27 Supplement, 0.033% BSA 7.5% solution, 50 µM β-mercaptoethanol, 2 mM Glutamax, 100 U/ml penicillin and 100 µg/ml streptomycin (all from Invitrogen). EpiSCs were passaged 1:4–1:10 every 3 days by triturating the colonies into small clumps using 0.5 mg/ml collagenase IV (Sigma).
To differentiate EpiSCs from ES cells, trypsinized ES cells were seeded at a density of 10,000 cells/cm^2 on gelatin and FCS coated plates in EpiSC medium supplemented with 1,000 U/ml LIF for the first passage. The cells were then passaged 1:4–1:10 every 3 days as small clumps using 0.5 mg/ml collagenase IV.
To revert EpiSCs to ESCs, EpiSCs were triturated to a single cell suspension in 0.5 mg/ml collagenase IV (Sigma) and seeded at a density of 2,000 cells/cm^2 in EpiSC medium on MEFs supplemented with 10µM the ROCK inhibitor Y-27632 (Stemgent). The next day, the medium was changed to N2B27 medium supplemented with LIF (1,000 U/ml), PD0325901 and CHIR99021. After 4 days the cells were stained for alkaline phosphatase activity using the SCR004 kit (Millipore) and the number of alkaline phosphatase-positive colonies counted.
Mouse ESCs were cultured in N2B27 medium supplemented with 1,000 U/ml LIF (Chemicon) and 250 ng/ml Wnt3a protein on gelatin coated plates.
WA01 (H1) and WA09 (H9) hESCs were cultured on irradiated mouse embryonic fibroblast feeder layers in medium consisting of DMEM/F12 supplemented with 20% Knockout Serum Replacement, 2 mM Glutamax, 1x MEM non-essential amino acids, 50 µM β-mercaptoethanol, 100 U/ml penicillin, 100 µg/ml streptomycin (all from Invitrogen) and supplemented with 10 ng/ml human bFGF (Millipore). For differentiation experiments cells were cultured on a layer of Matrigel (BD Biosciences) in medium consisting of DMEM/F12 supplemented with 20% Serum (HyClone), 2 mM Glutamax, 1x MEM non-essential amino acids, 50 µM β-mercaptoethanol, 100 U/ml penicillin, 100 µg/ml streptomycin (all from Invitrogen) and supplemented with 250 ng/ml Wnt3a, 50 ng/ml BMP4, or 2 µm IWP2, as indicated.
For feeder free culture, hESCs were cultured on a layer of Matrigel (BD Biosciences) in mTeSR1 medium (Stemcells Technologies) or TeSR-E8 medium (Stemcells Technologies).
Media, recombinant proteins and small molecules were changed daily in all experiments except when indicated otherwise. IWP2 (Merck or Stemgent), CHIR99021 (Axon Medchem or Stemgent), PD0325901 (Merck), LDN-193189 (Stemgent) and ROCK inhibitor Y-27632 (Stemgent) were diluted from 2 mM (IWP2), 0.2 mM (LDN-193189) or 10 mM (others) stocks in water (Y-27632) or dimethylsulphoxide (all others), and used at 2, 3, 0.9, 0.2 and 10 µM, respectively. Bmp4 (Invitrogen) was used at 15 ng/ml for EpiSCs, and 50 ng/ml for hESCs. Wnt3a and Fz8CRD proteins were used at 250 and 1,000 ng/ml, respectively. Recombinant mouse Wnt3a protein was produced in Drosophila S2 cells grown in suspension culture, and purified by Blue Sepharose affinity and gel filtration chromatography as described (Willert et al., 2003). Fz8CRD was produced as an Fc fusion protein as described (Hsieh et al., 1999).
Epiblast Stem Cell derivation. Epiblasts were dissected from E6.5 Rosa26-LacZ (Soriano, 1999) or Actin-GFP (Okabe et al., 1997) embryos and collected in DMEM with 10% FCS and 20 mM HEPES. After dissociation into small clumps using a brief trypsin-EDTA treatment, the clumps were plated on a MEF feeder layer in DMEM supplemented with 18% Knockout Serum

Replacement, 2% fetal bovine serum (Hyclone), 1 mM sodium pyruvate, 1x MEM non-essential amino acids, 50 µM β-mercaptoethanol, 100 U ml/1 penicillin, 100 µg ml/1 streptomycin (all from Invitrogen), 12 ng/ml bFGF (Peprotech) and 2 µM IWP2 (Stemgent). Four to seven days after initial plating, the epiblast outgrowths were passaged using 0.5 mg/ml collagenase IV and expand in MEF-containing culture. The MEFs were plated in the presence of 2 µM IWP2 prior to start of derivation or passaging to prevent the accumulation of endogenous Wnt proteins. Usually EpiSCs were transferred to feeder-free N2B27 media after passage 2.

EpiSCs and hESCs self-renewal assays. To quantify self-renewal over multiple passages, EpiSCs or hESCs were initially plated in 12-well plates at 1:10 ratio and the total number of cells was estimated. Every 2-3 days for EpiSCs and 5-7 days for hESCs cells were passaged at ratio that would result to a similar density (between 1:4 to 1:10 ratio) and at the same time cells were stained with SSEA1 or nuclear pluripotency markers for FACS analysis (see FACS marker staining). The cumulative number of positive cells was calculated by multiplying the cell counts by the dilution factor used for passaging.

Teratoma formation. EpiSCs and hESCs were harvested using 0.5 mg/ml collagenase IV (Sigma) and resuspended in PBS or 30% BD Matrigel in PBS (BD Biosciences), respectively. Between $2x10^6$ and $6x10^6$ cells were subcutaneously injected into the flank of NOD/SCID mice. After 5-8 weeks teratomas were removed, fixed in 4% PFA, embedded in paraffin, sectioned and stained with hematoxylin and eosin. All animal procedures were performed in accordance with institutional and national guidelines and regulations, and approved by the Erasmus MC Animal Experiment Committee (DEC).

Blastocyst injection. EpiSCs were recovered by treatment with Enzyme-Free Cell Dissociation Buffer (Gibco), and 10-15 cells were injected into blastocysts collected from C57Bl/6 mice. Blastocysts (10-15 per mouse) were transferred into the uterus of a pseudopregnant mouse and embryos recovered 7 days later.

Embryoid body formation. T-GFP and 7xtcf-GFP ESCs were triturated to a single cell suspension using trypsin-EDTA and resuspended in differentiation medium composed of DMEM plus 15% fetal bovine serum (Hyclone), 1x MEM non-essential amino acids, 50 µM β-mercaptoethanol, 100 U/ml penicillin, 100 µg/ml streptomycin (all from Invitrogen). Hanging drops were prepared from 2000 ESCs per 20 µl drop in differentiation medium. After 3 days embryoid bodies were transferred to low attachment plates for further culture in a shaking incubator. The embryoid bodies were collected at indicated time points and dissociated into single cells using collagenase IV in 5% FCS/PBS (5 minutes in 37°C) and collected for flow cytometry. Following markers were used for staining: SSEA1-PE (eBioscience, 1:50) and CD31-PE-Cy7 (eBioscience, 1:2000) in 5% FCS/PBS for 40 minutes at 4°C. 1µg/ml Hoechst 33258 (Molecular Probes) was used for live/dead cells assessment. Cells were analyzed using a FACSAria III flow cytometer and results analyzed by FlowJo.

Correlation between level of Brachyury reporter and ability to form EpiSC colonies or embryoid bodies. T-GFP EpiSCs were plated in N2B27 medium supplemented ActivinA and bFGF for 3 days, dissociated with 0.5 mg/ml collagenase IV (Sigma) for EpiSC colony formation assay or by 0.25% Trypsin-EDTA for embryoid body formation assay, resuspended in PBS with 10% serum and 1 µg/ml Hoechst 33258, and live cells sorted into 3 or 4 categories based on GFP intensity using a FACSAria III cell sorter (BD Biosciences). The gating strategies are shown in Figures S2D and S2E. Sorted cells were seeded at a density of 3000 or 6000 cells/cm^2 in N2B27 medium supplemented with bFGF, Activin A, IWP2 and ROCK inhibitor. After 6 days the cells were immunostained for Nanog and the number of positive colonies was counted by eye. For

embryoid body formation, 6000 sorted cells per 25 µl droplet were aggregated in hanging drops for 3 days, and the embryoid bodies collected and photographed.

Flow cytometry. For live flow cytometry experiments of EpiSCs, single cell suspensions were made using trypsin-EDTA (5 minutes in 37°C), washed with 5% FCS/PBS, and stained with SSEA1-PE (eBioscience, 1:50) for 40 minutes at 4°C. 1µg/ml Hoechst 33258 or 7AAD was used for live/dead cells assessment. Prior to the time course experiment of T-GFP EpiSCs treated with gastrulation-inducing factors, cells were cultured in the presence of IWP2 for one passage.
For live flow cytometry experiments of hESCs, single cell suspensions were made using Enzyme-Free Cell Dissociation Buffer (Gibco) for 30 min at 37ºC, washed with 5% FCS/PBS and stained with anti-APA or anti-ROR2 as described previously (Drukker et al., 2012). For the nuclear pluripotency markers, EpiSCs and hESCs were stained using Mouse or Human Pluripotent Stem Cell Transcription Factor Analysis Kits (BD Biosciences) according to the manufacturer's protocol. Cells were analyzed using FACSAria III, FACS Fortessa, or FACS SCAN flow cytometers (BD Biosciences), and data analyzed using FlowJo.

Real time RT-PCR analysis. Total RNA was prepared using a QIAGEN RNeasy mini kit with on-column DNase digestion, or using TriPure (Roche) according to the manufactures protocol, followed by reverse transcription using Superscript II (Invitrogen). Quantitative PCR was carried out on a Roche Lightcycler 480 using Lightcycler 480 SYBR Green Master mix (Roche). Relative quantification was carried out using Gapdh as a reference gene. All PCRs were carried out in triplicate, and the mean crossing point was used for quantification. Primer sequences were designed such that they spanned splice junctions whenever possible and are provided in Table S3.

Immunohistochemistry. Cells were fixed with 4% paraformaldehyde for 10 min at 4°C, permeabilized for 10 min with ice-cold methanol, washed with PBS/0.5% Triton X-100 (PBT), and blocked with 1% BSA (Sigma) and 5% normal donkey serum in PBT (blocking solution) for 1 hour. Samples were then incubated with primary antibody in blocking solution overnight at 4°C, washed three times with PBT, and primary antibodies detected by DyLight-488 or -594 labelled secondary antibodies (Jackson ImmunoResearch), followed by imaging. Antibodies and concentrations: goat-anti-Oct4 (Santa Cruz sc-8628, 1:250), rabbit-anti-Nanog (REC-RCAB0002P-F Cosmo Bio, 1:250), rabbit-anti-T (Santa Cruz sc-20109, 1:100), goat-anti-T (Santa Cruz sc-17743, 1:100) and rabbit-anti-Gata4 (Santa Cruz sc-9053, 1;100), goat-anti-Sox2 (Immune Systems, 1:1000), rabbit-anti- E-cadherin (Cell Signaling 24E10, 1:200), rabbit-anti-Neuronal Class III B-tubulin (Covance PRB-435P, 1:500), mouse-anti-Cdx2 (Biogenex, MU392A-UC 1:400). Human ESCs were stained for alkaline phosphatase according to manufacturer's protocol (Millipore, Alkaline Phosphatase Detection Kit SCR004).

X-gal staining. Embryos were fixed for 30 min and cells for 1 min in 0.5% glutaraldehyde and 1% paraformaldehyde in PBS, washed in PBS and incubated in X-Gal solution composed of 0.1% 5-Bromo-4-chloro-3-indolyl β-D-galactopyranoside, 0,02% Nonidet™ P 40, 0.01% Sodium Deoxycholate, 2mM magnesium chloride, 5mM potassium hexacyanoferrate(III), 5mM potassium hexacyanoferrate(II) trihydrate, 1mM ethylene glycol-bis(2-aminoethylether)-*N,N,N′,N′*-tetraacetic acid (all from Sigma) for 5 h to overnight at room temperature. Stained cells were counterstained with neutral red and photographed with an Olympus BX40 light microscope.

Micro-array analysis. Total RNA was prepared using TriPure (Roche) according to the manufacturer's protocol from GFP9 EpiSCs maintained in the presence or absence of IWP2 for 2 passages in EpiSC medium. RNA was converted to biotin-labeled cRNA, hybridized on the Affymetrix Mouse Genome 430 2.0 Array, and analyzed with the Affymetrix GeneChip Scanner 3000 at the Erasmus MC Center for Biomics (Rotterdam, The Netherlands) according to manufacturer's instructions. Raw intensity values were normalized by calling Variance

Stabilization (VSN) and calculating the summaries with the medianpolish algorithm of the Robust Multi-Array Average (RMA) expression (Huber et al., 2002; Irizarry et al., 2003). The probe sets gene annotations were based on Ensembl release 75 (Flicek et al., 2014). Quality control was investigated using the *qc* function from the *simpleaffy* R package. Differentially expressed genes were called with the *limma* package, using a threshold value of 0.05 for False Discovery Rate (FDR) adjusted p-value and minimal fold change of 2.
Gene Set Enrichment Analysis (Subramanian et al., 2005) was run on the vehicle versus IWP treated EpiSCs, with 1000 permutations per run. Permutation type was set to "phenotype". The enrichment statistic used was weighted and signal to noise was used as our preferred metric for gene ranking.
To combine gene expression data from Affymetrix GeneChip and Illumina BeadArray platforms, we used a similar approach as described previously (Heider and Alt, 2013). We first downloaded 112 gene expression datasets deposited in the Gene Expression Omnibus (GEO) database (GSE46227) (Kojima et al., 2014) and combined these data with our 9 Affymetrix GeneChip datasets. The probes and probesets were combined using the probe(set)s/gene annotation of Ensembl release 75 (Flicek et al., 2014). In each sample, genes with multiple probe/probesets were collapsed to their median value. This resulted in 17058 distinct genes from both platforms. Second, we quantile normalized the combined expression data (Bolstad et al., 2003). Third, we applied the Empirical Bayes method (Johnson et al., 2007) in a unsupervised mode using the CrOss-platform NOrmalization in R (CONVOR) package (Rudy and Valafar, 2011). We verified the proper unsupervised hierarchical clustering with euclidean distance of the cross-platform normalized data (data not shown). Subsequently we selected the gene expression values from EpiSCs and Epiblast/Ectoderm samples cultured in Tam's and our lab to conduct a Principal Component Analysis (PCA). Using R, the PCA was calculated based on the covariance matrix of 1117 genes that are differentially expressed with a FDR <0.05 and a fold change of at least 1.5.
RNA Seq. Total RNA was prepared using TriPure (Roche) according to the manufacturer's protocol from GFP9 EpiSCs treated for 48 hrs with Bmp4, Wnt3a, and/or IWP2 in EpiSC medium. RNA-Seq was performed at the Erasmus MC Center for Biomics (Rotterdam, The Netherlands) according to manufacturer's instructions (Illumina). Briefly, polyA containing mRNA molecules were purified using poly-T oligo attached magnetic beads. Following purification, the mRNA was fragmented into ~200 bp fragments using divalent cations under elevated temperature. The cleaved RNA fragments were copied into first strand cDNA using reverse transcriptase and random primers. This was followed by second strand synthesis using DNA polymerase I and RNaseH treatment. These cDNA fragments were end repaired, a single A base was added and Illumina adaptors were ligated. The products were purified and size selected on gel and enriched by PCR. The PCR products were purified by Qiaquick PCR purification and used for cluster generation according to the Illumina cluster generation protocols (www.illumina.com). The sample was sequenced for 36bp and raw reads were uploaded on the Galaxy main server (www.usegalaxy.org) (Goecks et al., 2010) and a standard pipeline for RNA-Seq analysis was applied, using modules from the Tuxedo suite. Samples were filtered and trimmed with FASTQ. The resulting files were aligned to the mm9 reference genome build using preSet settings. The aligned reads were imported to Cufflinks, using multi-read and effective length correction, and FPKM values calculated. The mm9 build was used as a reference annotation. Principal component analysis on the FPKM values was performed using Tibco Spotfire on the 9939 genes that had a FPKM value of 5 or more in at least one of the 4 samples.

PCR primer sequences		
Mouse	**Forward**	**Reverse**
Gapdh	TATGATGACATCAAGAAGGTGG	CATTGTCATACCAGGAAATGAG
Oct4	GAACATGTGTAAGCTGCGG	CAGACTCCACCTCACACG
Sox2	AGCTCGCAGACCTACATGAA	CCCTGGAGTGGGAGGAA
Nanog	AAAGGATGAAGTGCAAGCG	TCTGGCTGCTCCAAGTT
Fgf5	AATATTTGCTGTGTCTCAGG	TAAATTTGGCACTTGCATGG
Otx2	CATGATGTCTTATCTAAAGCAACCG	GTCGAGCTGTGCCCTAGTA
Dnmt3b	CCAAGGACACCAGGACGCGC	TCCGAGACCTGGTAGCCGGAA
Rex1	GCTCCTGCACACAGAAGAAA	GTCTTAGCTGCTTCCTTCTTGA
Pecam1	CAAAGTGGAATCAAACCGTATCT	CTACAGGTGTGCCCGAG
Stella	TTCAAAGCGCCTTTCCCAA	ACATCTGAATGGCTCACTG
Wnt1	ATGAACCTTCACAACAACGA	GGCGATTTCTCGAAGTAGAC
Wnt2b	CATGAACTTACACAACAACC	CAAAGTAGACAAGATCAGTCC
Wnt3	CAAGCACAACAATGAAGCAG	GGAGTTCTCGTAGTAGACCA
Wnt3a	AGTGAGGACATTGAATTTGG	GTTTCTCTACCACCATCTCC
Wnt4	GAATCTTCACAACAACGAGG	ATCTGTATGTGGCTTGAACTG
Wnt5a	TAATTCTTGGTGGTCTCTAGGT	GCACCTTCTCCAATGTACTG
Wnt5b	TATGCAGATAGGTAGCCGAG	TTGTTCTGTAGGTTCATGAGAG
Wnt7a	CATCATCGTCATAGGAGAAGG	GATAATCGCATAGGTGAAGG
Wnt7b	CATGAACCTTCACAACAATGAG	TTGTACTTCTCCTTGAGCAG
Wnt8b	GTACACCCTGACTAGAAACTG	ATTGTTGTGCAGATTCATGG
Wnt9a	AGTACAGCAGCAAGTTTGTC	GAGCGAGGTCTCATATTTGTG
Wnt10b	CGGGATTTCTTGGATTCCAG	TTGTGGGTATCGATAAAGATGG
Wnt11	GATCCCAAGCCAATAAACTG	AGATACACAAGTTCTGAGTCCT
Wnt16	CTCTTTGGCTATGAGCTGAG	CGTTGTTGTGTAGATTCATGG
T	GAACCTCGGATTCACATCG	GGCATCAAGGAAGGCTTTAG
Sp5	CGGGACCTATGAGCGCA	TTCGGGCGGAGGAGAAT
Sox17	TGTATGAGTTCTTTGGAGACAAAGTAG	ATAGGAAGGCTGAAATTCAGATG
Snail1	CTTGTGTCTGCACGACCTGT	CTTCACATCCGAGTGGGTTT
Klhl4	CAACAACTGCCACTCCAAATTG	TATGGATGCTGCTAAAGGCAC
Zfp42	TCGGGGCTAATCTCACTTTCAT	CCCTCGACAGACTGACCCTAA
Prdm14	AGCACCCAACCGACTTACAG	GTGGCACATCACCAAATGAG
Tbx3	CAGCAGCCCCCACTAACTG	AGATCCGGTTATCCCTGGGAC
Pou3f1	GGCGCATAAACGTCGTCCA	TCGAGGTGGGTGTCAAAGG
Lefty1	CGCGAAACGAACCAACTTGT	CCAACCGCACTGCCCTTAT
Pitx2	GTCCGTGAACTCGACCTTTTT	GCAGCCGTTGAATGTCTCTTC
Lrp2	GGCTGCATACATTGGGTTTTCA	AAAATGGAAACGGGGTGACTT
Slc39a8	GCCTAAGCATCCAGAGGGAGA	CAGGTATGTCCTGCTGATTGC
Prss23	GGCGTCGAAGTCTGCCTTAG	GGTGAGTCCCTACACCGTTC
Klhl4	CAACAACTGCCACTCCAAATTG	TATGGATGCTGCTAAAGGCAC
Spry4	TCTGGTCAATGGGTAAGATGGT	GCAGCGTCCCTGTGAATCC
Thbs1	CGGGGATCAGGTTGGCATT	GGGGAGATAACGGTGTGTTTG
Fn1	GCCCAGTGATTTCAGCAAAGG	ATGTGGACCCCTCCTGATAGT
Kit	GTCGCCAGCTTCAACTATTAACT	GCCACGTCTCAGCCATCTG
Map2k6	TTGGAGTCTAAATCCCGAGGC	ATGTCTCAGTCGAAAGGCAAG
Fgf15	CTGACACAGACTGGGATTGCT	ATGGCGAGAAAGTGGAACGG
Epas1	TGTGTCCGAAGGAAGCTGATG	CTGAGGAAGGAGAAATCCCGT
Rhox5	CCCTGGTGCCACTATCCTT	ACTCGGAAGAACAGCATGATG
Fgf4	GCTGCTCATAGCCACGAAGAA	GGGCATCGGATTCCACCTG
Klf2	CACGTTGTTTAGGTCCTCATCC	CTCAGCGAGCCTATCTTGCC
Alpl	GGCTACATTGGTGTTGAGCTTTT	CCAACTCTTTTGTGCCAGAGA
Tnfrsf19	AGAAAATTCAGCGCAGATGGAA	TTCTGTGGGGGACACGATG
Krt8	ATCGAGATCACCACCTACCG	TGAAGCCAGGGCTAGTGAGT
Krt19	TGACCTGGAGATGCAGATTG	AATCCACCTCCACACTGACC
Nedd9	CCACAGCACTCAAGGGGTAT	ATGGTGGAATGGCATAGACC
Plat	AGTGGTCTTGGGCAGAACAT	CTGCAGTAATGCGATGTCGT

Mnx1	GTTGGAGCTGGAACACCAGT	CTTTTTGCTGCGTTTCCATT
Lgr5	TAACAGGGAACCGAGCCTTA	CACTGTTGCCGTCGTCTTTA
Vil1	CTGGAAACCGAGACCTTGAG	AGTTTCCCAGCTCTGCCTTA
Fgf8	CCGGACCTACCAGCTCTACA	ACTCGGACTCTGCTTCCAAA
Id1	GAGTCTGAAGTCGGGACCAC	GAGTCCATCTGGTCCCTCAG
Cdh2	GGGGATATTGGGGACTTCAT	GAGTTGAGGGAGCTCAAGGA
Plet1	CTTGACATCCCAAAGCCAGT	GGTTGAGGCTGAGGTTGTA
Cdh1	GCCACCAGATGATGATACCC	GGAGCCACATCATTTCGAGT
Nodal	ACCATGCCTACATCCAGAGC	CATGTCCTTGTGGTGTTCCA
Axin2	AGGAGCAGCTCAGCAAAAAG	GCTCAGTCGATCCTCTCCAC
Human	**Forward**	**Reverse**
GAPDH	GGCCTCCAAGGAGTAAGACC	AGGGGTCTACATGGCAACTG
BRY	GCAAAAGCTTTCCTTGATGC	ATGAGGATTTGCAGGTGGAC
HOXB1	TCCCTGGGAACTTTGACAAC	GCTCTGACACCTTCGCTAGG
WNT3	GCTGACTTCGGCGTGTTAGT	CACTTGCATTTGAGGTGCAT
POU5F1	CGAAAGAGAAAGCGAACCAG	ACACTCGGACCACATCCTTC
KRT7	CAGGAACTCATGAGCGTGAA	CTGCCACCAGTGGAATTCAT
ENPEP	AAGAACATGGCCTGGAATTG	AGCTCTCCATCTGCCACAGT
GCM1	CCTCTGAAGCTCATCCCTTG	GCTCTTCTTGCCTCAGCTTC
SOX2	AACCCCAAGATGCACAACTC	CGGGGCCGGTATTTATAATC
NANOG	CAGAAGGCCTCAGCACCTAC	ACTGGATGTTCTGGGTCTGG
T	TCGGAACAATTCTCCAACCT	GGGTACTGACTGGAGCTGGT
MIXL1	AGTCCAGGATCCAGGTATGGT	GGGGCTTCAGACATTTCGT
FOXA2	GAGGGCTACTCCTCCGTGA	CACGTACGACGACATGTTCA
CGA	GGTGCCCCAATACTTCAGTG	CCCCATTACTGTGACCCTGT
SOX17	AGCAGAATCCAGACCTGCAC	TTGTAGTTGGGGTGGTCCTG
SIX3	CGGGAGTGGTACCTACAGGA	GGTGCTGGAGCCTGTTCTT
HESX1	TAGAGGCCGAAGACCAAGAA	ACGCCGATTTTGAAACCA
FOXD3	ACTCTGCCTCTCCCCAATTT	TCGGTTTTCGGTTTTACCTG
SOX1	AAAGTCAAAACGAGGCGAGA	AAGTGCTTGGACCTGCCTTA
PAX6	GCCAGCAACACACCTAGTCA	TGTGAGGGCTGTGTCTGTTC
ASCL1	GGACGAGGGCTCTTACGAC	AACGCCACTGACAAGAAAGC

Supplemental References

Bernemann, C., Greber, B., Ko, K., Sterneckert, J., Han, D.W., Arauzo-Bravo, M.J., and Scholer, H.R. (2011). Distinct developmental ground states of epiblast stem cell lines determine different pluripotency features. Stem cells (Dayton, Ohio) *29*, 1496-1503.

Bolstad, B.M., Irizarry, R.A., Astrand, M., and Speed, T.P. (2003). A comparison of normalization methods for high density oligonucleotide array data based on variance and bias. Bioinformatics *19*, 185-193.

Drukker, M., Tang, C., Ardehali, R., Rinkevich, Y., Seita, J., Lee, A.S., Mosley, A.R., Weissman, I.L., and Soen, Y. (2012). Isolation of primitive endoderm, mesoderm, vascular endothelial and trophoblast progenitors from human pluripotent stem cells. Nature biotechnology *30*, 531-542.

Flicek, P., Amode, M.R., Barrell, D., Beal, K., Billis, K., Brent, S., Carvalho-Silva, D., Clapham, P., Coates, G., Fitzgerald, S.*, et al.* (2014). Ensembl 2014. Nucleic Acids Res *42*, D749-755.

Goecks, J., Nekrutenko, A., Taylor, J., and Galaxy, T. (2010). Galaxy: a comprehensive approach for supporting accessible, reproducible, and transparent computational research in the life sciences. Genome biology *11*, R86.

Greber, B., Wu, G., Bernemann, C., Joo, J.Y., Han, D.W., Ko, K., Tapia, N., Sabour, D., Sterneckert, J., Tesar, P.*, et al.* (2010). Conserved and divergent roles of FGF signaling in mouse epiblast stem cells and human embryonic stem cells. Cell stem cell *6*, 215-226.

Heider, A., and Alt, R. (2013). virtualArray: a R/bioconductor package to merge raw data from different microarray platforms. BMC Bioinformatics *14*, 75.

Hsieh, J.C., Rattner, A., Smallwood, P.M., and Nathans, J. (1999). Biochemical characterization of Wnt-frizzled interactions using a soluble, biologically active vertebrate Wnt protein. Proceedings of the National Academy of Sciences of the United States of America *96*, 3546-3551.

Huber, W., von Heydebreck, A., Sultmann, H., Poustka, A., and Vingron, M. (2002). Variance stabilization applied to microarray data calibration and to the quantification of differential expression. Bioinformatics *18 Suppl 1*, S96-104.

Irizarry, R.A., Hobbs, B., Collin, F., Beazer-Barclay, Y.D., Antonellis, K.J., Scherf, U., and Speed, T.P. (2003). Exploration, normalization, and summaries of high density oligonucleotide array probe level data. Biostatistics *4*, 249-264.

Johnson, W.E., Li, C., and Rabinovic, A. (2007). Adjusting batch effects in microarray expression data using empirical Bayes methods. Biostatistics *8*, 118-127.

Kojima, Y., Kaufman-Francis, K., Studdert, J.B., Steiner, K.A., Power, M.D., Loebel, D.A., Jones, V., Hor, A., de Alencastro, G., Logan, G.J.*, et al.* (2014). The transcriptional and functional properties of mouse epiblast stem cells resemble the anterior primitive streak. Cell stem cell *14*, 107-120.

Okabe, M., Ikawa, M., Kominami, K., Nakanishi, T., and Nishimune, Y. (1997). 'Green mice' as a source of ubiquitous green cells. FEBS Lett *407*, 313-319.

Rudy, J., and Valafar, F. (2011). Empirical comparison of cross-platform normalization methods for gene expression data. BMC Bioinformatics *12*, 467.

Soriano, P. (1999). Generalized lacZ expression with the ROSA26 Cre reporter strain. Nature genetics *21*, 70-71.

Subramanian, A., Tamayo, P., Mootha, V.K., Mukherjee, S., Ebert, B.L., Gillette, M.A., Paulovich, A., Pomeroy, S.L., Golub, T.R., Lander, E.S., *et al.* (2005). Gene set enrichment analysis: a knowledge-based approach for interpreting genome-wide expression profiles. Proceedings of the National Academy of Sciences of the United States of America *102*, 15545-15550.

Willert, K., Brown, J.D., Danenberg, E., Duncan, A.W., Weissman, I.L., Reya, T., Yates, J.R., 3rd, and Nusse, R. (2003). Wnt proteins are lipid-modified and can act as stem cell growth factors. Nature *423*, 448-452.

Chapter 6

Discussion and future perspectives

General discussion and future direction

Pluripotency is an innate and, to a certain extent, flexible potential of cells to generate all embryonic lineages. This comprises mesoderm, definitive endoderm and ectoderm derivatives, along with germ cells. In the embryos of eutherian mammals, pluripotency first appears within the inner cell mass (ICM). Here, the first pluripotent tissue is the epiblast of the developing embryo. In preparation for deploying the adult organism blueprint, over a period of several days (in mouse) or approximately two weeks in human embryos, these cells undergo significant cellular, transcriptional and epigenomic changes. Pluripotency is often referred to as naïve or primed, two states that correspond to the pre- and post-implantation pluripotent populations in the embryo, and their *in vitro* counterpart stem cells: embryonic stem cells (ESCs) and epiblast stem cells (EpiSCs). Mouse ESCs (and the mouse pre-implantation epiblast) are characterized by the production of OCT4, SOX2, KLF4, TFCP2L1, ESRRB, TBX3 and NANOG, which are absent from the EpiSCs (and the post-implantation epiblast). These transcription factors form a "core pluripotency network" that controls and sustains naïve pluripotency. Upon differentiation of ESCs to EpiSCs, as the naïve factors are negatively regulated, the expressions of *Otx2* and *Oct6* increase. This triggers the differentiation of ESCs, i.e. loss of naïve pluripotency, and mirrors the transcriptional changes that occur in the late blastocyst. There, in an identical pattern, *Nanog* expression is repressed before implantation, concurrent with the increase in expression of *Otx2* and *Oct6*. Among the other factors that are differentially expressed between the two cell types, the *de novo* methyltransferases *Dnmt3a* and *Dnmt3b* are induced, which, both *in vivo* and *in vitro*, leads to a significant genome-wide increase in CpG methylation.

The transition from one state to the other (or its inhibition) is tightly regulated by several signaling pathways: LIF and WNT (for ESCs – naïve pluripotency) and FGF through MEK signaling and Activin (for EpiSCs – primed pluripotency). Despite knowing what factors are required for the maintenance of naïve pluripotency or the differentiation to primed pluripotency, it is still unclear what molecular mechanisms these signaling pathways trigger and whether they act in synergy. Our goal was to investigate the molecular cascades regulating the transition between different pluripotency states and their biological relevance. Clarifying these transitions can have a significant impact on improving reprogramming protocols and understanding how lineage decisions are affected and implemented.

Key thesis insights	
Chapter 2	▪ BMP induced differentiation in mouse EpiSCs is mediated by WNT signals; ▪ Endogenous WNT proteins induce differentiation and loss of pluripotency in EpiSCs; ▪ WNT inhibition maintains EpiSCs in a pregastrula epiblast stage; ▪ EpiSCs can contribute to blastocyst chimeras if their transcriptional profile corresponds to pregastrula epiblast; ▪ Inhibition of endogenous WNT signals prevents the accumulation of differentiated cells in human ESC cultures.
Chapter 3	▪ WNT signals block lumenogenesis and progression to a rosette-like state, while MEK inhibition does not affect this transition but blocks subsequent pluripotency progression to the primed state; ▪ MEK/WNT-inhibited cells display rosette-like features; ▪ MEK/WNT-inhibited cells display bivalent marking of primed genes; ▪ MEK/WNT-inhibited cells acquire rosette-specific formatting of pericentric heterochromatin; ▪ OTX2 regulates entry into the rosette-like state; ▪ MEK/WNT-inhibited cells represent a novel type of pluripotent cells, termed rosette stem cells (RSCs).
Chapter 4	▪ TCF7L1-/- ES cells inefficiently differentiate to RSCs; ▪ WNT activity induces significant changes in the binding pattern of TCF7L1 to protein complexes; ▪ Whereas the core pluripotency network in ESCs contains OCT4, SOX2, NANOG, KLF4 and TCF7L1, the one in RSCs only contains OCT4, SOX2 and TCF7L1, which may explain the faster differentiation of the RSCs to EpiSCs; ▪ WNT may direct Polycomb-mediated repression to genes involved in the transition to the primed state;
Chapter 5	▪ *Otx2* is among the first responders to reduced LIF and WNT activity, emphasizing its key role in coordinating the transition from naïve to primed pluripotency; ▪ DNA demethylation is not a key feature of ESCs, but rather a 'side-effect' of culture due to MEK inhibition; ▪ The cell motility observed in RSCs is repressed by MEK and supported by MEK inhibition.

In Chapter 2 we focused on investigating the effects of endogenous WNT signals on the differentiation and self-renewal of both human and mouse pluripotent cells. This work pinpoints endogenous WNT signals as mediators of differentiation decisions in response to BMP signaling, and demonstrate that these endogenous signals are the main cause of spontaneous differentiation in both human ESCs and mouse EpiSCs. In addition, we demonstrate that BMP4 induces two differentiation pathways, one WNT-dependent to primitive streak and one WNT-independent to trophoblast. We showed that endogenous WNT signals induce differentiation and loss of pluripotency in EpiSCs, leading to a new culture

condition that maintains homogenous EpiSC populations: serum free medium (N2B27) supplemented with FGF, Activin and IWP2 (inhibitor of WNT production 2). Our data shows that EpiSCs cultured without WNT signals more closely resemble the pre-gastrula stage of embryonic development, highlighted by the ability of these cells to contribute to chimeras upon blastocyst injections. Endogenous WNT signals push the EpiSCs to a phenotype resembling the late-gastrula stage epiblast, consisting of a mixture of EpiSCs in various stages of differentiation. In addition, we also showed that the inhibition of endogenous WNT signals prevents the accumulation of differentiated cells in human ESC cultures. An exciting recent development is the generation of synthetic embryos from ESCs and trophoblast stem cells (TSCs) (Rivron, et al., 2018). This allows the investigation of interactions between the different tissue types of the blastocyst and their roles in regulating development. Human TSCs have not been established yet, but if we can efficiently generate human trophoblast cells by using defined media as published in this chapter, we might be able to generate human trophoblast cells to create human synthetic embryos to address such questions.

In Chapter 3, we demonstrated that WNT and MEK signals act subsequently to arrest different states of pluripotency. Our work led to the description of a novel, third pluripotent state, which we termed rosette-like, after the *in vivo* equivalent of cells with similar characteristics. Whereas ESCs are reliant on LIF and WNT for their maintenance, and EpiSCs rely on the removal of WNT factors and activation of MEK, a novel pluripotency state can be stably maintained in culture through a combination of both WNT and MEK inhibition, in the presence of LIF (Figure 1). We showed that rosette-like stem cells (RSCs) share some characteristics with ESCs, such as the expression of a subset of genes considered specific for naïve pluripotency. These properties are relevant for a long-standing debate with regards to

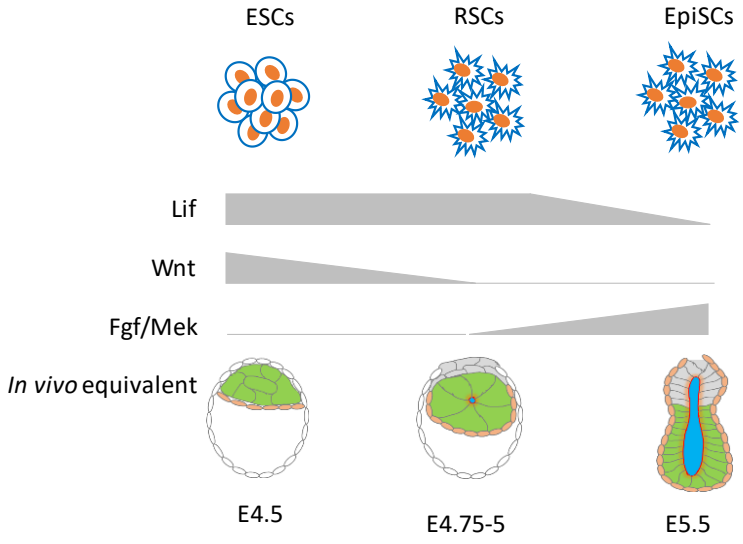

Figure 1. Schematic representation of the three pluripotent states and their signaling requirements, as defined in the mouse model

naïve pluripotency and its WNT requirement. Some groups have previously argued that WNT signals are not required for ESC maintenance, as some cells cultured in the absence of WNT are still able to generate chimeras and show a panel of naïve markers (Augustin, et al., 2017) (Biechele, Cockburn, Lanner, Cox, & Rossant, 2013). Chapter 3 demonstrates that this is not the case, and indicates that most likely, these groups were culturing RSCs. A still open question is on the status of ESCs cultured in LIF+serum. Although these cultures are still pluripotent, as demonstrated by their ability to generate high-contribution chimaeras with germline transmission, it is a well-established fact that ESCs maintained in serum are often morphologically heterogenous and also express pluripotency associated transcription factors in a heterogenous manner (Toyooka, Shimosato, Murakami, Takahashi, & Niwa, 2008) (Marks, et al., 2012). This mosaic transcription factor expression indicates that the ESCs cultured in serum are not only heterogenous ESCs, but cultures consisting of different cell types, including ESCs and RSCs, and perhaps EpiSCs due to the variability of serum composition.

Chapter 3 also includes a comprehensive description of RSC-specific characteristics, such as co-production of KLF4 and OTX2, apicobasal polarity, cell motility and accumulation of H3K27me3 in the pericentric heterochromatin. These features are consistent with the transformations occurring *in vivo* when transitioning from the inner cell mass to the epiblast, through the embryonic rosette. An important finding was that WNT blocks *Otx2* induction, lumenogenesis and the methylation of H3 at K27. Our data shows that the dynamic and global increase in DNA methylation that occurs as ESCs exit the naïve state and differentiate into RSCs creates a methylome intermediate between naïve and primed pluripotency. Our gene expression profiling indicates that the increased methylation in RSCs may be an artefact resulting from MEK inhibition, and not a driver/initiator of initial exit from naïve to rosette pluripotency, a hypothesis further investigated in Chapter 5. We observed the rosette pluripotent state as a naïve-primed intermediate both in vitro and in vivo, suggesting that it is a required intermediate. Our data lays the foundation of future studies that should provide an additional layer of insights into the molecular dynamics and drivers of transition through the three distinct stages of pluripotency. Equally important will be to verify whether the transition events we observe in our fully defined *in vitro* culture system are an accurate representation of the events occurring *in vivo*. In the embryo, the cells transition from naïve to primed pluripotency in a closely synchronized manner, whereas the *in vitro* differentiation

is more inconsistent, asynchronous and takes a longer time. Elucidation of the developmental program of transitions at a single-cell level is therefore fundamental in understanding how lineage decisions are set up and executed.

In light of our identification of RSCs in mouse, it would be important to investigate the existence of a similar state in human cells. A key question remains, of whether RSC-like human cells can be derived by conversion of human ESCs. Given that human ESCs more closely resemble mouse EpiSC, and the latter do not efficiently revert to RSCs, we hypothesize that it may be challenging to derive hRSCs from hESCs, without first describing a state in human cells that resembles naïve pluripotency. Similarly, exploring whether the ESC-RSC-EpiSC transition in human cells is triggered by the same factors or in the same order might generate insights relevant to IVF or oncology. For instance, human IVF embryos often implant but then fail to develop further. Our work provides some insight into the processes that regulate further development, in mouse. This thesis hints at signaling-regulated embryonic checkpoints, involving the different tissue types of the blastocyst.

In Chapter 4 we explored the role of TCF7L1 (also known as TCF3) in ESCs and RSCs, as despite the absence of WNT signaling, naïve genes are not repressed yet in the latter. This work focused on unravelling the molecular interactions that allow ESCs and RSCs to share naïve characteristics although they are maintained under opposite levels of WNT activity. First, we showed a direct correlation between TCF7L1 overexpression and a higher concentration of WNT required to counter-act its repressing effect, demonstrating that WNT relieves TCF7L1 repression to maintain naïve characteristics. In contrast, cells lacking TCF7L1 significantly slow down the transition of ESCs to RSCs. Additional work would be required to understand why the transition is not altogether stopped, and what other factors are involved in it.

An important outcome of Chapter 4 is a map of TCF7L1 interactors in RSCs, both when WNT signaling was inactive (true RSCs) and active (RSCs cultured with WNT for 4 hours). Our data showed NuRD and SWI/SNF as complexes pulled down irrespective of WNT activity. Moreover, we observed a compositional change of the TCF7L1 interactome, from a complex containing OCT4, SOX2, NANOG, KLF4 and TCF7L1 (in presence of WNT), to one only containing OCT4, SOX2 and TCF7L1 (in absence of WNT), providing insight into the faster differentiation of RSCs to EpiSCs, which we demonstrated in Chapter 3. This suggests KLF4 and NANOG may bring TCF7L1 to genomic binding sites specific to naïve pluripotency. To fully

define the existence of one complex containing all the factors above would require different pulldowns for each factor. Several complexes pulled down predominantly in the sample where WNT signaling was active indicate that WNT target genes are silenced in RSCs but become active within 4 hours of WNT activity. An important follow-up to this work would be to enrich this data with ChIP-Seq experiments to determine whether the changes in the TCF7L1 complex indeed result in changes in genomic localization. We also pulled down several Polycomb group proteins in the RSC sample treated with WNT, indicating a previously unknown connection between the repressive Polycomb complex and ESCs/RSCs. Additional pulldowns combined with knockdowns would further validate this link.

In addition to WNT signaling, MEK inhibition was also shown to support ESC self-renewal in the absence of LIF, when combined with GSK3 inhibitor (which activates the WNT pathway) or WNT3a soluble protein, although at a severely compromised level (Kurek & ten Berge, 2012). The mechanism hypothesized for this relies on the inhibition of autocrine FGF4 signals (Kunath, et al., 2007). As supporting evidence, it was shown that GSK3 inhibition is enough to support FGF4-/- ESCs (Ying, et al., 2008). In Chapter 5 we set out to confirm that ESC maintenance does not depend on MEK inhibition, and that this pathway is relevant for the maintenance of RSCs, through gene expression analysis. An important finding of this chapter is the early response of the *Otx2* gene to withdrawal of either LIF or WNT. The gene's upregulation is the highest when both factors are removed, consistent with the ESC-RSC-EpiSC transition and the effect of the signaling pathways on it. Previous literature showed that OTX2 and OCT4, a transcription factor of the core pluripotency network, bind to similar regulatory regions (Yang, et al., 2014). Previous to that, OTX2 had been shown to be an intrinsic determinant of the naïve state, and required for the transition to primed pluripotency (Acampora, Di Giovannantonio, & Simeone, 2013). Our data reveals OTX2 as the initial determinant controlling the ESC to RSC transition. How OTX2 manages to perform these functions is still unknown. This chapter also shows that the demethylation observed in ESCs cultured in LIF+2i is caused by the MEK inhibition, and is not an intrinsic attribute of ESCs. This finding can have important implications for efficient iPSC derivation from human tissues, as it was previously shown that previous somatic epigenetic signature is a limiting factor in iPSC derivation efficiency (Gomes, et al., 2017). Indeed, induced demethylation by miR-29b during mouse iPSC derivation was shown to increase iPSC quality (Wang, et al., 2017). A potential

follow-up on our work could aim at deriving mouse and human iPSCs in the presence of MEK inhibition and comparing the efficiency and quality with current state-of-the-art protocols. Our findings, in particular coupled with the identification of the RSCs (Chapter 3) will enable more studies that need to be done towards the precise identification of OTX2 target genes and its protein partners in regulating gene expression at specific timepoints in the ESC-RSC-EpiSC transition. A thorough time-series experiment combining protein pulldowns with gene expression analysis can answer these important questions.

To sum up, in this thesis we show that the signaling pathways associated with the maintenance and loss of pluripotency (in particular WNT and MEK) have different effects on the molecular machinery affecting pluripotency, depending on the particular developmental stage of the cells. We enrich the body of evidence demonstrating that ESCs are maintained solely by LIF and WNT. In addition, we describe a novel pluripotent state that significantly expands our knowledge on stem cell biology and how the balance of different signaling pathways affect pluripotency. While pluripotent cells are present in the embryo for a significant period of time during the course of development, since 2007 (the year EpiSCs were first described), only two pluripotent stem cell types have been described *in vitro*, limiting our view of pluripotency to either naïve ESCs or primed EpiSCs. This indicated that only a limited number of stable attractor states can be isolated and stably maintained. This thesis shows that a third pluripotent state can be arrested and maintained in culture, and that ESCs and RSCs can inter-convert *in vitro*. Therefore, our proposition is to view pluripotency as a series of discrete steps rather than a transitional continuum. Furthermore, modified culture conditions can induce novel characteristics in ESCs, RSCs or EpiSCs (for instance, different methylation levels), confirming that the functional definition of pluripotency can be fulfilled while encompassing a broad spectrum of additional properties. What remains unclear is whether bona fide counterparts of the three pluripotency states exist in the human embryo, neither of which are trivial questions to answer. A 2017 paper from the Zernicka-Goetz group indicates that to be the case, as they described the lumenogenesis process that occurs in human embryos with striking similarities with mouse, without deriving cell lines with RSC features (Shahbazi, et al., 2017). Our current knowledge relies on data generated using different types of basal media, cytokine combinations (and in different concentrations), functional assays and diverse transcriptional analysis platforms, making direct comparisons near impossible. This is

eased by embryonic analyses, which make comparisons possible, as well as investigating the roles of the various signaling pathways. To understand whether the differences between these states are representative of an endogenous developmental progression, one needs to determine how each state functionally and transcriptionally relates to another in parallel controlled experiments. This needs to be followed by comparisons to high-resolution data from the epiblast population of the embryo, through successive stages of embryonic development. Ideally, these comparisons would be at a single-cell level, as heterogeneity within cell cultures due to asynchronous transitions, as well as *in vivo* within the epiblast itself, may otherwise make the interpretation of these data challenging.

The naïve-primed transition is comparable to a reprogramming process that may also be reproduced during iPSC generation, as the same factors are involved. In a sense, naïve pluripotency is not yet functionally pluripotent. Only primed pluripotent cells can differentiate into the germ layers, naïve pluripotency can only become rosette/primed. Understanding this process and what enables the embryonic cells to do it so quickly and efficiently may hold lessons for understanding and improving reprogramming to induced pluripotency. For example, constitutive heterochromatin is a major barrier to iPSC generation, and RSCs simply remove it, which may be why they progress so quickly. The work in this thesis lays the groundwork to analyze the status of all heterochromatin during the naïve-rosette-primed transitions, and investigating whether the silencing of heterochromatin in RSCs is dependent on polycomb.

References

Acampora, D., Di Giovannantonio, L., & Simeone, A. (2013). Otx2 is an intrinsic determinant of the embryonic stem cell state and is required for transition to a stable epiblast stem cell condition. *Development* , 140: 43-55.

Augustin, I., Dewi, D., Hundshammer, J., Erdmann, G., Kerr, G., & Boutros, M. (2017). Autocrine Wnt regulates the survival and genomic stability of embryonic stem cells. *Sci Signal*, 10(461).

Biechele, S., Cockburn, K., Lanner, F., Cox, B., & Rossant, J. (2013). Porcn-dependent Wnt signaling is not required prior to mouse gastrulation. *Development*, 140(14): 2961-71.

Gomes, K., Costa, I., dos Santos, J., Dourado, P., Forni, M., & Ferreira, J. (2017). Induced pluripotent stem cells reprogramming: epigenetics and applications in the regenerative medicine. *Rev Assoc Med Bras*, 63(2): 180-189.

Kalkan, T., Olova, N., Roode, M., Mulas, C., Lee, H., Nett, I., . . . Smith, A. (2017). Tracking the embryonic stem cell transition from ground state pluripotency. *Development*, 144(7): 1221-34.

Kunath, T., Saba-El-Leil, M., Almousailleakh, M., Wray, J., Meloche, S., & Smith, A. (2007). FGF stimulation of the Erk1/2 signalling cascade triggers transition of pluripotent embryonic stem cells from self-renewal to lienage commitment. *Development*, 134(16): 2895-902.

Kurek, D., & ten Berge, D. (2012). The signaling requirements for mouse embryonic stem cells. *Cell Cycle*, 11(2): 207-8.

Marks, H., Kalkan, T., Menafra, R., Denissov, S., Jones, K., Hofemeister, H., . . . Stunnenberg, H. (2012). The Transcriptional and Epigenomic Foundations of Ground State Pluripotency. *Cell*, 149: 590-604.

Rivron, N., Frias-Aldeguer, J., Vrij, E., Boisset, J., Korving, J., Vivie, J., . . . Geijsen, N. (2018). Blastocyst-like structures generated solely from stem cells. *Nature*, 557(7703): 106-111.

Shahbazi, M., Scialdone, A., Skorupska, N., Weberling, A., Recher, G., Zhu, M., . . . Zernicka-Goetz, M. (2017). Pluripotent state transitions coordinate morphogenesis in mouse and human embryos. *Nature*, 552(7684): 239-43.

Toyooka, Y., Shimosato, D., Murakami, K., Takahashi, K., & Niwa, H. (2008). Identification and characterization of subpopulations in undifferentiated ES cell culture. *Development*, 135: 909-918.

Wang, G., Weng, R., Lan, Y., Guo, X., Liu, Q., Liu, X., . . . Kang, J. (2017). Synergetic effects of DNA methylation and histone modification during mouse induced pluripotent stem cell generation. *Scientific Reports*, 7: 39527.

Yang, S., Kalkan, T., Morissroe, C., Marks, H., Stunnenberg, H., Smith, A., & Sharrocks, A. (2014). Otx2 and Oct4 Drive Early Enhancer Activation during Embryonic Stem Cell Transition from Naive Pluripotency. *Cell Rep*, 7(6): 1968-81.

Ying, Q., Wray, J., Nichols, J., Batlle-Morera, L., Doble, B., Woodgett, J., . . . Smith, A. (2008). The ground state of embryonic stem cell self-renewal. *Nature*, 453(7194): 519-23.

Summary

Summary

This thesis aimed to thoroughly describe the effects key signaling pathways have on pluripotency, with a particular view towards providing a more complete view of the controversy of the role of WNT signaling in pluripotency. Our goal was to investigate how different signaling pathways (LIF, WNT and MEK) balance themselves to sustain different pluripotent states.

In Chapter 2 we show that BMP induces differentiation in mouse EpiSCs through a WNT-independent path to trophoblast, and through a WNT-dependent path to primitive streak. We also show that in contrast to ESCs, where WNT maintains naïve pluripotency, in EpiSCs it has the opposite effect, triggering differentiation and loss of pluripotency. This demonstrates that WNT inhibition maintains EpiSC pluripotency. Moreover, WNT inhibition in EpiSCs promotes a profile similar to pre-gastrula epiblast stage, which can lead to blastocyst chimera contribution. Lastly, this chapter shows that the inhibition of endogenous WNT signals prevents the accumulation of differentiated cells in human ESC cultures.

In Chapter 3, we demonstrate that WNT signals block lumenogenesis and progression to a rosette-like state, while MEK inhibition does not affect this transition but blocks subsequent pluripotency progression to the primed state. Moreover, the MEK/WNT-inhibited cells display rosette-like features, bivalent marking of primed genes and acquire rosette-specific formatting of pericentric heterochromatin. We also show that OTX2 regulates the entry into the rosette-like state. The MEK/WNT-inhibited cells represent a novel type of pluripotent cells, termed rosette stem cells (RSCs).

In Chapter 4 we started from the observation that both ESCs and RSCs share a subset of naïve pluripotency characteristics, even though WNT activity is on and off, respectively. We asked what role does TCF7L1 has in the transition and reversion from naïve to rosette-like and showed that *Tcf7l1*-/- cells inefficiently differentiate to RSCs. Moreover, our data shows that WNT activity induces significant changes in the binding pattern of TCF7L1 to protein complexes. Whereas the core pluripotency network in ESCs contains OCT4, SOX2, NANOG, KLF4 and TCF7L1, the one in RSCs only contains OCT4, SOX2 and TCF7L1, which may explain the faster differentiation of the RSCs to EpiSCs. For the first time, we also show that WNT may direct Polycomb-mediated repression to genes involved in the transition to the primed state.

In Chapter 5, we show that *Otx2* is among the first responders to reduced LIF and WNT activity, emphasizing its key role in coordinating the transition from naïve to primed pluripotency. In addition, we demonstrate that DNA methylation is not a key feature of ESCs, but rather a 'side-effect' of culture caused by MEK inhibition. In addition, we show that the cell motility observed in RSCs is repressed by MEK and supported by MEK inhibition.

In brief, in this thesis I describe a novel pluripotent state that allows an in-depth description of the effect different signaling pathways have on the transition from naïve to primed pluripotency, with relevance to the derivation of iPSCs, IVF and oncology.

Samenvatting

Samenvatting

Het doel van dit proefschrift was om de effecten van belangrijke signaleringsroutes op de pluripotentie grondig te beschrijven, met een visie om een vollediger beeld te krijgen van de controverse over de rol van WNT-signalering in pluripotentie. Ons doel was om te onderzoeken hoe verschillende signaalwegen (LIF, WNT en MEK) zich in evenwicht houden om verschillende pluripotente toestanden te ondersteunen.

In hoofdstuk 2 laten we zien dat BMP differentiatie induceert in EpiSC's van muizen via een WNT-onafhankelijke weg naar trofoblast, en via een WNT-afhankelijke weg naar primitieve streak. We laten ook zien dat in tegenstelling tot ESC's, waar WNT naïeve pluripotentie handhaaft, het in EpiSC's het tegenovergestelde effect heeft, waardoor differentiatie en verlies van pluripotentie wordt veroorzaakt. Dit toont aan dat WNT-remming EpiSC-pluripotentie handhaaft. Bovendien bevordert de WNT-remming in EpiSC's een profiel vergelijkbaar met het pre-gastrula-epiblaststadium, wat kan leiden tot een bijdrage van de blastocystchimera. Ten slotte laat dit hoofdstuk zien dat de remming van endogene WNT-signalen de accumulatie van gedifferentieerde cellen in menselijke ESC-culturen voorkomt.

In hoofdstuk 3 laten we zien dat WNT signalen de lumenogenese en progressie naar een rozetachtige toestand blokkeren, terwijl MEK-remming deze overgang niet beïnvloedt, maar de daaropvolgende pluripotentieprogressie naar de geprimede toestand blokkeert. Bovendien vertonen de MEK / WNT-geremde cellen rozetachtige kenmerken, bivalente markering van geprimede genen en verwerven ze rozet-specifieke opmaak van pericentrisch heterochromatine. We laten ook zien dat OTX2 de toegang tot de rozetachtige toestand regelt. De MEK / WNT-geremde cellen vertegenwoordigen een nieuw type pluripotente cellen, genoemd rozetstamcellen (RSC's).

In hoofdstuk 4 zijn we uitgegaan van de observatie dat zowel ESC's als RSC's een subset van naïeve pluripotentie-eigenschappen delen, hoewel WNT-activiteit respectievelijk aan en uit is. We onderzochten welke rol TCF7L1 heeft in de overgang en omkering van naïef naar rozetachtig en toonden aan dat *Tcf7l1-/-* cellen inefficiënt differentiëren tot RSC's. Bovendien laat onze data zien dat WNT-activiteit significante veranderingen in het bindingspatroon van TCF7L1 aan eiwitcomplexen induceert. Terwijl de kern pluripotentie netwerk in ESC's OCT4, SOX2, NANOG, KLF4 en TCF7L1 bevat, bevat dat in RSC's alleen OCT4, SOX2 en TCF7L1, wat de snellere differentiatie van de RSC's naar EpiSC's kan verklaren. Voor het eerst laten we ook

zien dat WNT door Polycomb gemedieerde repressie kan richten op genen die betrokken zijn bij de overgang naar de primer-toestand.

In hoofdstuk 5 laten we zien dat *Otx2* een van de eersten is die op vermindering van LIF- en WNT-activiteit reageert, wat zijn sleutelrol benadrukt in de coördinatie van de overgang van naïeve naar geprimeerde pluripotentie. Bovendien tonen we aan dat DNA-methylering geen belangrijk kenmerk is van ESC's, maar eerder een 'neveneffect' van het kweken veroorzaakt door MEK-remming. Bovendien tonen we aan dat de celmotiliteit waargenomen in RSC's wordt onderdrukt door MEK en wordt ondersteund door MEK-remming.

Samengevat, in dit proefschrift beschrijf ik een nieuwe pluripotente staat die een diepgaande beschrijving mogelijk maakt van het effect dat verschillende signaalroutes hebben op de overgang van naïeve naar geprimede pluripotentie, met relevantie voor de afleiding van iPSC's, IVF en oncologie.

Curriculum Vitae

Curriculum Vitae

Name: Alexandru Neagu

Address: Planetenbaan 94, 3721LC, Bilthoven, the Netherlands

Date of birth: September 29 1987

Email: alexvneagu@gmail.com

Phone number: 0031627047559

Nationality: Romanian

Work experience

2018 – present	Expert Evaluator, Horizon 2020 Innovation Fund
2018 – present	SME Instrument Business Coach
2016 – 2018	Science and Business Consultant at ttopstart B.V.
2015 – 2016	Business analyst at INKEF Capital

Education and research

2011 – 2015 Department of Cell Biology, Erasmus MC, Rotterdam, the Netherlands

- PhD student

2009 - 2011 Erasmus MC, Rotterdam, the Netherlands

- MSc Molecular Medicine

2010 - 2011 Erasmus Stem Cell Institute, Department of Cell Biology, Erasmus MC, Rotterdam, the Netherlands

- Internship in Prof. Dzierzak's group, supervised by Dr. Mihaela Crisan

2009 - 2010 Department of Cell Biology, Erasmus MC, Rotterdam, the Netherlands

- Internship in Prof. Grosveld's group, supervised by Dr. Robert-Jan Palstra

2006 - 2009 Faculty of Biology, 'Alexandru I. Cuza University', Iasi, Romania

- BSc Biochemistry

Courses / skills / languages

Courses

2014	Employability outside academia
2014	Research Based Business: Business development & Technology Transfer
2014	Science Based Business: Management
2013	Intellectual Property in high tech start-ups
2012	Biostatistics
2012	Laboratory animal science course (Article 9)
2012	Genetics
2012	Cell and Developmental Biology
2011	Biochemistry and Biophysics

Software skills

Microsoft Office programs (Word, Excel, PowerPoint)

Adobe (Photoshop, Illustrator)

Languages

English: fluent in reading, writing and speaking

Dutch: basic in reading, writing and speaking

Romanian: Native in reading, writing and speaking

List of publications

Neagu A., Escudero I., Kurek D., Lehmann J., Stel J., Dirks R., van Mierlo G., Maas A., Eleveld C., Ge Y., den Dekker A.T., Brouwer R., van Ijcken W., Modic M., Drukker M., Jansen J., Baart E., Marks H., ten Berge D. "WNT signals regulate the transition to rosette-stage pluripotency". *Under revision Nature Cell Biology*

Crisan M., Solaimani Kartalaei P., **Neagu A.**, Karkampouna S., Yamada-Inagawa T., Purini C., Vink CS., van der Linden R., van Ijcken W., Chuva de Sousa Lopes SM., Monteiro R., Mummery C., Dzierzak E. "BMP and Hedgehog Regulate Distinct AGM Hematopoietic Stem Cells Ex Vivo." *Stem Cell Reports 2016, 6(3): 383-395.*

Kurek D., **Neagu A.**, Tastemel M., Tuysuz N., Lehmann J., van de Werken HJG., Philipsen S., van der Linden R., Maas A., van Ijcken WFJ., Drukker M., ten Berge D. "Endogenous WNT signals mediate BMP-induced and spontaneous differentiation of epiblast stem cells and human embryonic stem cells." *Stem Cell Reports 2015, 4(1): 114-128*

PhD Portfolio Summary

Summary of PhD training and teaching activities

Name PhD student: Alexandru Neagu Erasmus MC Department: Cell Biology Research School: Biomedical Sciences	PhD period: 2011-2015 Promotor: Prof. Dr. Danny Huylebroeck and Prof. Dr. Elaine Dzierzak Co-promotor: Assoc. Prof. Dr. Derk ten Berge
1. PhD training	**Year**
Specific courses	
Biochemistry and Biophysics	2011
Cell and Developmental Biology	2012
Genetics	2012
Literature course	2012
Biostatistical methods I: basic	2012
Safely working in the lab	2012
Laboratory animal science course (Article 9)	2012
Seminars and workshops	
The 21st MGC symposium	2011
19th MGC PhD Workshop in Dusseldorf	2012
The 20th MGC PhD Workshop in Luxembourg (presentation)	2013
The 24th MGC Symposium	2014
The 22nd MGC PhD Workshop in Maastricht (presentation)	2015
Erasmus lectures in cell biology and development	2011-2015
Monday morning meetings	2011-2015
Other	
Intellectual Property in high-tech start-ups	2013
Science Based Business: Management	2014
	2014

Research Based Business: Technology Transfer	2014
Research Based Business: Business Development	2014
Employability outside academia	
2. Teaching	
BSc Nanobiology students	2014-2015
Master thesis student	2014-2015
Master thesis student	2012-2013